INFORMATION TO USERS

This manuscript has been reproduced from the microfilm master. UMI films the text directly from the original or copy submitted. Thus, some thesis and dissertation copies are in typewriter face, while others may be from any type of computer printer.

The quality of this reproduction is dependent upon the quality of the copy submitted. Broken or indistinct print, colored or poor quality illustrations and photographs, print bleedthrough, substandard margins, and improper alignment can adversely affect reproduction.

In the unlikely event that the author did not send UMI a complete manuscript and there are missing pages, these will be noted. Also, if unauthorized copyright material had to be removed, a note will indicate the deletion.

Oversize materials (e.g., maps, drawings, charts) are reproduced by sectioning the original, beginning at the upper left-hand corner and continuing from left to right in equal sections with small overlaps.

Photographs included in the original manuscript have been reproduced xerographically in this copy. Higher quality 6" x 9" black and white photographic prints are available for any photographs or illustrations appearing in this copy for an additional charge. Contact UMI directly to order.

ProQuest Information and Learning
300 North Zeeb Road, Ann Arbor, MI 48106-1346 USA
800-521-0600

UMI®

HETEROPOLYMETALATES CONTAINING LANTHANIDES: SOLUTION AND SOLID STATE CHEMISTRY

By

Qunhui Luo

A dissertation submitted to the Graduate Faculty in Chemistry in partial fulfillment of the requirements for the degree of Doctor of Philosophy, The City University of New York

2002

This manuscript has been read and accepted for the Graduate Faculty in Chemistry in satisfaction of the dissertation requirement for the degree of Doctor of Philosophy.

April 18, 2002
Date

Lynn C. Francesconi
Chair of Examining Committee

April 23, 2002
Date

Gerald Koppel
Executive Officer

Robert Beer

Charles Michael Drain

Malgorzata Ciszkowska
Supervisory Committee

The City University of New York

Abstract

HETEROPOLYMETALATES CONTAINING LANTHANIDES: SOLUTION AND SOLID STATE CHEMISTRY

by

Qunhui Luo

Adviser: Professor Lynn C. Francesconi

The monovacant heteropolyanions, $[\alpha\text{-}1\text{-}P_2W_{17}O_{61}]^{10-}$ (denoted α-1) and $[\alpha\text{-}2\text{-}P_2W_{17}O_{61}]^{10-}$ (denoted α-2), derived from the Wells-Dawson ion $[\alpha\text{-}P_2W_{17}O_{61}]^{6-}$ by removal of a $[WO]^{4+}$ unit are known to react with lanthanide (III) ions to form complexes. In this study, these complexes have been systematically characterized in solution and solid state.

Three lanthanide (Lu, Eu and Gd) α-2 1:2 complexes have been crystallized and their structures solved by X-ray crystallography. The molecule structures are in good agreement with solution structure characterizations.

The solution and solid state chemistry for Ln α-2 1:1 complexes has been studied by ^{31}P, ^{183}W NMR spectroscopy, fluorescence spectroscopy and X-ray crystallography. In solid state, $[Eu(\alpha\text{-}2\text{-}P_2W_{17}O_{61})]^{7-}$, exists as dimeric form, $[Eu(H_2O)_3(\alpha\text{-}2\text{-}P_2W_{17}O_{61})]_2^{14-}$. In solution, the dimeric form breaks down and $[Eu(\alpha\text{-}2\text{-}P_2W_{17}O_{61})]^{7-}$ exists as monomer, $[Eu(H_2O)_4(\alpha\text{-}2\text{-}P_2W_{17}O_{61})]^{7-}$. This is confirmed by ^{183}W NMR

spectrum and fluorescence lifetime measurement. Also there is equilibrium between Ln α-2 1:1 and Ln α-2 1:2 complexes in solution. The equilibrium constant is in the micromolar range.

The crystal structure of $[Lu(\alpha\text{-}1\text{-}P_2W_{17}O_{61})]^{7-}$ anion has been solved. The crystallographic results are in good agreement with the fluorescence and the ^{183}W NMR results.

A new complex of lanthanide $(\alpha\text{-}1\text{-}P_2W_{17}O_{61})^{10-}$ has been isolated. ^{31}P and ^{183}W NMR spectroscopy, fluorescence lifetime measurement and the elemental analysis data indicate that the formula of this new complex is $[Ln(\alpha\text{-}1\text{-}P_2W_{17}O_{61})_2]^{17-}$.

Ternary complexes of $[Ln(\alpha\text{-}1\text{-}P_2W_{17}O_{61})]^{7-}$ with organic ligands have been observed from titration of organic ligands to $[Ln(\alpha\text{-}1\text{-}P_2W_{17}O_{61})]^{7-}$ monitored by ^{31}P NMR. A chiral organic ligand, L-tartaric acid, was bound to the two optical isomers of $[Ln(\alpha\text{-}1\text{-}P_2W_{17}O_{61})]^{7-}$, as revealed from ^{31}P NMR titration to form diastereomeric pairs of Ln α-1-$P_2W_{17}O_{61}$ - L-tartaric acid complexes.

The protonation constants for $(\alpha\text{-}2\text{-}P_2W_{17}O_{61})^{10-}$ have been measured. Two methods have been developed to measure formation constant for Ln α-1 and Ln α-2 complexes: ligand-ligand competition method monitored by ^{31}P NMR and metal-ligand titration monitored by Eu(III) fluorescence excitation combined with lanthanide-lanthanide competition. The results from both methods are in good accord with each other and comparable with references.

Acknowledgements

It is a pleasure to acknowledge my debt to the many people involved in this work directly or indirectly.

My most heartfelt thanks go to my research advisor, Professor Lynn C. Francesconi, for her guidance, her encouragement, her understanding and support through these years.

I'd like to thank Professors Robert Beer, Charles M. Drain and Malgorzata Ciszkowska for serving on my thesis committee, especially Professor Robert Beer, for his thoughtful comments and encouragement.

Thanks also go to Professor Bill Horrocks for allowing me to use the luminescence facility at Penn State University and our productive collaboration; Dr. Victor Young and Dr. Robertha Howell for solving the crystal structures; Dr. Mark Antonio for his remarkable job on the paper we published together.

I appreciate the extraordinary effort of chemistry department at Hunter College and our lab to provide a congenial working environment. And special thanks to Professor William Grossman for his expert help in using analytical instruments and valuable advices; Dr. Michael Blumenstein for the discussion and suggestion in recording the NMR spectra; Melchor Cantorias for his help in the HPLC project; all the members in our lab for the good time and bad time we shared.

I am very grateful to my friends, Jiafang He, Zheming Ruan, Xinxu Shi, for helping me adjust to the new environment as I came to the United States.

I owe special thanks to Dr. Gertrude Elion for her spirit and financial support.

The most sincere gratitude must be extended to my husband, Xiaoming Fan, for his support; my son, Boyu, who always makes me proud; and my Mom and Dad, for their selfless and endless love.

TABLE OF CONTENT

LIST OF FIGURES

Chapter 1

Chapter 2

Chapter 3

Chapter 4

Chapter 5

Chapter 6

LIST OF TABLES

Chapter 2

Chapter 3

Chapter 4

Chapter 5

Chapter 6

Chapter 1

Introduction

1.1. General

Early transition metals, such as W(VI), Mo(VI), V(V) in their highest oxidation state, are able to form metal-oxygen cluster anions by a sequence of hydrolysis and condensation reactions. Such molecules are commonly called polyoxoanions or polyoxometalates. Key reviews can be found in an issue of Chemical Reviews devoted to polyoxometalates; Chem. Rev. 1998, 98. A hexametalate structure, $[M_6O_{19}]^{p-}$ (M=Mo, W, P=6; M=V, Nb, P=9), is shown in Figure 1.1a; the M ions are in distorted octahedral coordination environments, connected to each other by bridging oxygen atoms. The term isopolyanion is used when the

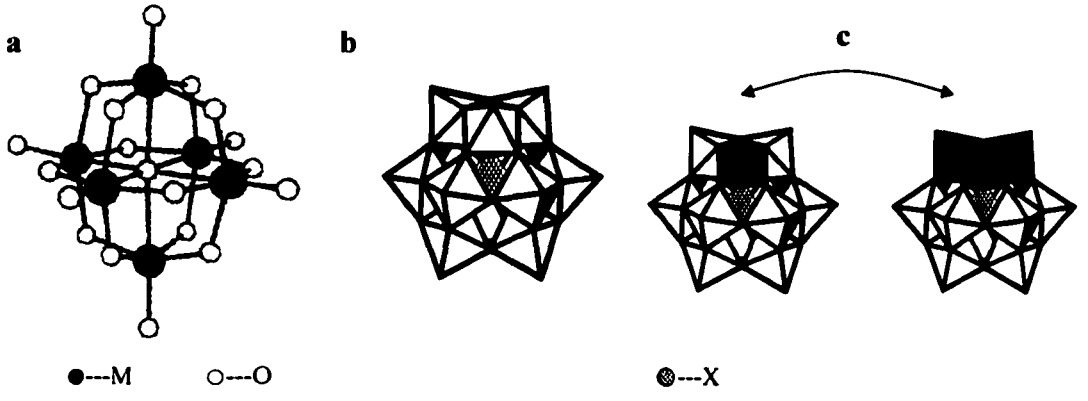

Figure 1.1. a: The hexametalate structure, $[M_6O_{19}]^{p-}$ (the charge, p depends on M: W^{6+}, Mo^{6+} or Nb^{5+}) in ball and stick representation. b: The common Keggin structure, $[XM_{12}O_{40}]^{q+}$ (the charge, q, depends on the heteroatom, X) in polyhedral representation. c: Two examples of lacunary structures result from "removal" of one or more MO_6 octahedrons.

structures are only composed of one type of metal atom, M, commonly called an addenda atom, and oxygen. Isopolyanions can be represented by the general formula:

$[M_mO_y]^{p-}$ M-----W(VI), Mo(VI), V(V), less commonly: Nb(V), Ta(V), Re(VII), I(VII).

Isopolyanions are able to incorporate other elements into their structures to form heteropolyanions. The general formula is:

$[X_xM_mO_y]^{q-}$ $(x \leq m)$ X---commonly called heteroatom

Fig. 1.1b shows the Keggin structure, $[XM_{12}O_{40}]^{x-}$, the heteroatom, X, is inside of the framework. Almost all of elements in the periodic table can be incorporated in isopolyanions. More than 65 other elements, including most nonmetals, transition metals and f elements, are found in heteropolyoxometalates. The ability of isopolyanion to incorporate heteroatoms leads to enormous number of complexes that display a large variety of structures.

The first report of polyoxometalates dates back to 1826, Berzelius described that a yellow precipitate was produced when ammonium molybdate was added to phosphoric acid. The complex formed we now know as the $[PMo_{12}O_{40}]^{5-}$ anion. The first systematic study was made by Marignac (1862-1864) who prepared and correctly analyzed both α and β isomers of 12-tungstosilicic acid and various salts. It was more than 100 years before any new tungstosilicates were unambiguously identified. The first step towards understanding the structures of polyoxometalate

anions was taken by Pauling in 1929. He proposed that the structure of the 12-tungsto anions were based on a central PO_4^{3-} or SiO_4^{4-}-tetrahedra surrounded by WO_6 octahedra. This proposal stimulated X-ray structural studies. By the beginning of the twentieth century several hundred heteropoly compounds had been prepared and analyzed by

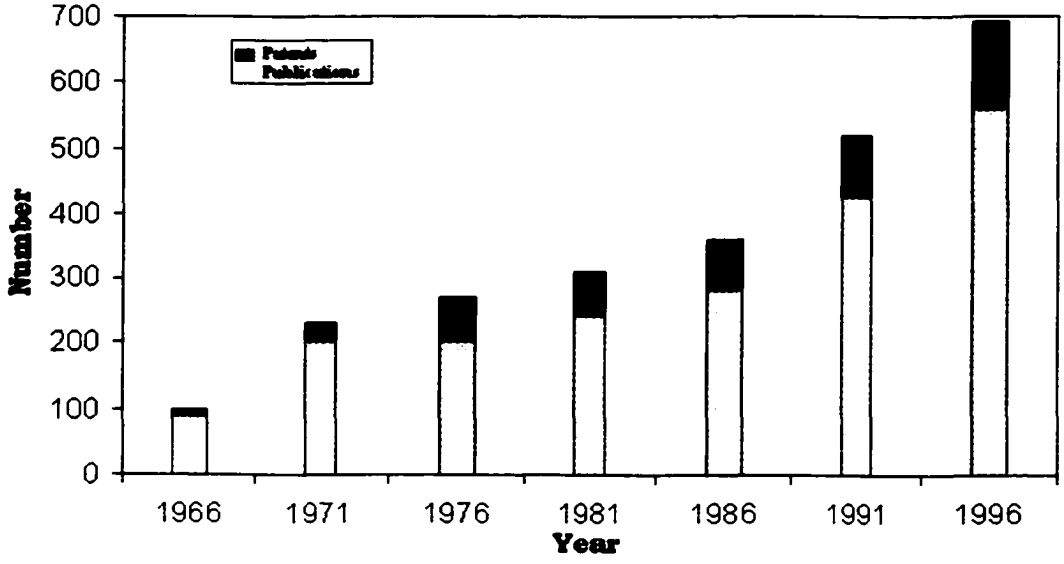

Figure 1.2. Publication and patent growth on polyoxometalates since 1966. [1] (From Katsoulis, D. E. "A Survey of Application of Polyoxometalates" *Chem. Rev.* **1998**, 98, 359.)

many research groups: The laboratory of A. Rosenheim produced some of the most productive and influential workers in the field until the mid 1930s. From the early 1940s into the mid-1970s, several laboratories worldwide were dedicated to polyoxometalates research, including the groups of Pierre Souchay in France, Ripan in Romanian and Baker and Pope in the United States. Systematic investigation started in the early

1970s followed by strong industrial applications in catalysis. Especially in the last two decades, due to advances in analytical instrumentation, polyoxometalate chemistry has developed into a new era. The present widespread availability of automated X-ray diffractometers with CCD detectors has enabled rapid solid-state structural characterization of polyoxometalates, and the number of known structure types has grown from fewer than 15 structural types known in 1970 to now hundreds of structural types. The commercially available NMR spectrometers with multinuclear capability also resulted in rapid structural characterization in solution. Figure 1.2 shows the growth of the polyoxometalates literature per year since 1966. [1]

1.2. Structures

Owing to the continuous growth of synthetic methods and the extreme variability of heteroatoms that can be incorporated into the framework of structures, a large variety of structures have been prepared and analyzed. By careful treatment with base many heteropoly species can produce so-called "lacunary" heteropoly species where one or more addenda atoms together with the oxygens have been removed from the structure. For instance, removal of one or three MO units from different positions of the Keggin structure, results in the $[XM_{11}O_{39}]^{p-}$ and $[XM_9O_{34}]^{q-}$ (A, B type) lacunary structures (Fig. 1.1c). These lacunary species generally react readily with a wide variety of metal ions (including addenda atoms) or nonmetal ions to refill the vacant sites. Many species

containing mixtures of addenda have been prepared, e.g., $[PV_2Mo_{10}O_{40}]^{5-}$ anion, two V(V) atoms substitute two Mo atoms' positions in the Keggin structure (Fig. 1.1b).

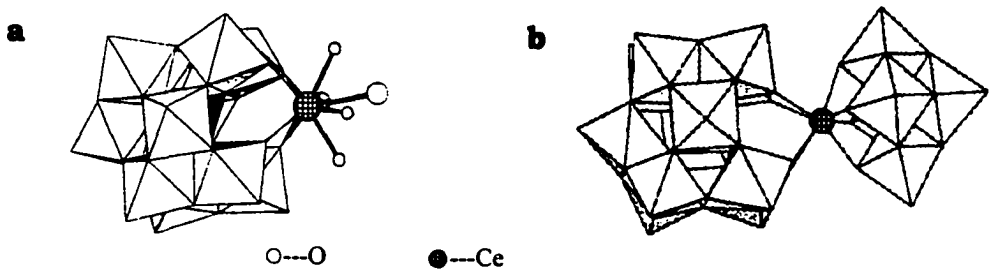

Figure 1.3. The structures of a: $[CeSiW_{11}O_{11}]^{5-}$ (From Sadakane, M.; Dickman, M. H.; Pope, M. T., *Angew. Chem. Int. Ed.* **2000**, 39(16), 2914.). b: $[Ce(W_5O_{18})(PW_{11}O_{39})]^{10-}$ (From Belai, N.; Sadakane, M.; Pope, M. T., *J. Am. Chem. Soc.* **2001**, 123(9), 2087.).

Figure 1.3a is the structure of $[CeSiW_{11}O_{39}]^{5-}$ anion [2], an example of the vacant sites in the Keggin lacunary structure refilled with a f element metal ion. The Ce ions are nine coordinated, so the five unshared coordinated positions are available for coordination to H_2O or to many other ligands. This complex is a hybrid between a heteropoly species and a coordination complex. Figure 1.3b is the structure of $[Ce(W_5O_{18})(PW_{11}O_{39})]^{10-}$ [3] where $[W_5O_{18}]^{6-}$ replaced the water molecules in $[CePW_{11}O_{39}]^{4-}$ structures. If organic ligands bind to the unshared coordination sites of metals, organic derivatives can be produced, e.g., the $[(MeO)TiW_5O_{18}]^{3-}$ anion [4] (Fig. 1.4a). In this example, the transition metal Ti atom refilled the vacant site of lacunary $[W_5O_{18}]^{6-}$ anion with an OMe group coordinated to the unshared coordinated site of Ti atom.

Organic ligands can also bond to a nonmetallic heteroatom, e.g., exterior oxygen atoms, or directly bonded to the metals through σ, π, 2π- binding

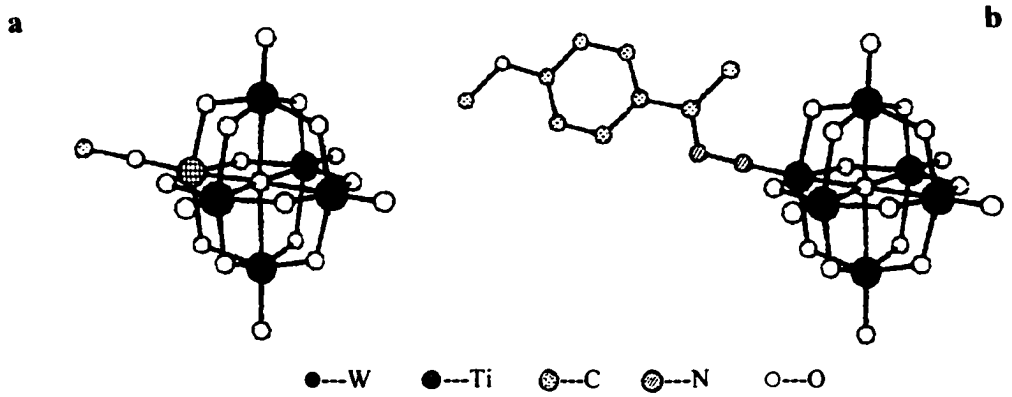

Figure 1.4. The structures of a: $[(MeO)TiW_5O_{18}]^{3-}$ (From Clegg, W.; Elsegood, M. R. J.; Errington, R. J.; Havelock, J., *J. Chem. Soc., Dalton Trans.*, **1996**, 681-690.). b: $[Mo_6O_{18}(NNC(PhOMe)Me)^{2-}$ (From Kwen, H.; Young, V. G., Jr.; Maatta, E. A., *Angew. Chem. Int. Ed. Engl.* **1999**, *38*, 1145.).

ligands, such as oxo, organoimido, cyclopentadienyl, nitrido and carbyne ligands. For more detail, refer to the review by Pierre Gouzerh [5] and the references within. Figure 1.4b is the structure of $[Mo_6O_{18}(NNC(PhOMe)Me)^{2-}$ anion [6], the organic ligand, -(PhOMe)Me, bonds to Mo through a C=N-N=Mo bridge.

Recently a new synthetic approach has emerged. The strategy is that the small metal-oxygen heteropolyoxometalates can serve as building blocks. Simple metal-oxygen building blocks or quasi-preoganized building blocks can be linked together to form new

structures. In polyoxometalate chemistry, the abundance of a large variety of linkable units, the possibility of generating new building blocks and the different ways of linking together these building blocks lead to a wide range of novel types of polyoxometalates structures. Figure 1.5a is the structure of a mixed-valence, electron-rich species $[Mo_{154}(NO)_{14}O_{420}(OH)_{28}(H_2O)_{70}]^{(25\pm5)-}$ [7]. 16 $\{Mo_8\}$ building blocks are connected

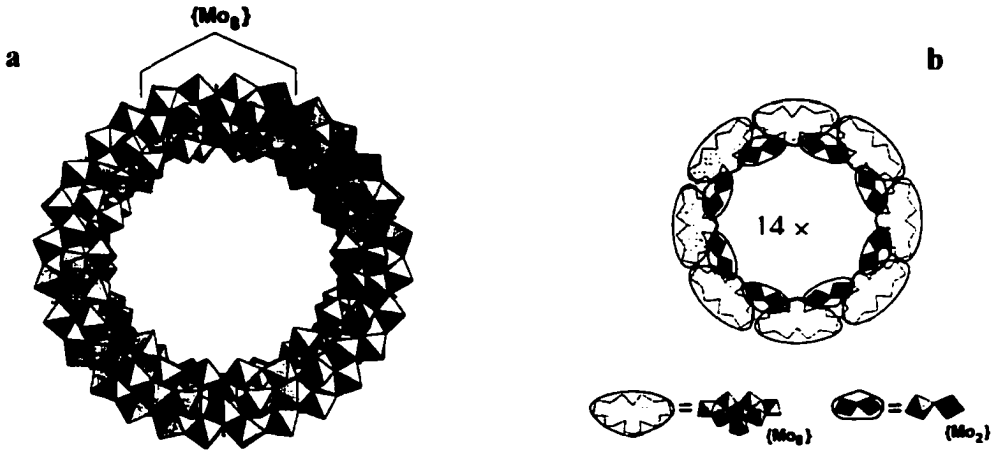

Figure 1.5. a: Structure of the cluster anion $[Mo_{154}(NO)_{14}O_{420}(OH)_{28}(H_2O)_{70}]^{28-}$; b: Scheme of this cluster being built up by the building blocks $\{Mo_2\}$ and $\{Mo_8\}$. (Both from Müller, A.; Kögerler, P.; Kuhlmann, C., *Chem. Commun.* **1999**, 1347.)

to each other to form an approximately ring shaped anion. The cavity at the equator is about 2 nm in diameter. Fig. 1.5b schematically shows how this huge cluster is built up by the building blocks $\{Mo_2\}$ and $\{Mo_8\}$ [7]. Building blocks can also be quasi-preorganized units, such as lacunary structures. Figure 1.6a is the structure of $[As_2W_{21}O_{69}(H_2O)]^{6-}$ anion [8], a simple example of two $\{AsW_9\}$ groups linking together by 3

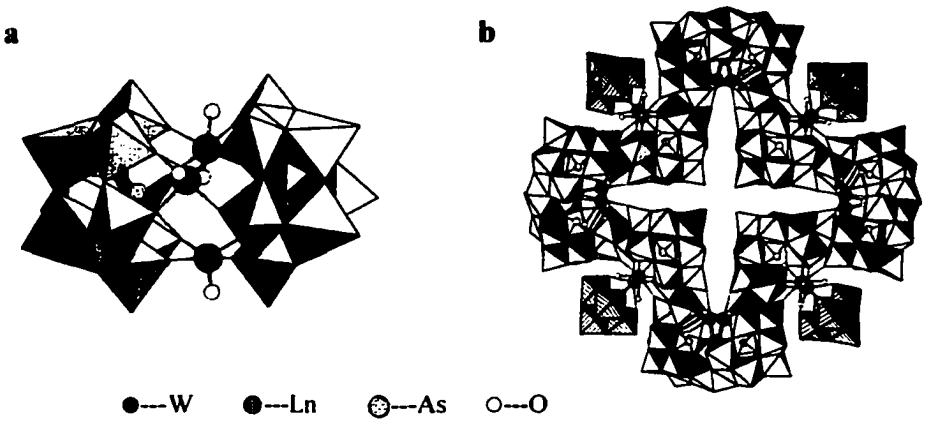

Figure 1.6. The structures of a: $[As_2W_{21}O_{69}(H_2O)]^{6-}$ anion (From 8-Jeannin, Y. J., *Cluster Sci.* **1992**, 3, 55.); b: $[Ln_6As_{12}W_{148}O_{524}(H_2O)_{36}]^{76-}$ anion (From Müller, A.; Plass, W.; Krichemeyer, E.; Dillinger, S.; Bögge, H.; Armatage, A.; Proust, A.; Bergholt, C.; Bergmann, U., *Angew. Chem. Int. Ed. Engl.* **1994**, 33, 849.).

{WO} units. Figure 1.6b is the structure of the anion $[Ln_6As_{12}W_{148}O_{524}(H_2O)_{36}]^{76-}$ [9], an example of more complex structure also built up by $\{AsW_9\}$ groups. 12 $\{AsW_9\}$ groups are linked by 4 $\{LnW_5\}$ groups and 20 {WO} units to form cyclic structure of about 4 nm in diameter.

1.3. Applications

Polyoxometalates have been found wide applications in many fields such as catalysis, medicine, magnetic properties, materials, photo- and electrochromism and nuclear waste treatment. The majority of the applications are found in the area of catalysis; about 70% of catalytic applications use the Keggin type heteropolyacids (HPA) and their salts.

Their popularity can be attributed to a large extent of the enormous volume of literature over several decades that describes their fundamental chemistry and to their commercial availability. HPAs have several advantages as catalysis that makes them economically and environmentally attractive. They are strong Brönsted acids (HPA>H_2SO_4, Zeolite, SiO_2-Al_2O_3). They have reversible redox properties and have the ability to activate O_2, H_2O_2, organic peroxides, etc. HPAs are thermally stable; highly soluble in polar solvents and transferable into hydrocarbons by changing counter ions. These properties render HPAs potentially as promising acid [10], redox [11], and bifunctional [12] catalysts in homogeneous as well as in heterogeneous or biphasic systems. In the last two decades, the broad utility of HPAs acid and oxidation catalysis has been demonstrated in a wide variety of synthetically useful selective transformations of organic substances. The

Industrial Processes Catalyzed by HPC			
Reaction	Catalyst	Typ	Start
CH_2=$CHCH_3$ + H_2O→$CH_3CH(OH)CH_3$	$H_4SiW_{12}O_{40}$	hom	1972
CH_2=$C(CH_3)CHO$ + O_2→CH_2=$C(CH_3)COOH$	Mo-V-P-HPA	het	1982
CH_2=$C(CH_3)_2$ + H_2O→ $(CH_3)_3COH$	$H_3PMo_{12}O_{40}$	hom	1984
nTHF + H_2O→$HO((CH_2)_4O)_nH$	$H_3PW_{12}O_{40}$	biph	1985
CH_3CH=$CHCH_3$ + H_2O→$CH_3CH(OH)CH_2CH_3$	$H_3PMo_{12}O_{40}$	hom	1989
CH_2=CH_2 + O_2→CH_3COOH	Pd-$H_4SiW_{12}O_{40}$	het	1997
CH_2=CH_2 + CH_3COOH→$CH_3CH_2O_2CCH_3$	$H_4SiW_{12}O_{40}/SiO_2$	het	2001

hom: homogeneous; het: heterogeneous gas-solid; biph: biphasic-liquid. (From Kozhevnikov, I. V., *Nato ASI, Polyoxometalate Molecular Science,* **2001**.)

table above [13] lists several industrial processes catalyzed by HPAs. Clearly, there is continuous growth of research activity in polyoxometalates catalysis.

Polyoxometalates provide excellent examples of magnetic clusters. Due to the large variety of well-characterized structures available in polyoxometalates chemistry, chemical control of the magnetic nuclearities is possible. Therefore, polyoxometalates are ideal candidates for studying the magnetic exchange interactions in clusters of increasing nuclearities and defined topologies at the molecular level [24].

Increasing attention is currently being paid to polyoxometalates in the domain of materials science due to their chemical, structural and electronic versatility. A focus in this respect is the exploration of organic-inorganic hybrid materials combining polyoxometalates and organic molecules and possessing a variety of interesting conducting, magnetic, electronic and optical properties. Until now, several synthetic methods have been adopted, including routine processes [14,15], hydrothermal reactions [17,16] and low thermal solid phase synthesis [18]. According to the role of organic ligands, polyoxometalate-based hybrids containing organic ligands can be divided into three types: (1) charge-compensating cations [19,20], (2) ligands bonded directly to the polyoxometalates skeletal framework [21], (3) ligands bonded to the heterometal site [16].

A recent development of polyoxometalates in material science deals with the use of soluble polyoxometalates as inorganic electron-accepting

moieties in new organic-inorganic charge transfer (CT) hybrid material based on organic π-electron donors such as substituted amides [22], or electron-rich substrates such as tetrathiafulvalenes (TTF), bis-(ethylenedithio)tetrathiafulvalene (BEDT-TTF or ET) [23] or decamethylferrocene ($FeCp^*_2$) [24]. The combination of these organic donors with polyoxometalates of various nuclearities, shapes, and charges has resulted in new types of magnetic, insulating, semiconducting, or even metallic CT salts.

Polyoxometalate-based hybrids have potential applications in many fields, but practical applications rely largely on the successful fabrication of polyoxometalates-based organic-inorganic films. Several main strategies have been used to prepare lamellar hybrids, including (1) doping polyoxometalates in electrically conductive polymers [25], (2) the Langmuir-Blodgett technique [26,27], (3) layer-by-layer self-assembly [28], and (4) electrochemical growth [29,30]. So far, the number of these hybrid materials has been rapidly growing due to their potential applications. However, the rational design and synthesis of polyoxometalates based materials with desired specific properties are still a challenge to be met.

Polyoxometalates also have potential application in medicine. Many polyoxometalates have been shown to be biologically active. For example, against Co-4 human colon cancer *in vivo*, $Na_5[IMo_6O_{24}]$ shows "effective" in the efficacy category compared with a "somewhat effective" rating for

ACNU or ADM (both are clinically approved agents). The SI (selectivity index, the bigger, the better) for $K_7[A\text{-}\alpha\text{-}GeNb_3W_9O_{40}]$ against RSV virus *in vitro* is more than 300 compared with less than 30 for Ribavirin (currently used as antiviral chemotherapeutic agents). The 'table 1' and 'table 2' in the review [31] by C. L. Hill list the biological behavior *in vitro* and *in vivo* for most of the polyoxometalates that have been investigated.

Polyoxometalates have two types of activities, antiviral activity and antitumoral activity. The mechanisms for these activities are still not clear, but research data up to date show that in spite of the size and charge, polyoxometalates can penetrate cell membranes and localize intracellularly. The reasons for biological activity may include ionic size and charge. For example, molecular mechanics studies suggest that $[(O_3POPO_3)_4W_{12}O_{36}]^{16-}$ inhibits HIV-1RT via docking at the DNA binding region of the enzyme through electrostatic interactions [32]. Redox properties (e.g., a single electron reduction/ oxidation cycle in isopolymolybdates may explain the antitumoral activity for this polyoxometalate [33]) and electron-transfer and reservoir properties (e.g., inhibition of biological electron transfer [34]) also may contribute to biological activities.

Another application of polyoxometalates is in radioactive waste remediation and that is mainly attributed to the lacunary Wells-Dawson polyoxometalates. This application will be discussed in the next section.

1.4. The Lacunary Wells-Dawson polyoxometalates containing Lanthanide

The monovacant lacunary Wells-Dawson polyoxometalates, [α-1-$P_2W_{17}O_{61}]^{10-}$ (denoted α-1 isomer) and [α-2-$P_2W_{17}O_{61}]^{10-}$ (denoted α-2 isomer), can be envisioned as the removal of a WO unit from "cap" or "belt" region of the plenary [α-$P_2W_{18}O_{62}]^{6-}$. Figure 1.7 shows the structures of the parent Well-Dawson structure and its two lacunary α-1

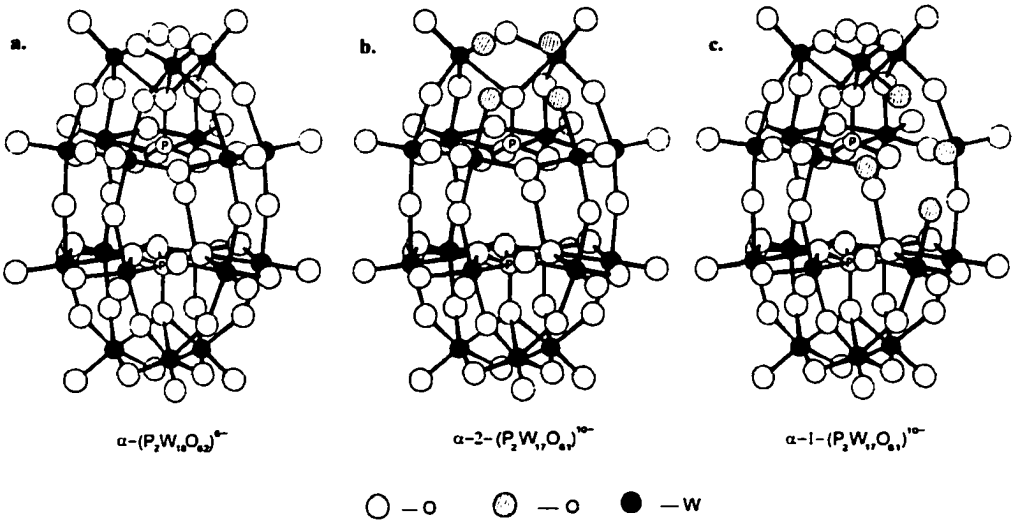

Figure 1.7. a: the [α-$P_2W_{18}O_{62}]^{6-}$ Wells-Dawson structure, b: the [α-2-$P_2W_{17}O_{61}]^{10-}$ isomer, c: the [α-1-$P_2W_{17}O_{61}]^{10-}$ isomers. The filled circles represent tungsten atoms. The open circles represent oxygen atoms, and the hatched circles represent oxygen atoms available for bonding to lanthanide ions.

and α-2 $[P_2W_{17}O_{61}]^{10-}$, the shaded oxygen atoms represent the four oxygen atoms available to bind to metal ions. The [α-1-$P_2W_{17}O_{61}]^{10-}$ possesses C_1 symmetry and [α-2-$P_2W_{17}O_{61}]^{10-}$ possesses C_s symmetry. Complexation of rare earth (RE) elements with these two lacunary

polyoxotungstates was discovered by Peacock and Weakley in 1971 [35]. The first RE complexes of $[P_2W_{17}O_{61}]^{10-}$ were prepared with what is now known as the α-2 isomer and had a 1:2 stoichiometry, $[RE^{n+}(\alpha\text{-}2\text{-}P_2W_{17}O_{61})_2]^{n-20}$. These complexes are of contemporary interest in stabilization of tetravalent Tb, Pr, Am, Cm and Cf ions. These valences are extremely unstable in other media.

The redox properties of rare earth elements are strongly affected by complexation with heteropolyanions, $PW_{11}O_{39}^{7-}$ and $[\alpha\text{-}2\text{-}P_2W_{17}O_{61}]^{10-}$. In fact, the $[P_2W_{17}O_{61}]^{10-}$ anion has been exploited as a valence-controlling complexant in solvent extraction techniques to separate trans-plutonium elements from Ln-elements [36,37]. The $[P_2W_{17}O_{61}]^{10-}$ anion stabilizes the otherwise reactive tetravalent oxidation states of americium, curium, berkelium, and californium [38-40]. We recently found that the tetravalent oxidation state of neptunium is stabilized by $[\alpha\text{-}2\text{-}P_2W_{17}O_{61}]^{10-}$ [41]. For the extraction of Ln(III) and An(III) ions with high-molecular-weight amines, $[P_2W_{17}O_{61}]^{10-}$ functions as a complexant [42-48]. The monovacant Wells-Dawson anion has also been tested in aqueous biphasic systems based on PEG—poly(ethylene glycol)—wherein it facilitates the transport of An(III) and An(IV) ions into the PEG-rich phase [49,50].

The technological prospects of polyoxometalates, in general, and of $[P_2W_{17}O_{61}]^{10-}$, in particular, for use in radioactive waste processing and remediation operations are due to, in part, the strength of their

interactions with Ln and An ions. The high charge-to-size ratio of Ln and An cations enhances their binding with $[P_2W_{17}O_{61}]^{10-}$. In addition to tight binding, selective Ln/An complexation occurs in the presence of other cations, including transition metals and Na^+, and other anions, including nitrate, which are often present in high concentrations in tank waste. The $[\alpha\text{-}2\text{-}P_2W_{17}O_{61}]^{10-}$ isomer is itself a robust ligand that can be prepared with a number of different counter cations [51]. For the most part, polyoxoanions are prepared by self-assembly, protonation and condensation reactions, and are relatively inexpensive compared to organic ligands often used for extraction processes. In some respects, the W-O framework structures shown in Figure 1.7 resemble discrete fragments of oxide mineral surfaces [52]. As testimony to their thermodynamic stability, polyoxoanions are presently used in commercial catalytic processes and the technology for bulk-quantity, high-yield syntheses is available today [53].

While the valence controlling aspects of $[\alpha\text{-}2\text{-}P_2W_{17}O_{61}]^{10-}$ and other heteropolymetalates and their practical utility in separations of actinides have been documented, the structural and solution chemistry on the molecular level is lacking. There is a dearth of metrical information about the coordination of RE ions in these otherwise well-characterized complexes of the α-1 and α-2 isomers of $[P_2W_{17}O_{61}]^{10-}$. No complete single-crystal X-ray diffraction structures have been determined before now because of difficulties in obtaining suitable-quality crystals. The sole

available structure determination, showing the tungsten framework only, was reported in 1979 for the 1:2 Ce(IV) complex $K_{16}[Ce(P_2W_{17}O_{61})_2]\cdot 50H_2O$ [54]. No Ce-O distances were reported because the O atoms were not located in the low-grade (R = 19%) structure determination. We and others have initiated such studies with lanthanides geared to providing understanding of the solid state and solution structures and chemistry of metal –heteropolyanion complexes [55-57]. Understanding the molecular level details concerning the structure, bonding and chemical properties of lanthanide/actinide ions bound to heteropolymetalates may allow improved design of these ligands as valence controlling complexants and their widespread use in practical solvent extraction techniques.

Therefore, in this study, we have (1) crystallized $[Ln(\alpha\text{-}2\text{-}P_2W_{17}O_{61})]^{17-}$ complexes and solved their structures by crystallography; (2) isolated and crystallized $[Ln(\alpha\text{-}2\text{-}P_2W_{17}O_{61})]^{7-}$ complexes, proved their structures by single crystal structure in solid state and by multinuclear NMR and fluorescence in solution state; (3) isolated the $[Ln(\alpha\text{-}1\text{-}P_2W_{17}O_{61})]^{7-}$ complexes, and proved their structures by single crystal structure; (4) isolated a new type of complex, $[Ln(\alpha\text{-}1\text{-}P_2W_{17}O_{61})_2]^{17-}$, and characterized the structure in solution; (5) identified ternary complexes of $[Ln(\alpha\text{-}1\text{-}P_2W_{17}O_{61})]^{7-}$ and provided data on their stability and (6) determined the formation constants for $[Ln(\alpha\text{-}1\text{-}P_2W_{17}O_{61})]^{7-}$, $[Ln(\alpha\text{-}2\text{-}$

$P_2W_{17}O_{61})]^{7-}$ and $[Ln(\alpha\text{-}2\text{-}P_2W_{17}O_{61})_2]^{17-}$ complexes by luminescence and multinuclear NMR techniques.

1.5. References:

1) Katsoulis, D. E., *Chem. Rev.* **1998**, 98, 359.

2) Sadakane, M.; Dickman, M. H.; Pope, M. T., *Angew. Chem. Int. Ed.* **2000**, 39(16), 2914.

3) Belai, N.; Sadakane, M.; Pope, M. T., *J. Am. Chem. Soc.* **2001**, 123(9), 2087.

4) Clegg, W.; Elsegood, M. R. J.; Errington, R. J.; Havelock, J., *J. Chem. Soc., Dalton Trans.* **1996**, 681-690.

5) Gouzerh, P.; Proust, A., *Chem. Rev.* **1998**, 98, 77.

6) Kwen, H.; Young, V. G., Jr.; Maatta, E. A., *Angew. Chem. Int. Ed. Engl.* **1999**, 38, 1145.

7) Müller, A.; Kögerler, P.; Kuhlmann, C., *Chem. Commun.* **1999**, 1347.

8) Jeannin, Y. J., *Cluster Sci.* **1992**, 3, 55.

9) Müller, A.; Plass, W.; Krichemeyer, E.; Dillinger, S.; Bögge, H.; Armatage, A.; Proust, A.; Bergholt, C.; Bergmann, U., *Angew. Chem. Int. Ed. Engl.* **1994**, 33, 849.

10) Misono, M.; Nojiri, N., *Appl. Catal.* **1990**, 64,1.

11) Nomiya, K.; Yanogibayashi, H.; Nozaki, C.; Kondoh, K.; Hiramatsu, E.; Shimizu, Y., *J. Mol. Catal. A* **1996**, 114, 181.

12) Shimizu, M.; Orita, H.; Hayakawa, T.; Takehira, T., *Tetrahedron Lett.* **1989**, 30, 471.

13) Kozhevnikov, I. V., *Nato ASI, Polyoxometalate Molecular Science,* **2001**.

14) Zhang, X.Y.; O'Connor, C. J.; Jameson, G. B., *Inorg. Chem.* **1996**, 35(1), 30.

15) Zhang, X.; Chen, Q.; Duncan, D. C., *Inorg. Chem.* **1997**, 36(20), 4381,

16) Hagrman, P. J.; Hagrman, D.; Zubieta, J., *Angew. Chem. Int. Ed.* **1999**, 38(18), 2638.

17) Nazar, L. F.; Koene, B. E.; Britten, J. F., *Chem. Mater.***1996**, 8(2), 327.

18) You, W.; Wang, E., *Inorg. Chem.*, **2001**, in press.

19) Nazar, L. F.; Koene, B. E.; Britten, J. F., *Chem. Mater.***1996**, 8(2), 327.

20) Koene, B. E.; Taylor, N. J.; Nazar, L. F., *Angew. Chem. Int. Ed.* **1999**, 38(19), 2888.

21) Soghomonian, V.; Chen, Q.; Haushalter, R. C.; Zubieta, J., *Angew. Chem. Int. Ed. Engl.* **1995**, 34(2), 223.

22) Niu, J. Y.; You, X. Z.; Duan, C. Y., *Inorg. Chem.* **1996**, 35(14), 4211.

23) Clemente-Juan, J. M.; Coronado, E.; Galán-Mascarós, J. R.; Gómez-Garciá, C. J., *Inorg. Chem.* **1999**, 38, 55.

24) Golhen, S.; Ouahab, L.; Grandjean, D., *Inorg. Chem.* **1998**, 37(7), 1499.

25) Lira-Cantu, M.; Gómez-Romero, P., *In Recent Research Developments in Physical Chemistry*; S. G. Pandalai, Ed.; *Transword Network*, **1997**.

26) Clemente-Leon, M.; Agricole, B.; Mingotaud, C., *Langmuir*, **1997**, 13(8), 2340.

27) Volkmer, D.; Du Chesne, A.; Kurth, D. G., *J. Am. Chem. Soc.* **2000**, 122(9), 1995.

28) Kurth, D. G.; Volkmer, D.; Ruttorf, M., *Chem. Mater.* **2000**, 12(10), 2829.

29) Cheng, L.; Niu, L.; Gong, J., *Chem. Mater.* **1999**, 11(6), 1465.

30) Tang, Z.; Liu, S.; Wang, E., *Langmuir,* **2000**, 16(13), 5806.

31) Rhule, J. T.; Hill, C. L.; Judd, D. A., *Chem. Rev.* **1998**, 98, 327.

32) Sarafianos, S. G.; Kortz, V.; Pope, M. T.; Modak, M. J., *Biochem. J.* **1996**, 319, 619.

33) Yamase, T., *Mol. Eng.* **1993**, 3, 241.

34) Chottard, G.; Michelon, M.; Hervé, M., *Biochim, Biophys. Acta.* **1987**, 916, 402.

35) Peacock, R.D.; R. Weakley, T. J., *J. Chem. Soc. A.* **1971**, 11, 1836.

36) Madic, C.; Bourges, J.; Dozol, J. F., *AIP Conf. Proc,* **1995**, *346*, 628.

37) Kamoshida, M.; Fukasawa, T.; Kawamura, F., *J. Nucl. Sci. Technol.* **1998**, *35*, 185- 189.

38) Saprykin, A. S.; Shilov, V. P.; Spitsyn, V. I.; Krot, N. N., *Doklady Chem., Engl. Trans* **1976**, *226*, 114-116.

39) Kosyakov, V. N.; Timofeev, G. A.; Erin, E. A.; Andreev, V. I.; Kopytov, V. V.; Simakin, G. A., *Soviet Radiochem., Engl. Transl.* **1977**, *19*, 418.

40) Erine, E. A.; Baranov, A. A.; Yu, V. A.; Chistyakov, V. M.; Timofeev, G. A., *J. Alloys Compd.* **1998**, *27*, 782.

41) Antonio, M. R.; Williams, C.; Solderholm, L.; Francesconi, L. C. *Chemical & Engineering News* **2001**, *Jan 14*, 48.

42) Milyukova, M. S.; Varezhkina, N. S.; Myasoedov, B. F. *J. Radioanal. Nucl. Chem., Letters* **1986**, *105*, 249-256.

43) Milyukova, M. S.; Varezhkina, N. S.; Myasoedov, B. F. *J. Radioanal. Nucl. Chem., Articles* **1988**, *121*, 403-408.

44) Milyukova, M. S.; Varezhkina, N. S.; Myasoedov, B. F. *Soviet Radiochem., Engl. Transl.* **1990**, *32*, 361-367.

45) Malikov, D. A.; Milyukova, M. S.; Myasoedov, B. F. *Soviet Radiochem., Engl. Transl.* **1989**, *31*, 425-430.

46) Malikov, D. A.; Milyukova, M. S.; Kuzovkina, E. V.; Myasoedov, B. F. *Soviet Radiochem., Engl. Transl.* **1993**, *35*, 465-471.

47) Myasoedov, B. F.; Milyukova, M. S.; Malikov, D. A. *Solv. Extr. Ion Exchan.* **1984**, *2*, 61-77.

48) Varezhkina, N. S.; Milyukova, M. S.; Myasoedov, B. F. *J. Radioanal. Nucl. Chem., Letters* **1989**, *135*, 67-76.

49) Molochnikova, N. P.; Frenkel, V. Y.; Myasoedov, B. F. *J. Radioanal. Nucl. Chem., Articles* **1988**, *121*, 409-413.

50) Molochnikova, N. P.; Frenkel, V. Y.; Myasoedov, B. F. *Sov. Radiochem., Engl. Transl.* **1989**, *31*, 322-326.

51) Bartis, J.; Dankova, M.; Blumenstein, M.; Francesconi, L. C. *Journal of Alloys and Compunds* **1997**, *249*, 56-68.

52) Mizuno, N. *Trends Phys. Chem* **1994**, *4*, 349-362.

53) Mizuno, N.; Misono, M. *Chem. Rev.* **1998**, 199-217.

54) Molchanov, V. N.; Kazanskii, L. P.; Torchenkova, E. A.; Simonov, V. I. *Sov. Phys. Crystallogr., Engl. Transl.* **1979**, *24*, 96-97.

55) Bartis, J.; Dankova, M.; Lessmann, J. J.; Luo, Q. H.; Horrocks, W. D., Jr.; Francesconi, L. C. *Inorganic Chemistry* **1999**, *38*, 1042-1053.

56) Luo, Q.H.; Howell, R. C.; Dankova, M.; Bartis, J.; Williams, C. W.; Horrocks, J., W.DeW.; Young, J., V.G.; Rheingold, A. L.; Francesconi, L. C.; Antonio, M. R. *Inorg. Chem.* **2001**, 40(8), 1894-1901.

57) Sadakane, M.; Dickman, M. H.; Pope, M. T. *Angew. Chem. Int. Ed.* **2000**, *39*, 2914-2916.

Chapter 2

Characterization of $[Ln(\alpha\text{-}2\text{-}P_2W_{17}O_{61})_2]^{17-}$ by X-ray Crystallography

Lanthanide (Ln) ions react with $(\alpha\text{-}2\text{-}P_2W_{17}O_{61})^{10-}$ to form two complexes, $[Ln(\alpha\text{-}2\text{-}P_2W_{17}O_{61})]^{7-}$ and $[Ln(\alpha\text{-}2\text{-}P_2W_{17}O_{61})_2]^{17-}$, denoted Ln α-2 1:1 and 1:2, respectively. The lanthanide α-2 1:2 complexes have been prepared and their solution structure and chemistry have been studied by ^{31}P and ^{183}W NMR spectroscopy [1]. A crystal structure of this species, prepared by Dr. Judit Bartis [16] was solved in 1997, but the data was not publishable. After thoroughly studying crystallization of these complexes, I have crystallized three different lanthanides α-2 1:2 complexes: $K_{17}[Eu(\alpha\text{-}2\text{-}P_2W_{17}O_{61})_2]$, $K_{17}[Gd(\alpha\text{-}2\text{-}P_2W_{17}O_{61})_2]$ and $K_{17}[Lu(\alpha\text{-}2\text{-}P_2W_{17}O_{61})_2]$. The structure of $K_{17}[Lu(\alpha\text{-}2\text{-}P_2W_{17}O_{61})_2]$ has been published [2]. Here I provide all the information of crystallization and refinement of these three structures, the discussion of structure of $K_{17}[Eu(\alpha\text{-}2\text{-}P_2W_{17}O_{61})_2]$ and the comparison of the three structures.

2.1. Experimental

2.1.1. Synthesis of $K_{17}[Gd(\alpha\text{-}2\text{-}P_2W_{17}O_{61})_2]$

$K_{10}[\alpha\text{-}2\text{-}P_2W_{17}O_{61}]$(2.0 g) was dissolved in 30 mL of water at ca. 40°C. After stirring for about 15 minutes the solution was clear. 0.30 mL of 1M $GdCl_3$ aqueous solution was added dropwise; the solution was stirred for a few minutes followed by potassium chloride (2.4 g). The

white precipitate was separated by filtration and dried under air suction for 2 hours.

2.1.2. Crystallization

Crystallization was set up using 4 mL vials as the inner vial and 25 mL vial as the outer vial. Solid sample dissolved in 1mL of solvent in a 4mL vial at room temperature to obtain a clear solution. Saturated KCl was added dropwise, the solution remained clear. This vial was then placed into a larger vial (25mL). The outside solvent was added and the samples were left at different temperatures for several days. Different

Table 2.1. Crystallization conditions have been tried for Ln α-1 and Ln α-2 complexes

Complex Concentration: 2mM-10mM
Solvent: H_2O, Lithium acetate (0.5 M), sodium acetate (0.5M)
Solvent pH: 2.5-5.5
Temperature: room temperature, 4°C
Outside solvent: ethanol, 0.5M-4.5M KCl, sodium acetate solution.

conditions have been tried for crystallization of Ln α-1 and Ln α-2 complexes. The conditions are listed in table 2.1.

Crystals of $K_{17}[Lu(\alpha\text{-}2\text{-}P_2W_{17}O_{61})_2]$, $K_{17}[Eu(\alpha\text{-}2\text{-}P_2W_{17}O_{61})_2]$ and $K_{17}[Gd(\alpha\text{-}2\text{-}P_2W_{17}O_{61})_2]$ for crystallography were obtained using the following conditions:

The solid sample was dissolved in water to get 0.8 mL of saturated solution in 2 mL vial. 0.2 mL of water and 2 drops (1 mL syringe) of

saturated KCl was added. The cap was covered loosely; the vials remained at room temperature for about 2 days. Colorless crystals were formed.

2.1.3. Crystallography

Crystallography data was collected by Dr. R. Howell using the diffractometor at the University of Delaware. The structures were solved by Dr. Howell and myself.

A single crystal of $K_{17}[Ln(\alpha\text{-}2\text{-}P_2W_{17}O_{61})_2]$ was attached to a glass fiber and mounted on a Siemens SMART system for data collection at 173(2) K with Mo Kα radiation (0.71073 Å). The raw data were corrected for Lorentz-polarization and absorption effects (face-indexed numerical correction) using SAINT/SADABS. The structure was solved by direct methods. Tungsten, lanthanide, and potassium atoms were refined anisotropically by full matrix least squares on the F^2 data (SHELXTL-Plus V5.0). All other atoms were not refined anisotropically due to a low data/parameters ratio and absorption effects. No hydrogen atoms were included. The resulting structure was triclinic and of the P1 bar space group. The data were further subjected to an empirical absorption correction by means of the program DIFABS [3]; the refinement continued after this correction was applied. The largest residual peaks are located close to the metal atoms in a final difference map. Large residual peaks in the final difference map are a common problem

encountered in the solution and refinement of polyoxotungstate structures [4-9].

We have obtained Ln α-2 1:2 complex crystal structures of three analogs, $[Lu(\alpha\text{-}2\text{-}P_2W_{17}O_{61})_2]^{17-}$ [2], $[Eu(\alpha\text{-}2\text{-}P_2W_{17}O_{61})_2]^{17-}$ and $[Gd(\alpha\text{-}2\text{-}P_2W_{17}O_{61})_2]^{17-}$. The details of data collection and refinement are contained in table 2.2 for $K_{17}[Eu(\alpha\text{-}2\text{-}P_2W_{17}O_{61})_2]$, table 2.3 for $K_{17}[Lu(\alpha\text{-}2\text{-}P_2W_{17}O_{61})_2]$, table 2.4 for $K_{17}[Gd(\alpha\text{-}2\text{-}P_2W_{17}O_{61})_2]$.

Table 2.2. Crystal data, data collection, and solution and refinement for $K_{17}[Eu(\alpha\text{-}2\text{-}P_2W_{17}O_{61})_2]$.

Crystal Data	
Empirical formula	$K_{16}EuO_{164}P_4W_{34}$
Crystal Habit, color	Plate, Colorless
Crystal system	Triclinic
Space group	P-1
Unit cell dimensions	a = 14.408 (2) Å α =95.079 (3)°
	b = 22.420 (4) Å β =102.148 (3)°
	c = 24.562 (4) Å γ =100.591 (3)°
Volume	7557 (2) Å^3
Z	2
Formula weight	9776.23
Density (calculated)	4.327 mg/m^3
Absorption coefficient	26.771 mm^{-1}
F (000)	8648
Data Collection	
Diffractometer	Bruker SMART, CCD area detector
Wavelength	0.71073 Å
Temperature	173(2) K
θ range for data collection	1.18 to 25.16°
Index ranges	$-17 \le h \le 16$, $-26 \le k \le 26$, $0 \le l \le 29$
Reflections collected/unique	26841 / 26841 (R_{int} = 0.0000)
Completeness to θ=25.16	99.0%
Solution and Refinement	
System used	SHELXTL-V5.054
Solution	Direct methods
Refinement method	Full-matrix least-squares on F^2
Absorption correction	SADABS (Sheldrick, 1996)
Data / restraints / parameters	26841 / 0 / 1215
Final R indices (I>2σ(I))	R1 = 0.0846, wR2 = 0.2162
R indices (all data)	R1 = 0.1385, wR2 = 0.2510
Goodness-of-fit on F^2	1.354
Largest diff. Peak and hole	4.649 and -5.643 eÅ^{-3}

Table 2.3. Crystal data, data collection, and solution and refinement for $K_{17}[Lu(\alpha\text{-}2\text{-}P_2W_{17}O_{61})_2]$.

Crystal Data		
Empirical formula	$K_{17}LuO_{176}P_4W_{34}$	
Crystal Habit, color	Plate, Colorless	
Crystal size	0.2×0.2×0.2 mm	
Crystal system	Triclinic	
Space group	P-1	
Unit cell dimensions	a = 14.4722 (6) Å	α =95.103 (2)°
	b = 22.3719 (8) Å	β=102.618 (2)°
	c = 24.4501 (9) Å	γ =99.954 (3)°
Volume	7542.3 (5) Å^3	
Z	2	
Formula weight	10030.45	
Density (calculated)	4.417 mg/m^3	
Absorption coefficient	27.101 mm^{-1}	
F (000)	8756	
Data Collection		
Diffractometer	Bruker SMART, CCD area detector	
Wavelength	0.71073 Å	
Temperature	173(2) K	
θ range for data collection	1.18 to 28.31°	
Index ranges	$-19 \le h \le 18$, $-29 \le k \le 28$, $0 \le l \le 32$	
Reflections collected/unique	34303/ 29785 (R_{int} =>2sigma(I))	
Completeness to θ=28.31	99.0%	
Solution and Refinement		
System used	SHELXTL-V5.054	
Solution	Direct methods	
Refinement method	Full-matrix least-squares on F^2	
Absorption correction	SADABS (Sheldrick, 1996)	
Data / restraints / parameters	34303/ 0 / 1199	
Final R indices (I>2σ(I))	R1 = 0.0860, wR2 = 0.2303	
R indices (all data)	R1 = 0.0964, wR2 = 0.2424	
Goodness-of-fit on F^2	1.063	
Largest diff. Peak and hole	7.575 and -6.735 eÅ^{-3}	

Table 2.4. Crystal data, data collection, and solution and refinement for $K_{17}[Gd(\alpha\text{-}2\text{-}P_2W_{17}O_{61})_2]$.

Crystal Data		
Empirical formula	$K_{16}GdO_{150}P_4W_{34}$	
Crystal Habit, color	Plate, Colorless	
Crystal system	Triclinic	
Space group	P-1	
Unit cell dimensions	a = 14.5105 (4) Å	α =95.373 (2)°
	b = 22.4097 (6) Å	β=102.533 (2)°
	c = 24.6183 (7) Å	γ =100.227 (2)°
Volume	7617 (2) Å^3	
Z	2	
Formula weight	9557.28	
Density (calculated)	4.167 mg/m^3	
Absorption coefficient	26.572 mm^{-1}	
F (000)	8288	
Data Collection		
Diffractometer	Bruker SMART, CCD area detector	
Wavelength	0.71073 Å	
Temperature	173(2) K	
θ range for data collection	1.18 to 28.31°	
Index ranges	$-19 \le h \le 19$, $-30 \le k \le 29$, $-31 \le l \le 32$	
Reflections collected/unique	35688 /35688 (R_{int} = 0.0000)	
Completeness to θ=28.31	99.0%	
Solution and Refinement		
System used	SHELXTL-V5.054	
Solution	Direct methods	
Refinement method	Full-matrix least-squares on F^2	
Absorption correction	SADABS (Sheldrick, 1996)	
Data / restraints / parameters	35688 / 0 / 846	
Final R indices (I>2σ(I))	R1 = 0.0940, wR2 = 0.2162	
R indices (all data)	R1 = 0.1491, wR2 = 0.2540	
Goodness-of-fit on F^2	1.320	
Largest diff. Peak and hole	13.35 and -15.14 eÅ^{-3}	

2.2. Results and Discussions

We used methods discussed in the experimental section to crystallize three complexes, $[Eu(\alpha\text{-}2\text{-}P_2W_{17}O_{61})_2]^{17-}$, $[Gd(\alpha\text{-}2\text{-}P_2W_{17}O_{61})_2]^{17-}$ and $[Lu(\alpha\text{-}2\text{-}P_2W_{17}O_{61})_2]^{17-}$. Selected bond distances are given in table 2.5, table 2.6 and table 2.7, respectively. These are the first complete structures of lanthanide $[\alpha\text{-}2\text{-}P_2W_{17}O_{61}]^{10-}$ 1:2 complexes. One of the structures, $[Eu(\alpha\text{-}2\text{-}P_2W_{17}O_{61})_2]^{17-}$ is shown in Figure 2.1. It demonstrates that one Eu(III) ion substitutes for two $[WO]^{4+}$ units in the "cap" regions of two $[\alpha\text{-}2\text{-}P_2W_{17}O_{61}]^{10-}$ unit. The Eu(III) ion is in a square antiprismatic coordination environment with 8 oxygen atoms: 4 from each of the two $[\alpha\text{-}2\text{-}P_2W_{17}O_{61}]^{10-}$ ligands. Unlike the 1:1 complex which is discussed in Chapter 3, no water molecules are bound to the Eu(III) ion in this molecule, consistent with the results of fluorescence. The two polyoxometalate "lobes" are disposed in a *syn* fashion. This structure is similar to the partial structure of $[Ce^{4+}(\alpha\text{-}2\text{-}P_2W_{17}O_{61})_2]^{16-}$ [10]. The tungsten-oxygen and phosphate bonds and angles of the two polyoxoanion ligands are consistent with the structure of $[\alpha\text{-}2\text{-}P_2W_{17}O_{61}]^{10-}$ and similar complexes [2,11,12]. The molecule has C_2 point group symmetry, consistent with ^{31}P and ^{183}W solution NMR spectroscopic results [13].

We have obtained three crystal structures of different lanthanides for α-2 1:2 complexes: Eu, Gd and Lu. Therefore it is possible for us to

Table 2.5. Selected bond length (Å) for $[Eu(\alpha\text{-}2\text{-}P_2W_{17}O_{61})_2]^{17-}$ anion.

W(1)—O(1)	1.778(2)	W(4)—O(9)	1.807(3)
W(1)—O(5)	2.114(2)	W(4)—O(13)	2.411(3)
W(1)—O(6)	1.926(3)	W(4)—O(18)	1.691(2)
W(1)—O(7)	1.884(3)	W(4)—O(22)	1.893(1)
W(1)—O(10)	1.715(2)	W(4)—O(23)	1.833(2)
W(1)—O(12)	2.279(2)	W(4)—O(29)	1.962(4)
W(17)—O(53)	1.798(4)	W(10)—O(29)	1.833(3)
W(17)—O(54)	1.823(3)	W(10)—O(34)	2.363(4)
W(17)—O(37)	2.323(3)	W(10)—O(39)	1.698(2)
W(17)—O(58)	1.690(1)	W(10)—O(44)	1.867(3)
W(17)—O(60)	2.035(3)	W(10)—O(45)	1.865(3)
W(17)—O(61)	2.006(4)	W(10)—O(51)	1.929(2)
W(6)—O(3')	1.783(3)	W(6)—O(24)	1.949(3)
W(6)—O(14)	2.313(3)	W(6)—O(25)	1.897(3)
W(6)—O(19)	1.727(3)	W(6) —O(31)	2.094(2)
Eu1 ----O(1)	2.372(3)	Eu1 ----O(2)	2.366(3)
Eu1 ----O(3)	2.347(4)	Eu1 ----O(4)	2.375(5)
Eu1 ----O(1')	2.353(4)	Eu1 ----O(2')	2.463(6)
Eu1 ----O(3')	2.406(3)	Eu1 ----O(4')	2.349(4)

compare these structures. In general, the terminal W=O bond average lengths are 1.72 Å. The bridging W-O bond average lengths are 1.92Å and the W-O (P) bond average lengths are 2.35 Å, which are consistent with reports of similar compounds [11,12,14]. Since the "cap" W=O is replaced by Ln, bond lengths of these W-O (W-O-Ln) are changed, bond lengths W-O(Ln) decrease from 1.92 Å to 1.76 Å, bond lengths W-O(W) increase from 1.92 Å to 2.09 Å. The bond lengths from Ln(III) to the

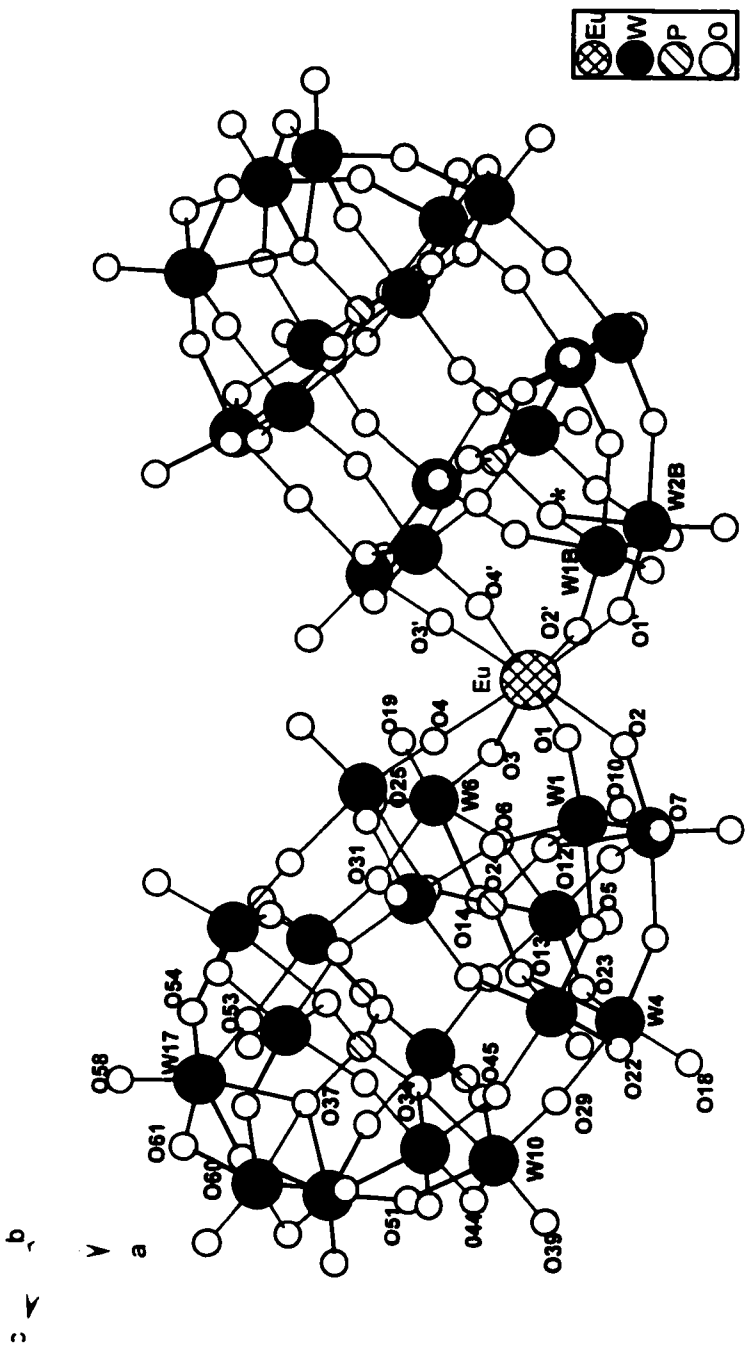

Figure 2.1. Crystal structure of $[Eu(\alpha\text{-}2\text{-}P_2W_{17}O_{61})_2]^{17-}$ anion in stick and ball representation.

oxygen atoms of the polyoxometalate framework are similar and average 2.38Å, 2.38Å and 2.32Å for Eu(III), Gd(III) and Lu(III) complexes.

The bond lengths of the atoms in the tungsten-oxygen framework of $[Ln(\alpha\text{-}2\text{-}P_2W_{17}O_{61})_2]^{17-}$ compare favorably with the those reported for the Wells-Dawson parent structure and the crystal structures of the $[\alpha\text{-}2\text{-}P_2W_{17}O_{61}]^{10-}$ isomer and the Co(III)(H_2O) adduct [11]. The pattern of edge shared WO_6 octahedra and corner shared WO_6 octahedra, observed in the Wells-Dawson ion and the lacunary $[\alpha\text{-}2\text{-}P_2W_{17}O_{61}]^{10-}$ isomer, are

Table 2.6. Selected bond length (Å) for $[Gd(\alpha\text{-}2\text{-}P_2W_{17}O_{61})_2]^{17-}$ anion.

W(21)—O(7)	2.271(2)	W(7)—O(47)	1.762(2)
W(21)—O(53)	1.742(2)	W(7)—O(91)	1.880(2)
W(21)—O(42)	2.061(1)	W(7)—O(119)	1.991(2)
W(21)—O(99)	1.913(2)	W(7)—O(141)	2.347(3)
W(21)—O(100)	1.922(1)	W(7)—O(30)	1.819(2)
W(21)—O(134)	1.777(2)	W(7)—O(17)	1.903(3)
W(19)—O(124)	1.804(3)	W(22)—O(121)	1.701(1)
W(19)—O(54)	1.760(3)	W(22)—O(21)	2.004(2)
W(19)—O(72)	1.983(2)	W(22)—O(43)	1.865(2)
W(19)—O(27)	2.064(2)	W(22)—O(73)	2.378(2)
W(19)—O(58)	2.368(4)	W(22)—O(8)	1.963(2)
W(19)—O(64)	1.926(1)	W(22)—O(143)	1.866(2)
W(9)—O(107)	1.734(2)	W(9)—O(30)	2.015(1)
W(9)—O(33)	1.890(2)	W(9)—O(12)	1.868(3)
W(9)—O(130)	1.797(1)	W(9) —O(85)	2.357(2)
Gd1 ----O(8)	2.432(2)	Gd1 ----O(111)	2.360(2)
Gd1 ----O(71)	2.403(2)	Gd1 ----O(23)	2.380(3)
Gd1 ----O(54)	2.320(2)	Gd1 ----O(108)	2.332(2)
Gd1 ----O(26)	2.383(2)	Gd1 ----O(134)	2.433(4)

retained in these structures. Both of the cap regions show edge shared octahedral while the belt regions show the alternating pattern of corner and edge shared octahedral. The introduction of the Ln(III) into one of the caps disrupts the pattern of edge and corner sharing as the Ln is connected via a corner shared octahedron. Overall, the Ln(III) introduces a relatively minor perturbation into the parent Wells-Dawson framework.

Table 2.7. Selected bond length (Å) for $[Lu(\alpha\text{-}2\text{-}P_2W_{17}O_{61})_2]^{17-}$ anion.

W(1B)—O(1B)	1.762(2)	W(5B)—O(10B)	1.754(2)
W(1B)—O(6B)	1.915(2)	W(5B)—O(13B)	1.973(3)
W(1B)—O(4B)	1.740(3)	W(5B)—O(14B)	1.898(2)
W(1B)—O(3B)	1.935(2)	W(5B)—O(20B)	1.734(3)
W(1B)—O(7B)	2.088(1)	W(5B)—O(27B)	2.134(2)
W(1B)—O(54B)	2.288(3)	W(5B)—O(56B)	2.360(4)
W(3B)—O(18B)	1.737(2)	W(9B)—O(36B)	1.683(2)
W(3B)—O(8B)	1.835(1)	W(9B)—O(25B)	1.820(2)
W(3B)—O(12B)	1.883(4)	W(9B)—O(30B)	1.897(3)
W(3B)—O(17B)	1.947(2)	W(9B)—O(35B)	1.944(2)
W(3B)—O(25B)	2.020(1)	W(9B)—O(42B)	2.005(2)
W(3B)—O(55B)	2.333(3)	W(9B)—O(58B)	2.356(3)
W(17B)—O(53B)	1.726(2)	W(17B)—O(50B)	1.967(3)
W(17B)—O(44B)	1.856(2)	W(17B)—O(45B)	1.834(2)
W(17B)—O(49B)	1.963(2)	W(17B) —O(61B)	2.361(3)
Lu1—O(1B)	2.388(4)	Lu1—O(2B)	2.314(3)
Lu1—O(10B)	2.249(3)	Lu1—O(11B)	2.349(2)
Lu1—O(1A)	2.321(2)	Lu1—O(2A)	2.326(2)
Lu1—O(11A)	2.272(3)	Lu1—O(10A)	2.325(4)

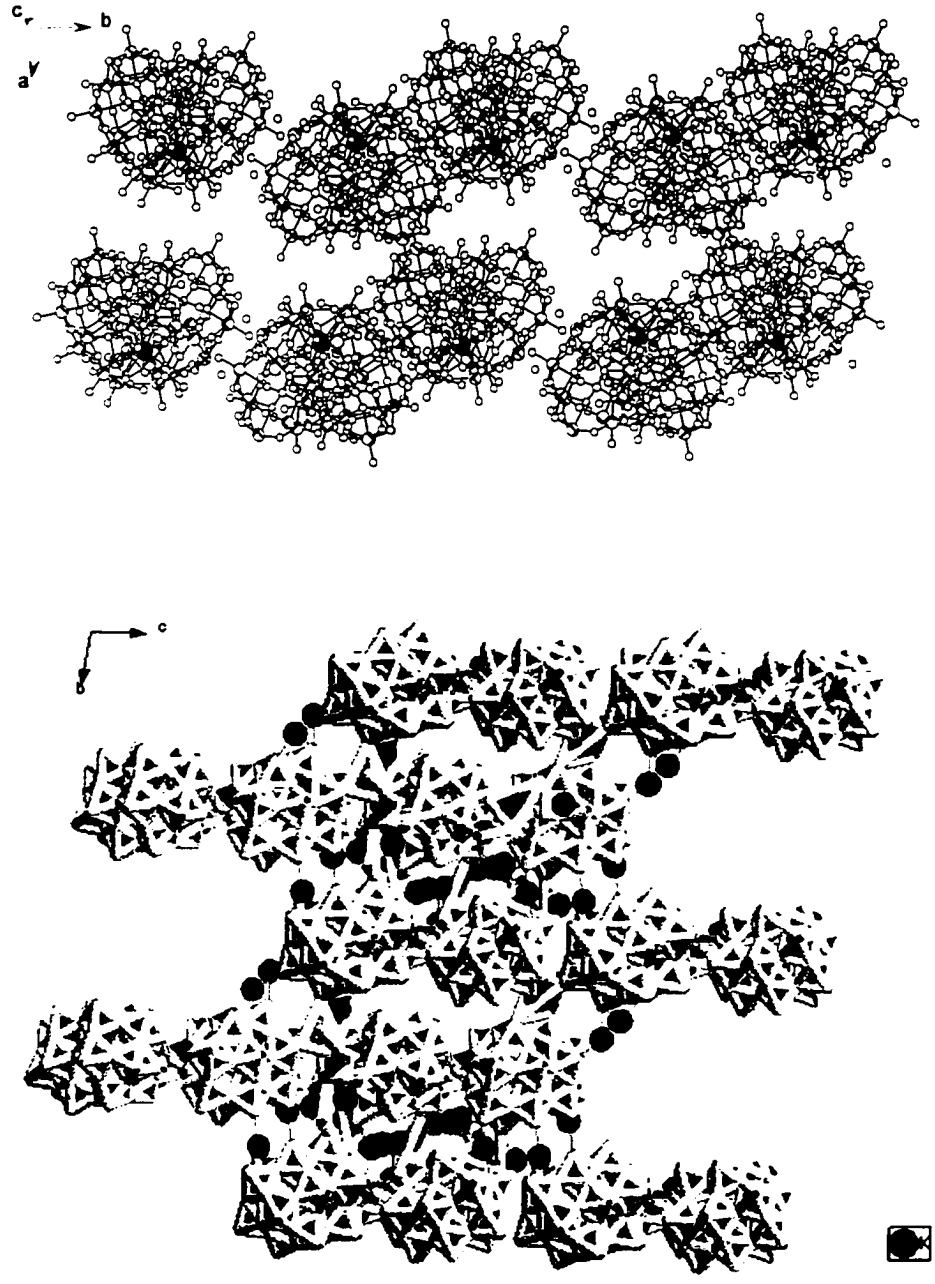

Figure 2.2. Packing diagrams of $[Eu(\alpha\text{-}2\text{-}P_2W_{17}O_{61})_2]^{17-}$. Upper: the ball and stick representation. Bottom: the polyhedral representation.

The ionic radii of these three lanthanides are 1.15 Å (Eu), 1.14 Å (Gd) and 1.05 Å (Lu) [10]. The average Ln-O bond lengths of these three Ln ions are 2.379(4) Å (Eu), 2.380(2) Å (Gd) and 2.318(3) Å (Lu). We can see that the radii of Eu and Gd are almost the same (1.14-1.15 Å) and their Ln-O bond length are similar (2.38 Å). The ionic radius of Lu is smaller than that of Gd and Eu, the Ln-O bond length is smaller also. Ionic radius of W(VI) (coordination number 6) is 0.68 Å [10], since ionic radius of Lu(III) is close to that of W(VI), Lu(III) can bind to oxygen atoms in the 'defect' cavity deeply. The binding of these two $[\alpha\text{-}2\text{-}P_2W_{17}O_{61}]^{10-}$ units to lanthanides is not affected by steric hindrance of these two "lobes" because the 'defect' place is in the "cap" region.

Figure 2.2 shows the packing diagrams of $[Eu(\alpha\text{-}2\text{-}P_2W_{17}O_{61})_2]^{17-}$ anion. From the upper picture, we can see that the molecules next to each other are like butterflies pointing in different directions to form a more compact structure. In the bottom picture, there is a big void space between molecules, which can be filled with different kinds of atoms and molecules, e.g., here the K atoms as counter ion are distributed among the channels; this opens a door for further research on guest inclusion properties.

2.3. Conclusion

Three lanthanide (Lu, Eu and Gd) α-2 1:2 complexes have been crystallized and their structures solved by X-ray crystallography. The structures compare favorably with the Wells-Dawson parent structure and the crystal structures of the $[\alpha\text{-}2\text{-}P_2W_{17}O_{61}]^{10-}$ isomer and the Co(III)(H_2O) adduct. The molecule structure is in good agreement with solution structure characterization. The molecule has C_2 point group symmetry, which is consistent with ^{31}P and ^{183}W solution NMR spectroscopic results [1]. No water molecules are bound to Eu(III) ion which is consistent with the results of fluorescence (Chapter 3).

2.4. References:

1) Bartis, J.; Sukal, S.; Dankova, M.; Kraft, E.; Kronzon, R.; Blumenstein, M.; Francesconi, L. C. *J. Chem. Soc., Dalton Trans.* **1997**, 1937.

2) Luo, Q. H.; Howell, R. C.; Dankova, M.; Bartis, J.; Williams, C. W.; Horrocks, J., W.DeW.; Young, J., V.G.; Rheingold, A. L.; Francesconi, L. C.; Antonio, M. R. *Inorg. Chem.* **2001**, 40(8), 1894-1901.

3) Walker, N.; Stuart, D. *Acta Cryst.* **1983**, *A39*, 158-166.

4) Casan-Pastor, N.; Gomez-Romero, P.; Jameson, G. B.; Baker, L. C. W. *J. Am. Chem. Soc.* **1991**, *113*, 5658-5663.

5) Ortega, F.; Pope, M. T.; Evans, J., H.G. *Inorg. Chem.* **1997**, *36*, 2166-2169.

6) Sazani, G.; Dickman, M. H.; Pope, M. T. *Inorg. Chem.* **2000**, *39*, 939-943.

7) Wasserman, K.; Lunck, H. J.; Palm, R.; Fuchs, J.; Steinfeldt, N.; Pope, M. T. *Inorg. Chem.* **1996**, *35*(11), 3273-3279.

8) Xin, F.; Pope, M. F. *Inorg. Chem.* **1996**, *35*, 5693-5695.

9) Zhang, X. Y.; O'Connor, C. J.; Jameson, G. B.; Pope, M. T. *Inorg. Chem.* **1996**, *35*, 30-34.

10) Molchanov, V. N.; Kazanskii, L. P.; Torchenkova, E. A.; Simonov, V. I. *Sov. Phys. Crystallogr., Engl. Transl.* **1979**, *24*, 96-97.

11) Weakley, T. J. R. *Polyhedron*, **1987**, 6, 931.

12) Dawson, B. *Acta Cryst.* **1953**, 6, 113.

13) Bartis, J.; Dankova, M.; Blumenstein, M.; Francesconi, L. C. *J. Alloys Compds.* **1997**, 249, 56.

14) Luo, Q. H.; Howell, R. C.; Bartis, J.; Dankova, M.; Horrocks, W. DeW. Jr.; Rheingold, A. L.; Francesconi, L. C., *Inorg. Chem.* **2002**, accepted.

15) *Principles and Applications of Inorganic Geochemistry*, Gunter Faure, Macmillan, New York, **1991**.

16) Batis, J., *Doctoral Dissertation*, Chemistry Department of The City University of New York, **1997**.

Chapter 3

Characterization of $[Ln(\alpha\text{-}2\text{-}P_2W_{17}O_{61})]^{7-}$

Lanthanide (Ln) ions react with $(\alpha\text{-}2\text{-}P_2W_{17}O_{61})^{10-}$ to form two complexes, $[Ln(\alpha\text{-}2\text{-}P_2W_{17}O_{61})]^{7-}$ and $[Ln(\alpha\text{-}2\text{-}P_2W_{17}O_{61})_2]^{17-}$, denoted Ln α-2 1:1 and 1:2, respectively. The Ln α-2 1:2 complex has been discussed in Chapter 2. This Chapter will discuss in detail the characterization of Ln α-2 1:1 complex by fluorescence spectroscopy and ^{31}P, ^{183}W NMR spectroscopy in aqueous solution and by X-ray crystallography in the solid state. This work was submitted to *Inorganic Chemistry* and has been accepted.

3.1. Experiments

3.1.1. Synthesis of $K_7[Ln(\alpha\text{-}2\text{-}P_2W_{17}O_{61})]$ (Ln=La, Eu, Nd, Gd, Lu)

$K_{10}[\alpha\text{-}2\text{-}P_2W_{17}O_{61}]$(0.2 mmol) was dissolved in 15 mL of water at ca. 35°C. After stirring for about 15 minutes the solution was clear. 0.30 mL of 1M $LnCl_3$ (0.3 mmol) solution was added dropwise; the solution was stirred for a few minutes followed by addition of potassium chloride (0.7g). The white precipitate was separated by filtration and dried under air suction for 2 hours.

3.1.2. Crystallization of $[Ln(\alpha\text{-}2\text{-}P_2W_{17}O_{61})]^{7-}$ (Ln=Eu)

$K_7[Ln(\alpha\text{-}2\text{-}P_2W_{17}O_{61})]$ was dissolved in water to form 1 mL of saturated solution in 2 mL vial. 2 drops (from 1 mL syringe) of saturated

KCl was added. The solution remained clear. The vial was covered loosely and the vial remained at room temperature for ca. 2 days. Colorless crystals were formed.

3.1.3. Crystallography

X-ray crystallography was performed by Dr. Robertha C. Howell. Data was collected at the University of Delaware in Professor Arnold Rheingold's Laboratory.

A single crystal of $[Eu(\alpha\text{-}2\text{-}P_2W_{17}O_{61})]^{7-}$ was attached to a glass fiber and mounted on a Brüker Siemens diffractometer equipped with a SMART CCD detector and a graphite monochromator (K_α wavelength = 0.71073 Å) for data collection at 173(2)K. The raw data was corrected for Lorentz-polarization and absorption effects (face-indexed numerical correction) using SAINT/SADABS. The structure was solved using direct methods and standard difference map techniques, and was refined by full matrix least-squares procedures using SHELXTL. No hydrogen atoms were included. The data were further subjected to an empirical absorption correction by means of the program DIFABS [1]; the refinement continued after this correction was applied. The largest residual peaks are located close to the metal atoms in a final difference map. Large residual peaks in the final difference map are a common problem encountered in the solution and refinement of polyoxotungstate structures [2-7]. The details of data collection and refinement are

Table 3.1. Crystal data, data collection, and solution and refinement for $K_7[Eu(\alpha\text{-}2\text{-}P_2W_{17}O_{61})]$.

Crystal Data		
Empirical formula	$Cl_2K_{15}Eu_2O_{178}P_4W_{34}$	
Crystal Habit, color	Plate, Colorless	
Crystal size	0.2 x 0.2 x 0.3 mm	
Crystal system	Triclinic	
Space group	P-1	
Unit cell dimensions	a = 12.7214 (5) Å	α =71.550(3)°
	b = 14.7402 (7) Å	β=84.019(3)°
	c = 22.6724 (9) Å	γ =74.383(3)°
Volume	3883.2 (3) Å^3	
Z	1	
Formula weight	10184.10	
Density (calculated)	4.355 mg/m^3	
Absorption coefficient	26.466 mm^{-1}	
F (000)	4445	
Data Collection		
Diffractometer	Siemens SMART, CCD area detecter	
Wavelength	0.71073 Å	
Temperature	173(2) K	
θ range for data collection	1.50 to 28.54°	
Index ranges	$-15 \le h \le 16$, $-18 \le k \le 19$, $0 \le l \le 29$	
Reflections collected/unique	17930/17930 (R_{int} = 0.0000)	
Completeness to θ =28.54	90.7%	
Solution and Refinement		
System used	SHELXTL-V5.054	
Solution	Direct methods	
Refinement method	Full-matrix least-squares on F^2	
Absorption correction	SADABS (Sheldrick, 1996)	
Data / restraints / parameters	17930 / 0 / 605	
Final R indices (I>2σ(I))	R1 = 0.0520, wR2 = 0.1287	
R indices (all data)	R1 = 0.0679, wR2 = 0.1450	
Goodness-of-fit on F^2	1.098	
Largest diff. Peak and hole	4.156 and -4.274 eÅ^{-3}	

contained in table 3.1 for $K_7[Eu(\alpha\text{-}2\text{-}P_2W_{17}O_{61})]$.

3.1.4. NMR experiments

NMR spectra were performed on a Jeol GX-400 spectrometer. ^{31}P spectra at 161.8 MHz were acquired using either a 10 mm broad band probe or the broad band decoupler coil of a 5 mm inverse detection probe. ^{183}W spectra at 16.7 MHz were recorded utilizing a 10 mm low frequency broad band probe. Typical acquisition parameters for ^{31}P spectra included: spectral width: 10,000Hz; acquisition time: 0.8 s; pulse delay: 1s; pulse width: 15μsec (50 degree tip angle). From 200 to 500 scans were required. For ^{183}W spectra, typical conditions included: spectral width: 10,000Hz; acquisition time: 1.6 s; pulse delay: 0.5s; pulse width: 50 μsec (45 degree tip angle). From 1,000 to 30,000 scans were acquired. ^{31}P spectra were referenced to 85% H_3PO_4. ^{183}W spectra were referenced to 2.0 M Na_2WO_4. For ^{31}P and ^{183}W chemical shifts, the convention used is that the more negative chemical shifts denote up field resonance.

3.1.5. Fluorescence experiments

3.1.5.1. General

Luminescence excitation spectra and excited state lifetimes of Eu(III) were measured using the laser luminescence spectroscopic technique in the lab of Professor William DeW. Horrocks, Jr. of Penn State University [8-9]. A pulsed (10 Hz) Nd : YAG laser-pumped dye

laser (Continuum), with a mixture of Rhodamine 590 and 610 dyes, was used to excite the $^7F_0 \rightarrow {}^5D_0$ transition of Eu(III) in the 578-581 nm region; emission ($^5D_0 \rightarrow {}^7F_2$) was monitored at 614 nm. Titration of metal to ligand or ligand to metal was monitored by measurement of excitation photon flux needed by $[Eu(\alpha\text{-}2\text{-}P_2W_{17}O_{61})]^{7-}$ complex controlled the emission ($^5D_0 \rightarrow {}^7F_2$) at 614 nm. All measurements were carried out at 25±0.1 °C. The commercially available Peakfit program, which employs a nonlinear regression method, was used in the data analysis [10-11].

The concentration of the samples used for the measurements was in 0.1μM–500μM range. The potassium salt of $[\alpha\text{-}2\text{-}P_2W_{17}O_{61}]^{10-}$ was converted to the more soluble Li^+ salt using ion exchange at pH=4.7 [12]. For titration experiments, standardized $Li_{10}[\alpha\text{-}2\text{-}P_2W_{17}O_{61}]$(0.0122M, pH=4.7, 0.5M lithium acetate buffer) was diluted to 400μM (ligand-to-metal) and 200nM (metal-to-ligand) with D_2O. The standardization of the Li^+ salt of $[\alpha\text{-}2\text{-}P_2W_{17}O_{61}]^{10-}$ was accomplished by spectrophotometric titration with cobalt(III) [13]. Eu(III) was standardized by EDTA (standard solution from Aldrich) with arsenazo as indicator (5 drops of pyridine was added to sharpen the end point).

3.1.5.2. Titration

For metal–to-ligand titration, 2mL of standardized $Li_{10}[\alpha\text{-}2\text{-}P_2W_{17}O_{61}]$ solution (200nM) is placed into a 4mL quartz sample cell,

using volumetric pipette, a total of 0.96 nmol of $EuCl_3$ was added in 5 μL increments of a 8 μM $EuCl_3$ stock solution.

For ligand-to-metal titration, 2mL of $EuCl_3$ stock solution (10 μM) is placed into a 4mL quartz sample cell, using volumetric pipette, a total of 0.06 μmol of $Li_{10}[\alpha\text{-}2\text{-}P_2W_{17}O_{61}]$ was added in 5 μL increments of a 400 μM standardized $Li_{10}[\alpha\text{-}2\text{-}P_2W_{17}O_{61}]$ solution.

3.1.5.3. Excited State Lifetime Measurements

Excited-state lifetime measurements in H_2O and D_2O solution were used to obtain the number of water molecules coordinated to Eu(III) ion, using the method of Horrocks and Sudnick [10,29]. The 1:1 complex was prepared as described in the experimental section. The 1:2 complex was prepared following method, which was reported previously by our lab [12]. Samples where the lifetime was recorded in D_2O were recrystallized 3 times from D_2O.

3.2. Results and Discussions

3.2.1. Crystallographic Characterization of $[Eu(\alpha\text{-}2\text{-}P_2W_{17}O_{61})]^{7-}$

The Ln α-2 1:1 complexes, $[Ln(\alpha\text{-}2\text{-}P_2W_{17}O_{61})]^{7-}$, have been isolated and characterized by elemental analysis (table 3.2), ^{31}P NMR, ^{183}W NMR spectroscopy and fluorescence spectroscopy.

Table 3.2. Elemental Analysis Data for $K_7[Lu(\alpha\text{-}2\text{-}P_2W_{17}O_{61})]$ and $K_7[Eu(\alpha\text{-}2\text{-}P_2W_{17}O_{61})]$

$K_7LuP_2W_{17}O_{61} \cdot 16H_2O$			$K_{13}H(EuP_2W_{17}O_{61})_2 \cdot 2KCl \cdot 56H_2O$		
	Observed(%)	Calculated(%)		Observed(%)	Calculated(%)
K	5.50	5.58	K	5.67	5.70
P	1.18	1.26	P	1.32	1.20
W	62.04	63.78	W	61.20	60.70
Lu	3.06	3.57	Eu	3.10	2.95

Figure 3.1 shows the crystal structure of $[Eu(\alpha\text{-}2\text{-}P_2W_{17}O_{61})]^{7-}$ anion. The structure shows clearly that two identical $[Eu(H_2O)_3(\alpha\text{-}2\text{-}P_2W_{17}O_{61})]^{7-}$ moieties are connected through two Eu–O–W bonds, one from each polyoxometalate unit. An inversion center relates these two units. The Eu(III) ion is substituted for a $[WO]^{4+}$ unit in the "cap" region of the tungsten-oxygen framework of the parent Wells-Dawson ion. The point group of the dimeric molecule is C_i.

The Eu(III) is in a square antiprismatic coordination geometry, bound to four oxygen atoms of the tungsten oxygen framework, three

water molecules and to an oxygen atom of a terminal W=O of another $[Eu(H_2O)_3(\alpha\text{-}2\text{-}P_2W_{17}O_{61})]^{7-}$ moiety. The Eu(III) is not bound to an oxygen of a phosphate. Thus, the Eu(III) is displaced outward and away from the normal eighteenth position in the Wells-Dawson framework. This type of bonding has been seen in crystal structures of lanthanide derivatives of the α-monovacant Keggin ions [14] and $[Ln(III)W_{10}O_{36}]^{9-}$ [15,16]. In contrast, transition metal ions bond to the phosphate oxygen and to another "axial" ligand, such as a water molecule, to complete the octahedral coordination sphere, as seen in the Co derivative of the lacunary $(\alpha\text{-}2\text{-}P_2W_{17}O_{61})^{10-}$ species [17].

The bond lengths from Eu(III) to the oxygen atoms of the polyoxometalate framework are similar and average 2.369(3)Å. The average bond length of the Eu(III) to the three water molecules is 2.413(4)Å. The Eu -O (oxygen atom of a terminal W=O) bond length is 2.434(4), in the range of Eu-O (H_2O) bond distance. The bond length of 1.736 (4) Å for the terminal W=O bound to the Eu(III) is at the high end of the range typically found for terminal W=O bonds. Selected bond lengths are shown in table 3.3.

The bond lengths of the atoms in the tungsten-oxygen framework of $[Eu(H_2O)_3(\alpha\text{-}2\text{-}P_2W_{17}O_{61})]^{7-}$ compare favorably with the those reported for the Wells-Dawson parent structure and the crystal structures of the $[\alpha\text{-}2\text{-}P_2W_{17}O_{61}]^{10-}$ isomer and the Co(III)(H_2O) adduct [17]. The pattern of

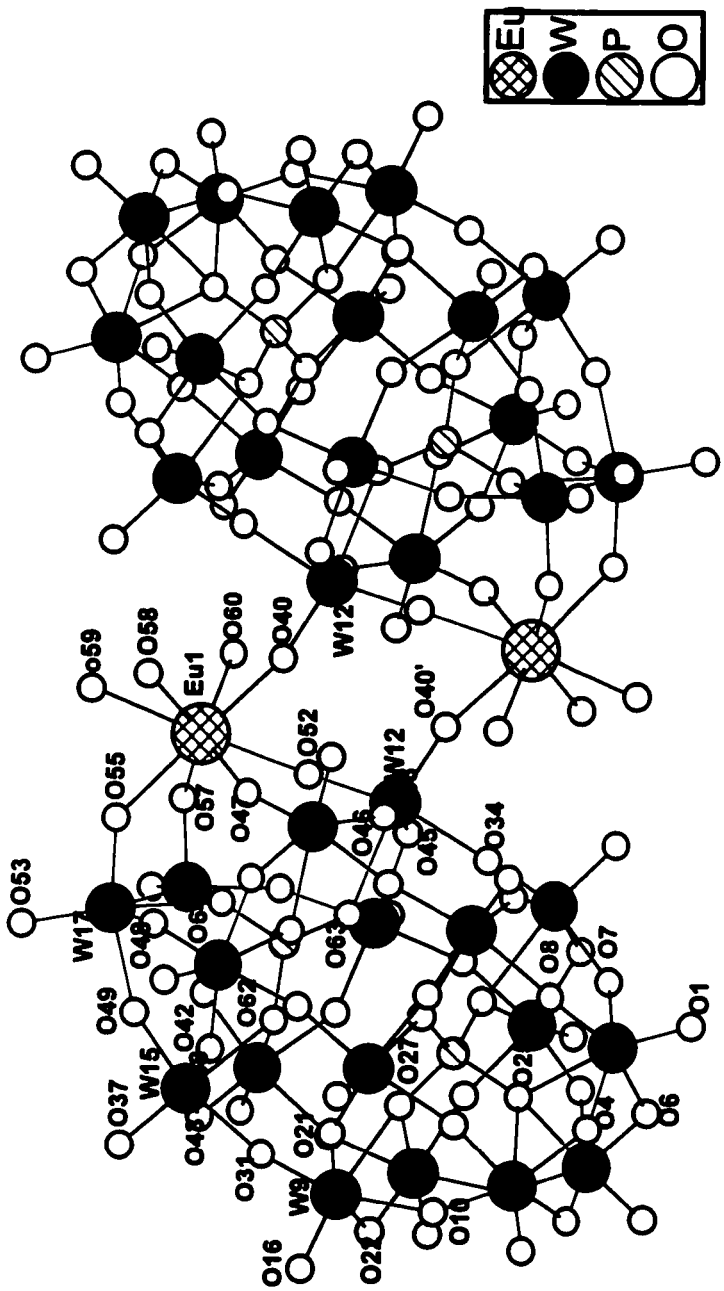

Figure 3.1. Crystal structure of $[Eu(H_2O)_3(\alpha\text{-}2\text{-}P_2W_{17}O_{61})]^{7-}$ anion in ball and stick representation.

edge shared WO_6 octahedra and corner shared WO_6 octahedra, observed in the Wells-Dawson ion and the lacunary $[\alpha\text{-}2\text{-}P_2W_{17}O_{61}]^{10-}$ isomer, are retained in this structure. Both of the cap regions show edge shared octahedra while the belt regions show the alternating pattern of corner and edge shared octahedra. The introduction of the $Eu(III)(H_2O)_3$ into one of the caps disrupts the pattern of edge and corner sharing as the Eu is connected via a corner shared octahedron. However, overall, the $Eu(III)(H_2O)_3$ unit introduces a relatively minor perturbation into the parent Wells-Dawson framework.

The structure of $[Eu(H_2O)_3(\alpha\text{-}2\text{-}P_2W_{17}O_{61})]^{7-}$ can be compared with the structures of the 1:1 La(III)/Ce(III): $SiW_{11}O_{39}^{8-}$ complexes, see below [14], and to the crystal structure of $[Lu(H_2O)_4(\alpha\text{-}1\text{-}P_2W_{17}O_{61})]^{7-}$, another 1:1 lanthanide polyoxometalate; in the latter case four water molecules are bound to the Lu(III) ion [18]. There is no bonding between the Lu(III) ion and a terminal oxygen atom of another $[Lu(\alpha\text{-}1\text{-}P_2W_{17}O_{61})]^{7-}$ moiety possibly due to the high basicity of the oxygen atoms at the α-1 defect site and steric incumbrance at the α-1 defect site [18]. Both the La(III) and Ce(III) cations in the 1:1 La/Ce: $\alpha\text{-}SiW_{11}O_{39}^{8-}$ complexes were reported recently [14]. In these complexes, the La(III) and Ce(III) are coordinated by nine oxygen atoms in a distorted monocapped square antiprism environment, involving bonding to the four oxygen atoms of the lacunary polyoxoanion; the cerium(III) analog is additionally

coordinated by two neighboring α-$SiW_{11}O_{39}^{8-}$ moieties and to three oxygen atoms of water molecules. Two types of La ions alternate in the lanthanum analog: one La(III) is coordinated to two α-$SiW_{11}O_{39}^{8-}$ moieties and three water molecules and the second La(III) is coordinated to one α-$SiW_{11}O_{39}^{8-}$ moiety and four water molecules. The bonding to two terminal oxygen atoms each from a different α-$SiW_{11}O_{39}^{8-}$ species allows these species to form polymeric chains connected by Ln-O-W bonding in the solid state.

Table 3.3. Selected bond length (Å) for $[Eu(H_2O)_3(\alpha\text{-}2\text{-}P_2W_{17}O_{61})]^{7-}$ anion.

W(1)—O(1)	1.711(2)	W(15)—O(37)	1.723(3)
W(1)—O(4)	1.955(4)	W(15)—O(42)	1.914(3)
W(1)—O(6)	1.946(2)	W(15)—O(43)	1.915(2)
W(1)—O(7)	1.846(2)	W(15)—O(49)	1.812(1)
W(1)—O(8)	1.843(2)	W(15)—O(31)	2.065(2)
W(1)—O(25)	2.366(3)	W(15)—O(62)	2.352(4)
W(9)—O(16)	1.711(4)	W(17)—O(49)	2.058(4)
W(9)—O(10)	1.990(2)	W(17)—O(53)	1.712(2)
W(9)—O(21)	1.899(3)	W(17)—O(55)	1.768(4)
W(9)—O(22)	1.939(1)	W(17)—O(48)	1.913(3)
W(9)—O(27)	2.344(5)	W(17)—O(64)	2.286(3)
W(9)—O(31)	1.826(2)	W(17)—O(56)	1.922(3)
W(12)—O(40')	1.736(4)	W(12)—O(45)	1.922(2)
W(12)—O(46)	1.911(3)	W(12)—O(34)	2.084(2)
W(12)—O(63)	2.337(6)	W(12) —O(52)	1.765(2)
EU1 ----O(58)	2.369(1)	EU1 ----O(60)	2.455(4)
EU1 ----O(59)	2.416(3)	EU1 ----O(40)	2.434(4)
EU1 ----O(55)	2.374(4)	EU1 ----O(57)	2.390(4)
EU1 ----O(47)	2.340(3)	EU1 ----O(52)	2.372(3)

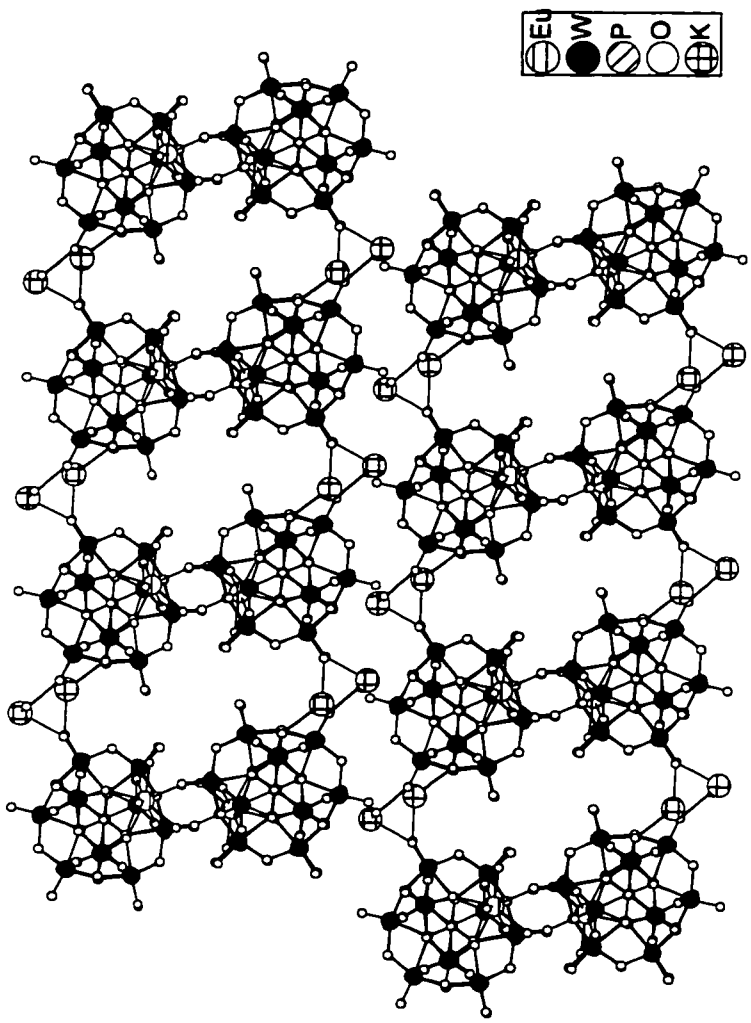

Figure 3.2. Packing diagram of $[Eu(H_2O)_3(\alpha\text{-}2\text{-}P_2W_{17}O_{61})]^{7-}$ anion.

The extended structure is composed of the anions of $[Eu(H_2O)_3(\alpha\text{-}2\text{-}P_2W_{17}O_{61})]^{7-}$ linked together by surface bound potassium cations. The potassium ions bind to terminal oxygen atoms of two dimers giving rise to chains along the crystallographic *a* axis, and a mesh-like structure along the crystallographic *b* and *c* axes. The surface bound potassium ions results in the formation of discrete channels forming a porous 3D structure (Fig. 3.2) [20,21]. The approximate cross-sectional area of the gaps in $[Eu(H_2O)_3(\alpha\text{-}2\text{-}P_2W_{17}O_{61})]^{7-}$ are of the order of 19 × 12 Å ^{2}. The K-O distances of terminal bound K cations range from 2.75 to 2.85 Å. The separations between adjacent layers are 12.7 Å, 14.7 Å and 22.7 Å for the crystallographic *a*, *b*, and *c* axes respectively.

3.2.2. NMR experiment

Figure 3.3 shows the ^{31}P NMR and ^{183}W NMR of $[Nd(\alpha\text{-}2\text{-}P_2W_{17}O_{61})]^{7-}$ complex. ^{31}P NMR shows two resonances corresponding to the two nonequivalent phosphorus atoms in the molecule upon substitution of the lanthanide ion. P1 (down field) represents the phosphorus atoms close to lanthanide and P2 (up field) denotes the phosphorus far away from lanthanide. 9 resonances (integration ratio: 2:2:1:2:2:2:2:2:2) are observed in the ^{183}W NMR spectrum. The ^{31}P and ^{183}W NMR spectra clearly illustrate the C_s symmetry of the molecule, consistent with substitution in the "cap" region. The chemical shifts of the ^{183}W NMR resonances are different from the chemical shifts of the

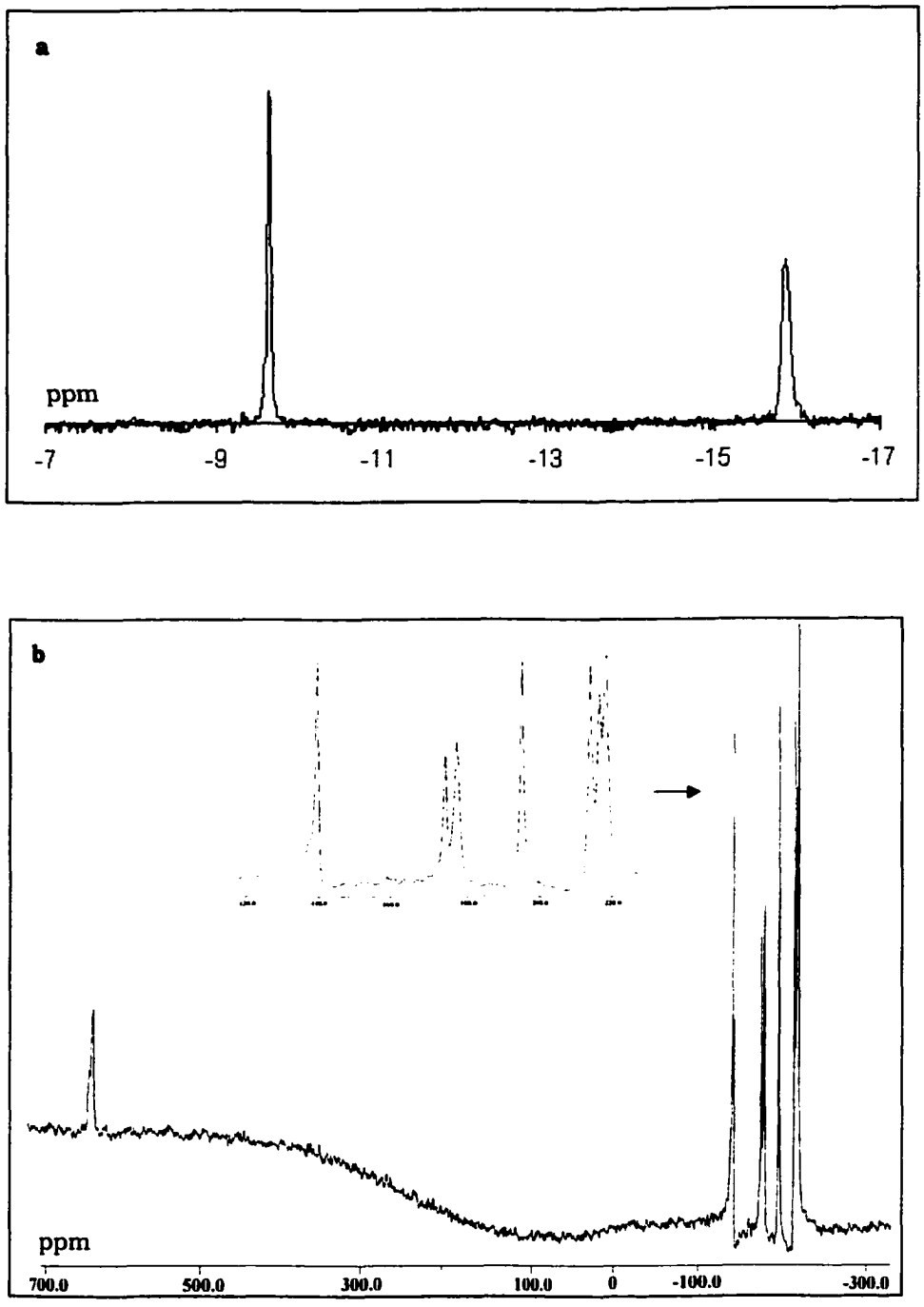

Figure 3.3. a: ^{31}P NMR spectrum of $[Nd(\alpha\text{-}2\text{-}P_2W_{17}O_{61})]^{7-}$. b: ^{183}W NMR spectrum of $[Nd(\alpha\text{-}2\text{-}P_2W_{17}O_{61})]^{7-}$, the inside spectrum is the enlargement.

lacunary species [22,23] and that of the "sandwich" $[Ln(\alpha\text{-}2\text{-}P_2W_{17}O_{61})_2]^{17-}$ complex [18]. The ^{183}W NMR spectroscopy gives cogent data suggesting that the dimeric $[Ln(\alpha\text{-}2\text{-}P_2W_{17}O_{61})]^{7-}$ complexes dissociate in aqueous solution. If the dimer remained intact in solution all seventeen tungsten atoms in one lacunary unit would be nonequivalent to each other while each lacunary half would be related to the other by an inversion center. Therefore, seventeen peaks of equal intensity would be observed in the ^{183}W NMR spectrum. Nine peaks are observed, clearly indicating C_s symmetry of the lacunary $(\alpha\text{-}2\text{-}P_2W_{17}O_{61})^{10-}$ unit.

3.2.3. Fluorescence spectroscopy

Lanthanide ions are distinguished among metallic cations in their ability to luminesce in solution at room temperature. Eu(III) and Tb(III) are the most strongly emitting members of the Ln series [8] Laser excited Eu(III) luminescence spectroscopy is a powerful tool for monitoring the binding of this ion to ligands in solution. The $^7F_0 \rightarrow {}^5D_0$ transition of Eu(III) ion in the range 578-581 nm is excited by a tunable dye laser while the $^5D_0 \rightarrow {}^7F_2$ emission band at 614 nm is monitored. Since the $^7F_0 \rightarrow {}^5D_0$ transition occurs between nondegenerate energy levels, neither of which can be split by a ligand field, a single environment gives rise to only a single transition. If more than one Eu(III) environment is present, each will have its characteristic transition energy [9].

3.2.3.1. Lifetime measurement to determine the number of H_2O molecules bonded to Eu(III)

The excited state lifetime of the Eu(III) is very sensitive to the number of water molecules coordinated to the ion, because the weak vibronic coupling between the excited electronic state and the O-H vibrational manifold of coordinated water provides an efficient radiationless deexcitation pathway. Replacement of H_2O with D_2O eliminates the efficient deexcitation pathway and causes the lifetime to increase dramatically [9-11]. Based on this observation Horrocks and Sudnick developed a method for determining the number of water molecules coordinated to the Eu(III). From measurements of lifetimes separately in H_2O and D_2O solution, it is possible to determine the number of coordinated molecules [8,28], q, with uncertainly of 0.3, from:

$q = 1.11[\tau^{-1}(H_2O) - \tau^{-1}(D_2O) - 0.31]$ (τ : lifetime in msec)

Using this equation the lifetime of the $K_7[Eu(\alpha\text{-}2\text{-}P_2W_{17}O_{61})]$ and $K_{17}[Eu(\alpha\text{-}2\text{-}P_2W_{17}O_{61})_2]$ are measured in H_2O and D_2O respectively.

For $K_7[Eu(\alpha\text{-}2\text{-}P_2W_{17}O_{61})]$:

$$\tau\,(H_2O) = 0.23\text{msec}, \quad \tau\,(D_2O) = 2.8\text{msec}, \qquad q = 4.08$$

For $K_{17}[Eu(\alpha\text{-}2\text{-}P_2W_{17}O_{61})_2]$:

$$\tau\,(H_2O) = 3.02\text{msec}, \quad \tau\,(D_2O) = 4.79\text{msec}, \qquad q = 0.14$$

These results are in agreement with the 1:2 formulation of the $K_{17}[Eu(\alpha\text{-}2\text{-}P_2W_{17}O_{61})_2]$ complex where the Eu(III) binds to eight oxygen atoms of the polyoxoanion with no open coordination sites for binding

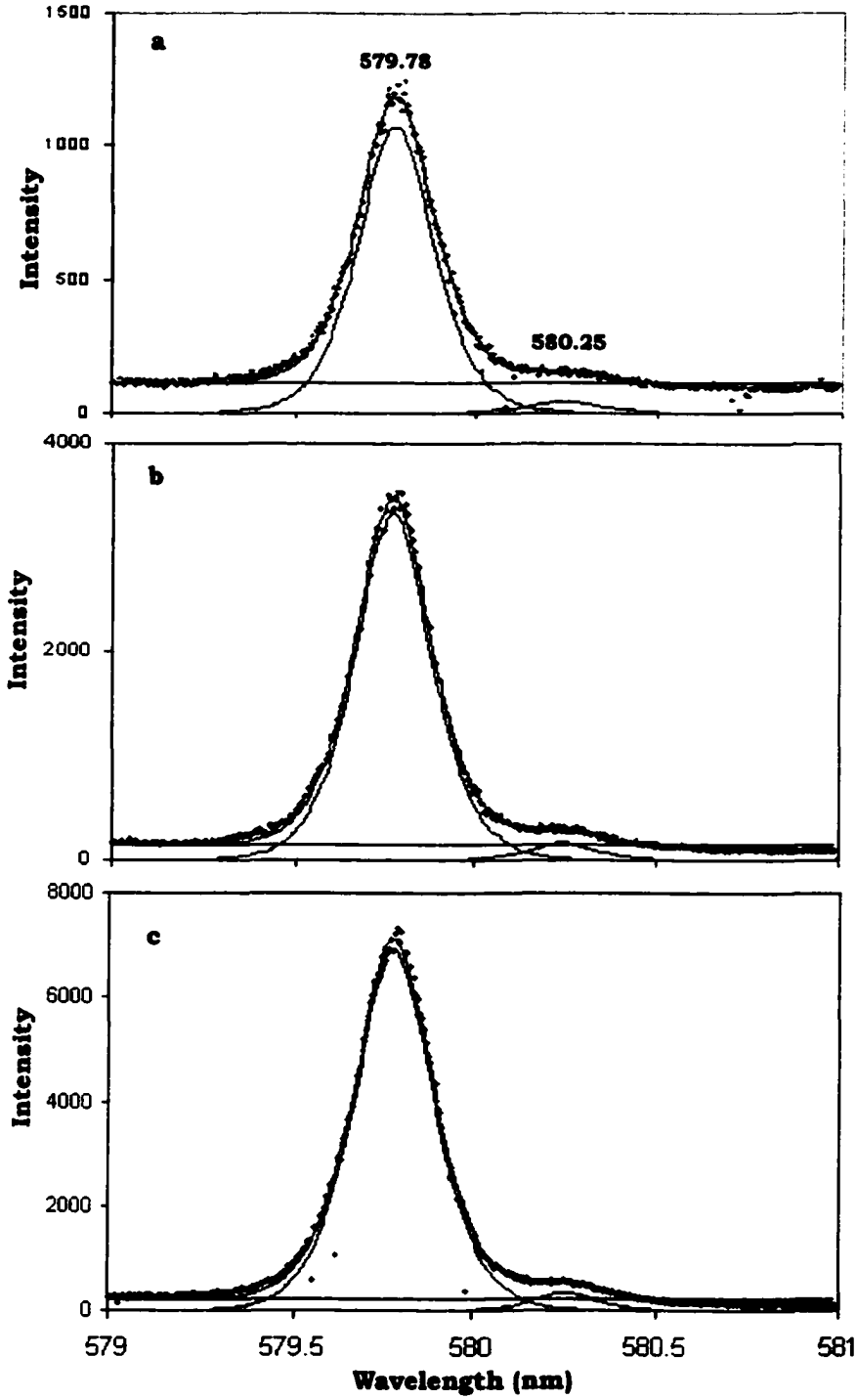

Figure 3.4. Excitation spectra of $K_7[Eu(\alpha\text{-}2\text{-}P_2W_{17}O_{61})]$ at different concentrations. a: 200nM, b: 40μM, c: 500μM. λ_{em}=614 nm.

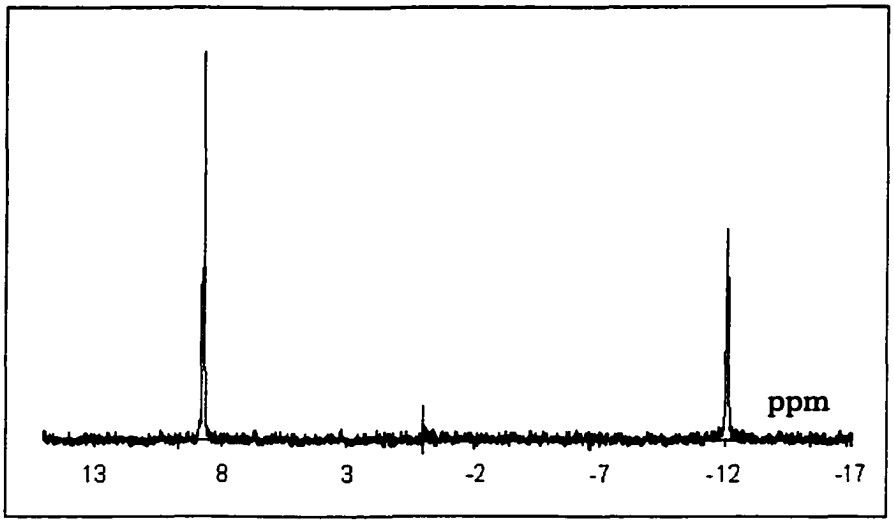

Figure 3.5. ^{31}P NMR spectrum of $K_7[Eu(\alpha\text{-}2\text{-}P_2W_{17}O_{61})]$ in aqueous solution.

water molecules; this is consistent with its crystal structure discussed in Chapter 2. The luminescence lifetime measurements provide compelling evidence that the $[Eu(\alpha\text{-}2\text{-}P_2W_{17}O_{61})]_2^{14-}$ dimeric complex dissociates in aqueous solution to form the monomeric $[Eu(H_2O)_4(\alpha\text{-}2\text{-}P_2W_{17}O_{61})]^{7-}$ complex. These measurements indicate that Eu(III) binds to 4 oxygen atoms of the polyoxoanion and the remaining four coordination sites are taken by water molecules.

3.2.3.2. Observation on concentration dependence of $K_7[Eu(\alpha\text{-}2\text{-}P_2W_{17}O_{61})]$ and $K_{17}[Eu(\alpha\text{-}2\text{-}P_2W_{17}O_{61})_2]$

The excitation spectra of $K_7[Eu(\alpha\text{-}2\text{-}P_2W_{17}O_{61})]$ solutions show one major peak at 579.78 nm and another peak of very lower intensity at 580.25 nm, as shown in Figure 3.4. The major peak represents the Eu α-2 1:1 complex. The low intensity peak is attributed to the Eu α-2 1:2

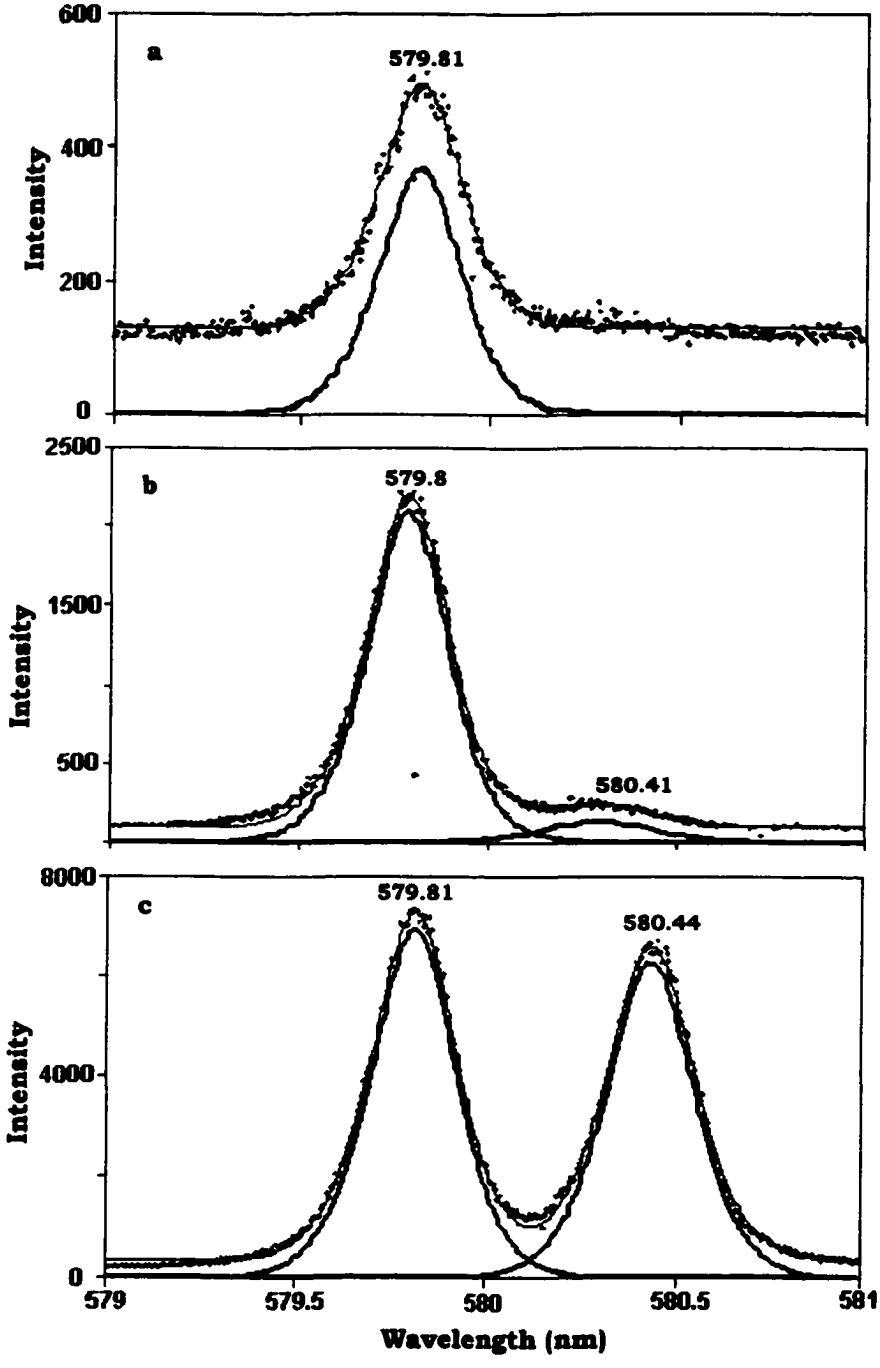

Figure 3.6. Excitation spectra of $K_{17}[Eu(\alpha\text{-}2\text{-}P_2W_{17}O_{61})_2]$ at different concentrations. a: 100nM, b: 20μM, c: 250μM. λ_{em}=614 nm.

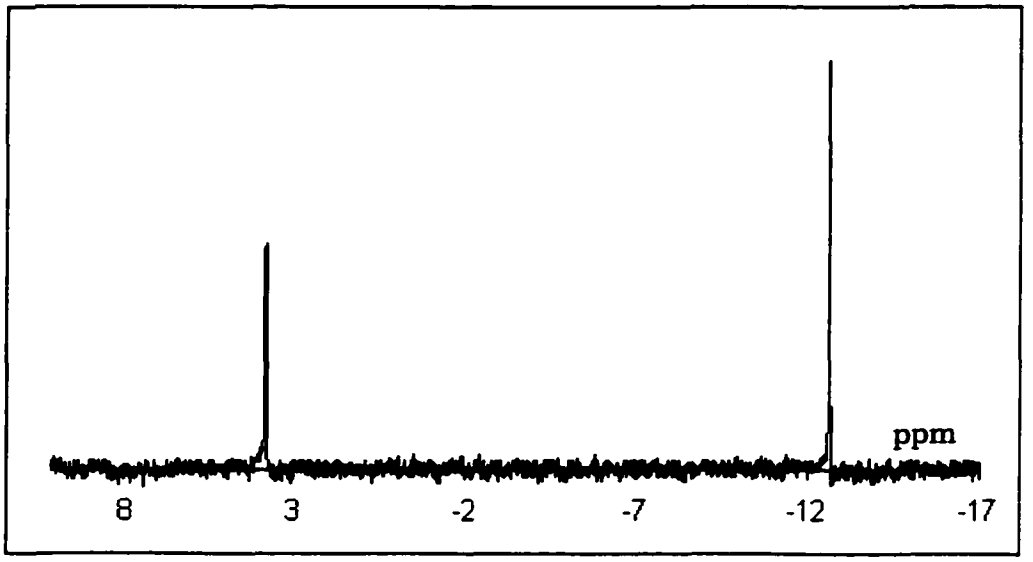

Figure 3.7. ^{31}P NMR spectrum of $K_{17}[Eu(\alpha\text{-}2\text{-}P_2W_{17}O_{61})_2]$ in aqueous solution.

complex contained in the sample, although the ^{31}P NMR spectrum of the same sample of $K_7[Eu(\alpha\text{-}2\text{-}P_2W_{17}O_{61})]$, which used for the fluorescence experiments, did not show the presence of this component (Fig. 3.5). From the spectra of different concentrations in Figure 3.4, the ratios (peak area) of 1:2/1:1 are in the 4-6% range, they almost don't change as the solution concentration increases. Since the detection limit of NMR is much higher than fluorescence, the small amount of Eu α-2 1:2 complex cannot be detected by NMR.

The excitation spectrum of Eu α-2 1:2 complex, $K_{17}[Eu(\alpha\text{-}2\text{-}P_2W_{17}O_{61})_2]$, shows one peak at 579.8 nm and one at 580.4 nm as shown in Figure 3.6, revealing two different Eu(III) environments. The 579.8 nm peak is attributed to Eu α-2 1:1 complex and the 580.4 nm peak is

attributed to Eu α-2 1:2 complex. The ratio of the peak areas of 1:2 to 1:1 increases from almost 0 to 0.902 as solution concentration increases from 100nM to 250μM. These concentrations bracket the equilibrium of the Eu: $[\alpha\text{-}2\text{-}P_2W_{17}O_{61}]^{10-}$ 1:1 and 1:2 species. The formation constant for the equilibrium:

$$[Eu(\alpha\text{-}2\text{-}P_2W_{17}O_{61})]^{7-} + [\alpha\text{-}2\text{-}P_2W_{17}O_{61}]^{10-} \rightleftharpoons [Eu(\alpha\text{-}2\text{-}P_2W_{17}O_{61})_2]^{17-}$$

is in the micromolar range, consistent with my work for a series of lanthanides measurements (Chapter 6) and other work for the Eu(III) and Ce(III) complexes [25-27].

We did not observe the two species in the ^{31}P NMR spectrum (Fig. 3.7) for the same sample that was used for fluorescence experiment, because the solution concentration used for NMR measurements is usually in mM range, and the above equilibrium is shifted to the right side, so only Eu α-2 1:2 complex exists in solution.

3.2.3.3. Titration

We performed a titration monitoring the intensity of the excitation spectra of Eu α-2 1:1 complex trying to obtain stoichiometric information for Eu α-2 1:1 and 1:2 complexes. We observed one breakpoint for 1:1 complex as shown in Figure 3.8. Increasing the ligand/metal ratio to 2 or 3 did not show any 1:2 complex. These results do not change when the titration is performed in reverse order.

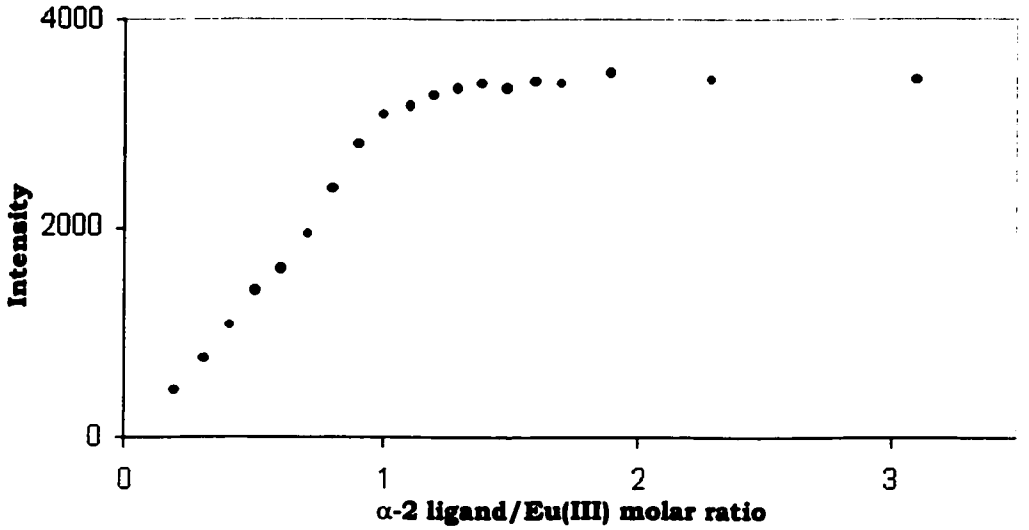

Figure 3.8. Titration of Eu(III) solution (10μM) with $(\alpha\text{-}2\text{-}P_2W_{17}O_{61})^{10-}$ monitored by $^7F_0 \rightarrow {}^5D_0$ excitation spectra of $[Eu(\alpha\text{-}2\text{-}P_2W_{17}O_{61})]^{7-}$. λ_{em} =614 nm, pH ca.6.

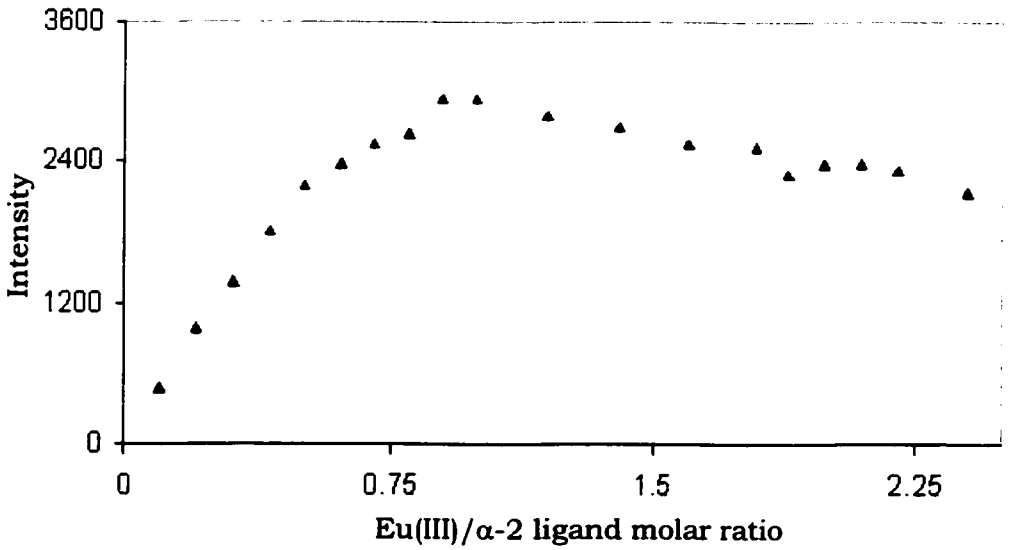

Figure 3.9. Titration of $(\alpha\text{-}2\text{-}P_2W_{17}O_{61})^{10-}$ solution (200nM) with Eu(III) monitored by $^7F_0 \rightarrow {}^5D_0$ excitation spectra of $[Eu(\alpha\text{-}2\text{-}P_2W_{17}O_{61})]^{7-}$. λ_{em} =614 nm, pH ca.6.

We ran another titration experiment at Eu(III) concentration of 200nM, pH ca. 6, in an attempt to measure the formation constant of the Eu α-2 1:1 complex (Fig. 3.9). But since the solution pH was ca. 6, we only observe a breakpoint at 1:1 ligand/metal ratio. Lowering the pH results in the appropriate curvature of titration curve [27], which gives the formation constant K. This experiment will be discussed thoroughly in Chapter 6. Figure 3.9 shows that the curve decreases after the 1:1 breakpoint. This is probably due to excess Eu(III) ion quenching the luminescence of $[Eu(\alpha\text{-}2\text{-}P_2W_{17}O_{61})]^{7-}$ ion.

3.3. Conclusion

The solution and solid state chemistry for $[Ln(\alpha\text{-}2\text{-}P_2W_{17}O_{61})]^{7-}$ has been fully studied by ^{31}P, ^{183}W NMR spectroscopy, luminescence spectroscopy and X-ray crystallography. In solid state, $[Eu(\alpha\text{-}2\text{-}P_2W_{17}O_{61})]^{7-}$ exists as dimeric form, $[Eu(H_2O)_3(\alpha\text{-}2\text{-}P_2W_{17}O_{61})]_2^{14-}$. The point group of the dimeric molecule is C_i. In solution, the ^{183}W NMR spectrum shows 9 resonances denoting C_s symmetry for the molecule. From the fluorescence lifetime measurement, four water molecules are coordinated to Eu(III) in solution. Both results indicate that in solution the dimeric form breaks down and $[Eu(\alpha\text{-}2\text{-}P_2W_{17}O_{61})]^{7-}$ exists as monomer, $[Eu(H_2O)_4(\alpha\text{-}2\text{-}P_2W_{17}O_{61})]^{7-}$. In solution, there is equilibrium between Ln α-2 1:1 and Ln α-2 1:2 complexes, as the solution concentration increases, the percentage of the Ln α-2 1:2 complex increases. The formation constant for the equilibrium is in the micromolar range.

3.4. References:

1) Walker, N.; Stuart, D. *Acta Cryst.* **1983**, *A39*, 158-166.

2) Casan-Pastor, N.; Gomez-Romero, P.; Jameson, G. B.; Baker, L. C. W. *J. Am. Chem. Soc.* **1991**, 113, 5658-5663.

3) Ortega, F.; Pope, M. T.; Evans, J., H.G. *Inorg. Chem.* **1997**, 36, 2166-2169.

4) Sazani, G.; Dickman, M. H.; Pope, M. T. *Inorg. Chem.* **2000**, 39, 939-943.

5) Wasserman, K.; Lunck, H. J.; Palm, R.; Fuchs, J.; Steinfeldt, N.; Pope, M. T. *Inorg. Chem.* **1996**, *35*.

6) Xin, F.; Pope, M. F. *Inorg. Chem.* **1996**, *35*, 5693-5695.

7) Zhang, X. Y.; O'Connor, C. J.; Jameson, G. B.; Pope, M. T. *Inorg. Chem.* **1996**, 35, 30.

8) Horrocks, W. DeW., Jr. *Methods Enzymol.* **1993**, *226*, 495.

9) Horrocks, W. DeW., Jr.; Sudnick, D. R. *Acc. Chem. Res.* **1981**, 14, 384.

10) Horrocks, W. DeW., Jr.; Sudnick, D. R. *J. Am. Chem. Soc.* **1979**, 101, 334.

11) Horrocks, W. DeW., Jr.; Wu, S. R. *Inorg. Chem.* **1995**, 34, 3724.

12) Bartis, J.; Sukal, S.; Dankova, M.; Kraft, E.; Kronzon, R.; Blumenstein, M.; Francesconi, L. C. *J. Chem. Soc., Dalton Trans.* **1997**, 1937.

13) Bartis, J.; Dankova, M.; Lessmann, J. J.; Luo, Q. H.; Horrocks, W. D., Jr.; Francesconi, L. C. *Inorg. Chem.* **1999**, 38, 1042-1053.

14) Sadakane, M.; Dickman, M. H.; Pope, M. T. *Angew. Chem. Int. Ed.* **2000**, 39, 2914-2916.

15) Yamase, T.; Ozeki, T.; Ueda, K. *Acta Crystallographica Section C* **1993**, 49, 1572-1574.

16) Yamase, T.; Ozeki, T. *Acta Cryst* **1993**, C49, 1577-1580.

17) Weakley, T. J. R. *Polyhedron*, **1987**, 6, 931.

18) Luo, Q. H.; Howell, R. C.; Dankova, M.; Bartis, J.; Williams, C. W.; Horrocks, J., W.DeW.; Young, J., V.G.; Rheingold, A. L.; Francesconi, L. C.; Antonio, M. R. *Inorg. Chem.* **2001**, 40(8), 1894-1901.

19) Ciabrini, J.-P.; Contant, R. *J. Chem. Research (M).* **1993**, 2720-2744.

20) Son, J.-H.; Choi, H.; Kwon, Y.-U. *J. Am. Chem. Soc.* **2000**, 122, 7432.

21) Müller, A.; Serain, C. *Acc. Chem. Res.* **2000**, 33, 2.

22) Jorris, T. L.; Kozik, M.; Casan-Pastor, N.; Domaille, P. J.; Finke, R. G.; Miller, W. K.; Baker, L. C. W. *J. Am. Chem. Soc.* **1987**, 109, 7402.

23) Bartis, J.; Dankova, M.; Blumenstein, M.; Francesconi, L. C. *Journal of Alloys and Compunds* **1997**, 249, 56-68.

24) Crans, D. C. *Comments Inorg. Chem.* **1994**, 16, 35.

25) Ciabrini, J. P.; Contant, R. *J. Chem. Res., Synop.* **1993**, 10, 391.

26) Luo, Q. H.; W. DeW.;Jr.; Francesconi, L.C., manuscript in preparation.

27) S. L. Wu and W. DeW. Horrocks, Jr. *J. Chem. Soc., Dalton trans.*, **1997**, 1497-1502.

28) Supkouski, R. M.; Horrocks, W. DeW., Jr., *Inorg. Chem.* Acta. **2002**, in press.

Chapter 4

Characterization of $[Ln(\alpha\text{-}1\text{-}P_2W_{17}O_{61})]^{7-}$ by X-ray Crystallography

Lanthanide (Ln) ions react with $(\alpha\text{-}1\text{-}P_2W_{17}O_{61})^{10-}$ forming $[Ln(\alpha\text{-}1\text{-}P_2W_{17}O_{61})]^{7-}$ and $[Ln(\alpha\text{-}1\text{-}P_2W_{17}O_{61})_2]^{17-}$, denoted Ln α-1 1:1 and 1:2, respectively. The synthesis and characterization of 1:2 complex will be discussed in Chapter 5. The 1:1 complex was first isolated by our lab [1] and characterized with NMR and fluorescence spectroscopy. However, solid state crystallographic data has never been obtained for Ln α-1 1:1 complex, possibly due to the rapid isomerization and instability of α-1 isomer. Here I report the first single crystal structure of $[Lu(\alpha\text{-}1\text{-}P_2W_{17}O_{61})]^{7-}$. This structure has been published [2].

4.1. Experiments

4.1.1. Synthesis of $K_7[Lu(\alpha\text{-}1\text{-}P_2W_{17}O_{61})]$

$K_{10}[\alpha\text{-}1\text{-}P_2W_{17}O_{61}]$ (10g) was dissolved in 100 mL of lithium acetate buffer (0.285 M) at pH=4.7. 3 mL of an aqueous 1 M $LuCl_3$ solution was added dropwise; the solution was stirred for a few minutes followed by potassium chloride (7g). The resulting suspension was cooled in the freezer for 10 hours and a small amount of solid was filtered. The filtrate was cooled in the freezer again for another 2 days. White crystals formed. The crystals were separated by filtration, and dried under air suction.

4.1.2. Crystallization of $K_7[Lu(\alpha\text{-}1\text{-}P_2W_{17}O_{61})]$

Two grams of $K_{10}[\alpha\text{-}1\text{-}P_2W_{17}O_{61}]$ was dissolved in 20 mL of lithium acetate buffer (0.285 M) at pH=4.7. $LuCl_3$ (0.6 mL of 1 M aqueous solution) was added; the solution was stirred for a few minutes. Potassium chloride (1.4g) was added. The resulting suspension was cooled in the freezer for 10 hours and filtered. The filtrate was cooled in the freezer again for another 2 days to yield white crystals.

4.1.3. Crystallography

The data collection and crystal structure solution were performed by Dr. Victor Young, University of Minnesota, X-ray crystallography facility.

A single crystal of $K_7[Lu(\alpha\text{-}1\text{-}P_2W_{17}O_{61})]\bullet 18.7H_2O\bullet {}^1/_2CH_3COOK$ was attached to a glass fiber and mounted on a Siemens SMART system for data collection at 173(2) K with Mo Kα radiation (0.71073 Å). The space group $P2_1/n$ was determined based on systematic absences and intensity statistics (SHELXTL-Plus V5.0, Siemens Industrial Automation, Inc., Madison, WI). A successful direct-methods solution was calculated which provided most non-hydrogen atoms from the E-map. Several full matrix least squares/difference Fourier cycles were performed which located the remainder of the non-hydrogen atoms. All non-hydrogen and non-oxygen atoms were refined with anisotropic displacement parameters. Crystal data and structure refinement parameters are listed in table 4.1.

Table 4.1. Crystal data, data collection, and solution and refinement for $K_7[Lu(\alpha\text{-}1\text{-}P_2W_{17}O_{61})]\cdot 18.7H_2O\cdot 1/2CH_3COOK$

Crystal Data	
Empirical formula	$H_0K_5LuO_{81.30}P_2W_{17}$
Crystal Habit, color	Plate, Colorless
Crystal size	0.40×0.25×0.11 mm
Crystal system	Monoclinic
Space group	$P2_1/n$
	a = 18.6997(2) Å α =90°
	b = 26.1617(4) Å β=106.417°(1)
	c = 19.2653(1) Å γ =90°
Volume	9040.6(2) Å^3
Z	4
Formula weight	4858.70
Density (calculated)	3.570 mg/m^3
Absorption coefficient	22.977 mm^{-1}
F (000)	8418
Data Collection	
Diffractometer	Siemens SMART Platform CCD
Wavelength	0.71073 Å
Temperature	173(2) K
θ range for data collection	1.34 to 24.93°
Index ranges	$-21 \le h \le 21$, $0 \le k \le 30$, $0 \le l \le 22$
Reflections collected	53627
Independent reflections	15174 (R_{int} = 0.0749)
Solution and Refinement	
System used	SHELXTL-V5.0
Solution	Direct methods
Refinement method	Full-matrix least-squares on F^2
Weighting scheme	$w = [\sigma^2(F_o^2) + (AP)^2 + (BP)^{-1}$, where $P = (F_o^2 + 2Fc^2)/3$, A = 0.119500, and B = 59.004102
Absorption correction	SADABS (Sheldrick, 1996)
Max. and min. transmission	1.0000 and 0.4055
Data / restraints / parameters	15171 / 243 / 577
R indices (I>2 (I) = 10379)	R1 = 0.0732, wR2 = 0.1915
Goodness-of-fit on F	1.054
Largest diff. Peak and hole	6.103 and -3.303 eÅ^{-3}

4.2. Results and Discussions

Lanthanide α-1 1:1 complexes were isolated by Dr. Judit Bartis [3] and characterized by ^{31}P NMR and ^{183}W NMR spectroscopy as shown in Figure 4.1a and Figure 4.1b, respectively, fluorescence spectroscopy (Figure 4.1c) and a stoichiometric study of the lutetium analog. These techniques are quite useful to illustrate the solution structure and stoichiometry. The ^{31}P NMR spectrum shows two resonances corresponding to the two nonequivalent phosphorus atoms in the molecule. The ^{183}W NMR spectrum shows 17 different tungsten peaks, clearly illustrating the C_1 symmetry of the molecule, consistent with substitution in the "belt" region. Luminescent lifetime measurements show four water molecules coordinated to the Eu(III), consistent with the 1:1 stoichiometry [1]. However, a single crystal structure is the most convincing evidence to illustrate a structure in solid state. Also, as we have observed with the Ln α-2 1:1, the solution structure can be different from the solid state structure. A complete characterization of the chemistry of these novel polyoxometalates should include solid state X-ray crystallographic analysis.

The $[\alpha\text{-}1\text{-}P_2W_{17}O_{61}]^{10-}$ ligand is not stable and easily isomerizes to $(\alpha\text{-}2\text{-}P_2W_{17}O_{61})^{10-}$ (refer to section 5.2.1). After binding to lanthanide, the complex, $[Ln(\alpha\text{-}1\text{-}P_2W_{17}O_{61})]^{7-}$ is more stable than the ligand itself. But still some amount of $[Ln(\alpha\text{-}2\text{-}P_2W_{17}O_{61})]^{7-}$ will be formed after the [Ln(α-

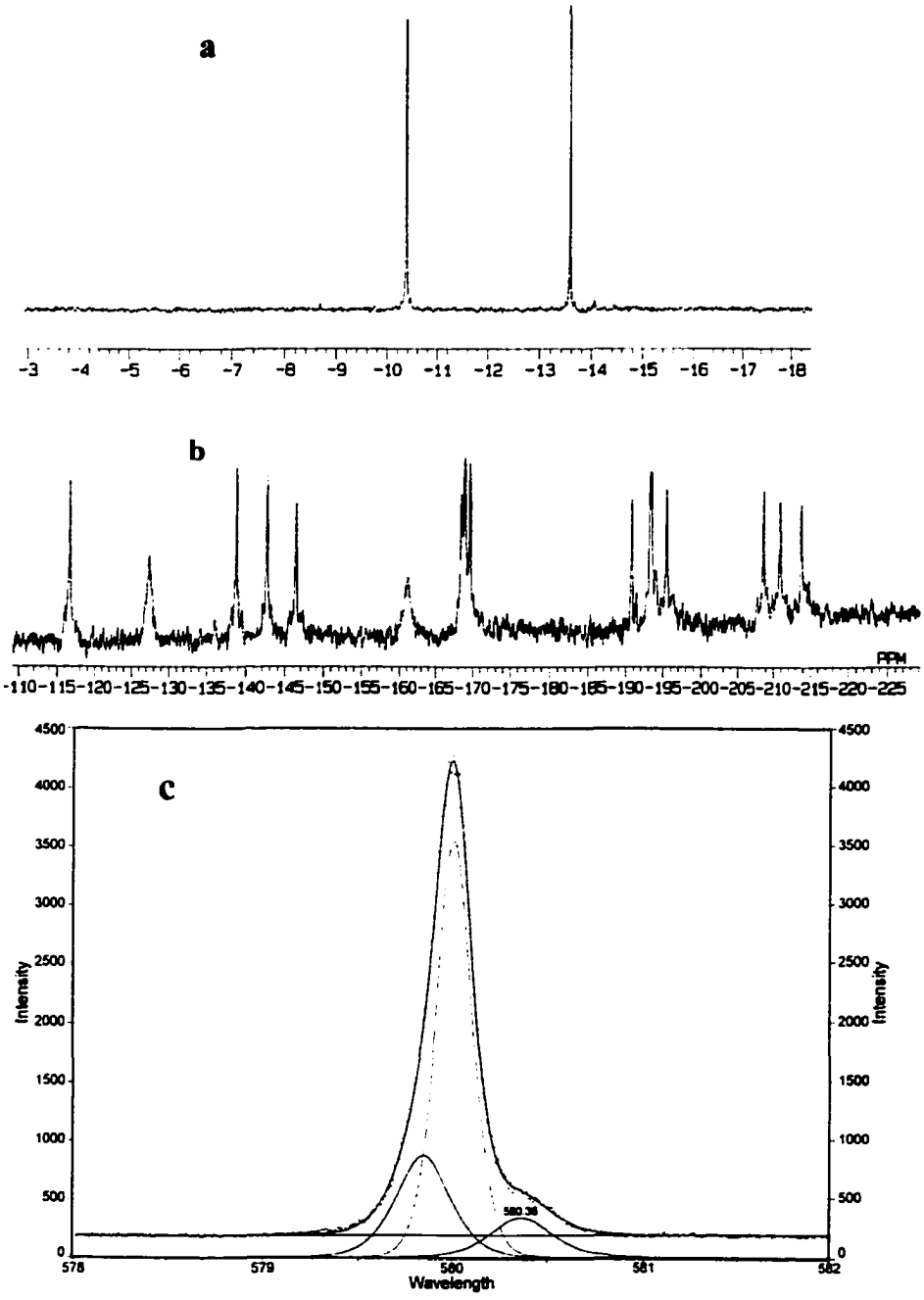

Figure 4.1. a: ^{31}P NMR spectrum of $TBA_xH_y[Lu(\alpha\text{-}1\text{-}P_2W_{17}O_{61})]$, b: ^{183}W NMR spectrum of $TBA_xLi_y[Lu(\alpha\text{-}1\text{-}P_2W_{17}O_{61})]$, c: Excitation spectrum of $K_7[Lu(\alpha\text{-}1\text{-}P_2W_{17}O_{61})]$.

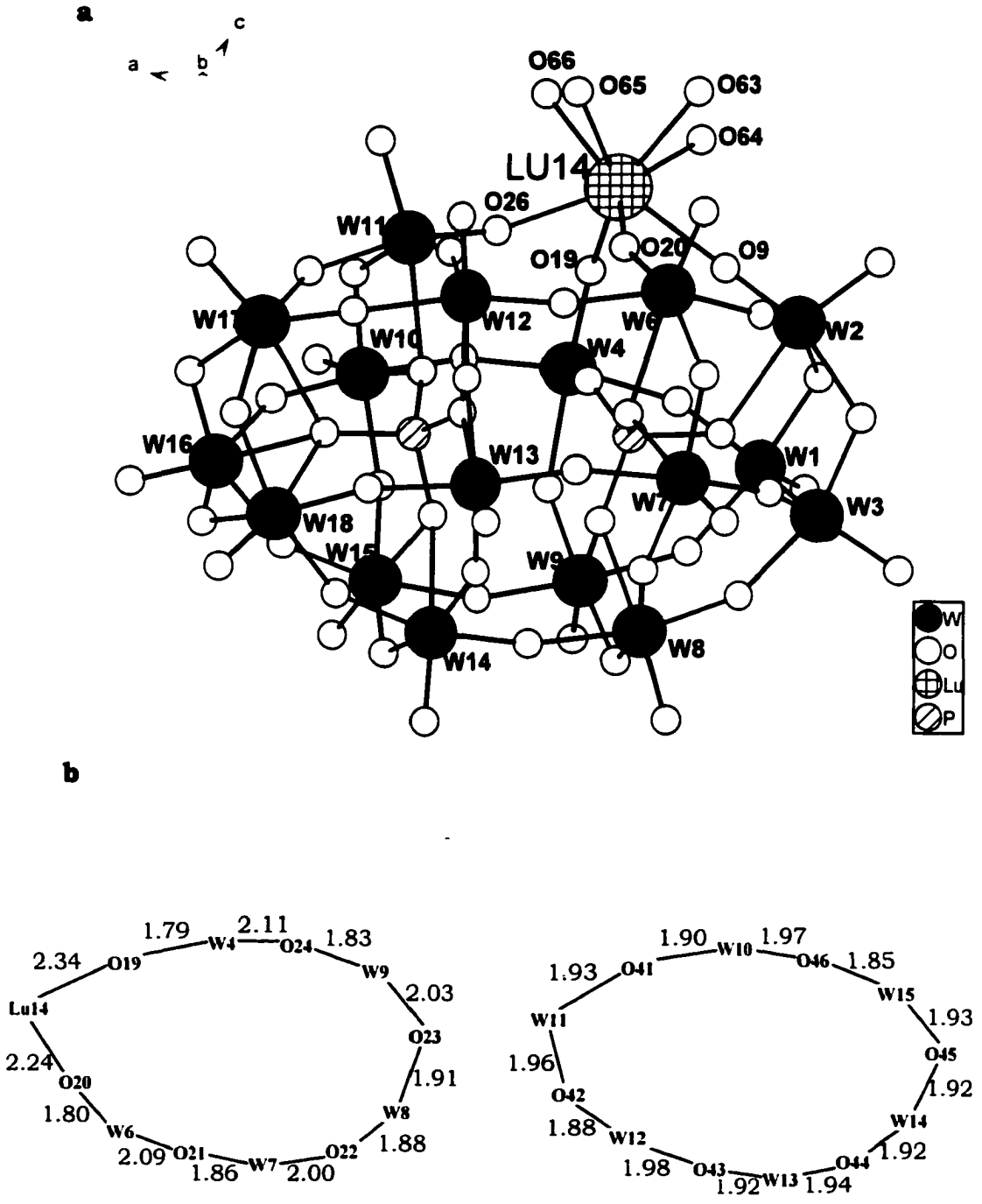

Figure 4.2. a: The crystal structure of $[Lu(\alpha\text{-}1\text{-}P_2W_{17}O_{61})]^{7-}$ anion in stick and ball representation. b: W-O bond lengths in W-O-W rings in the two belt regions.

1-$P_2W_{17}O_{61}$)]$^{7-}$ solutions remain at room temperature for periods of time, rendering crystallization of these complexes difficult. The temperature, lithium ion and pH of the solution not only affect the stability of [Ln(α-1-$P_2W_{17}O_{61}$)]$^{7-}$ anion, but also the crystallization. After optimizing these conditions, I was able to crystallize and Dr. Young could solve the first crystallographic structure for Ln α-1 1:1 complex.

Figure 4.2a, the crystal structure of the [$(H_2O)_4$Lu(α-1-$P_2W_{17}O_{61}$)]$^{7-}$ anion, shows that the Lu(III) ion is substituted for a $[WO]^{4+}$ unit in the "belt" region of the tungsten-oxygen framework of the parent Wells-Dawson ion, [α-$P_2W_{18}O_{62}$]$^{6-}$ [6]. The bond lengths from Lu to the four oxygen atoms of the framework are 2.26(2) Å, 2.34(2) Å, 2.24(2) Å, and 2.34(2) Å. Moreover, the crystal structure shows that four water molecules are bound to Lu(III), with Lu-O distances of 2.38(3), 2.44(2), 2.39(3) and 2.45(2) Å, so that Lu is fully coordinated with 8 oxygen atoms in a square antiprism geometry. The presence of 4 H_2O molecules bound to Lu(III) is consistent with luminescence lifetime measurements of the analogous Eu complex that show four water molecules are bound to Eu(III) [1]. The water molecules are clearly an integral part of the coordination environment of Lu in the structure of [Lu(α-1-$P_2W_{17}O_{61}$)]$^{7-}$ anion. As such, the anion's stoichiometry is best described by the formula [$(H_2O)_4$Lu(α-1-$P_2W_{17}O_{61}$)]$^{7-}$. Substitution of Lu(III) into the belt region results in a structure of C_1 symmetry, consistent with the solution ^{183}W NMR data for a series of lanthanide analogs.

The Lu(III) ion in the structure of $[Lu(\alpha\text{-}1\text{-}P_2W_{17}O_{61})]^{7-}$ anion is eight-coordinate with a square antiprismatic environment of oxygen atoms. Four oxygen atoms are from the W-O framework of one $[\alpha\text{-}1\text{-}P_2W_{17}O_{61}]^{10-}$ ligand and the remaining four O atoms are from four bound water molecules. The average Lu-$(OH_2)_4$ bond distance of 2.42(5) Å is larger than the average Lu-$O_4(\alpha\text{-}1\text{-}P_2W_{17}O_{61})^{10-}$ distance of 2.30(4) Å. The average distance for all 8 Lu-O interactions is 2.36(6) Å. Lutetium in the structure of $[Lu(\alpha\text{-}1\text{-}P_2W_{17}O_{61})]^{7-}$ anion is not bound to an oxygen of a phosphate group. Thus, the Lu ion is displaced outward and away from the normal eighteenth position in the Wells-Dawson framework. This type of bonding, also seen in $[Lu(\alpha\text{-}2\text{-}P_2W_{17}O_{61})_2]^{17-}$ (Chapter 2) and $[Ce(IV)(\alpha\text{-}2\text{-}P_2W_{17}O_{61})_2]^{16-}$ [7] has been observed for crystal structures of lanthanide derivatives of the α-monovacant Keggin ions and $[Ln(III)W_{10}O_{36}]^{9-}$ derivatives [8,9]. In contrast, transition metal ions bond to the phosphate oxygen and to another "axial" ligand, such as a water molecule, to complete the octahedral coordination sphere, is seen in the Co derivative of the lacunary $\alpha\text{-}2\text{-}[P_2W_{17}O_{61}]^{10-}$ species [4]. The 8-coordinate $[Lu(OH_2)_8]^{3+}$ aqua ion has bond lengths of 2.31-2.338 Å [10,11]. The Lu-OH_2 bond lengths are longer than in the aqua ion, and the Lu-O bonds with the W-O framework in are on the same order as the aqua ion.

The bond lengths of the atoms in the tungsten-oxygen framework of $[Lu(\alpha\text{-}1\text{-}P_2W_{17}O_{61})]^{7-}$ structure compare favorably with those reported

for the Wells-Dawson parent structure [6] and the crystal structures of the lacunary α-2-$[P_2W_{17}O_{61}]^{10-}$ isomer and the Co(III)H_2O adduct [4]. Table 4.2 shows the selected bond lengths. The bond lengths and angles of the two phosphate tetrahedra range from 1.53(2) to 1.64(2) Å and 106.7(9) to 114.0(10)°, respectively, well within the ranges observed in the previous structures. Terminal W-O bonds are in the 1.73(2) - 1.80(2) Å range. The W -O (phosphate) bonds range from 2.34(2) - 2.43(2) Å. The W-O bond lengths in the belt containing the Lu atom range from 1.83(2) -

Table 4.2. Selected bond length (Å) for $[Lu(\alpha\text{-}1\text{-}P_2W_{17}O_{61})]^{-7}$

W(2)—O(2)	1.730(1)	W(13)—O(38)	1.74( )
W(2)—O(5)	2.117(1)	W(13)—O(50)	1.913(0)
W(2)—O(4)	2.035(0)	W(13)—O(28)	1.860(1)
W(2)—O(9)	1.787(1)	W(13)—O(44)	1.942(0)
W(2)—O(10)	1.943(0)	W(13)—O(43)	1.922(1)
W(2)—O(31)	2.406(0)	W(13)—O(60)	2.430(1)
W(6)—O(15)	1.778(0)	W(17)—O(54)	1.769(1)
W(6)—O(20)	1.804(1)	W(17)—O(56)	1.966(0)
W(6)—O(21)	2.093(1)	W(17)—O(48)	1.838(0)
W(6)—O(10)	1.951(0)	W(17)—O(49)	1.899(0)
W(6)—O(27)	2.058(1)	W(17)—O(57)	1.988(0)
W(6)—O(26)	2.421(0)	W(17)—O(62)	2.388(1)
W(8)—O(17)	1.732(1)	W(11)—O(36)	1.751(1)
W(8)—O(12)	1.891(1)	W(11)—O(48)	2.109(1)
W(8)—O(29)	1.955(1)	W(11)—O(26)	1.804(0)
W(8)—O(22)	1.88( )	W(11)—O(42)	1.956(0)
W(8)—O(23)	1.941(0)	W(11)—O(41)	1.933(0)
W(8)—O(36)	2.341(1)	W(11)—O(59)	2.357(1)
LU14—O(63)	2.385(0)	LU14—O(64)	2.454(0)
LU14—O(66)	2.382(1)	LU14—O(65)	2.437(1)

2.03(2) Å. These bonds show a significant *trans* bond alternation where each W atom in the ring is involved in a "short" W-O bond *trans* to a "long" W-O bond (Figure 4. 2b). This phenomenon is not significant for the second W_6 ring. Oxygen atoms, O19 and O20, bridge the Lu14 atom and W4 and W6, respectively; the W4-O19 and W6-O20 bonds are shorter than for other bridging oxygen atoms with bond lengths (1.78(2) Å and 1.80(2) Å, respectively) approaching terminal W-O bond lengths. In the two caps, bridging W-O bonds range from 1.93(2) – 1.99(2) Å. The pattern of edge shared WO_6 octahedra and corner shared WO_6 octahedra, observed in the Wells-Dawson ion and the lacunary α-2-$[P_2W_{17}O_{61}]^{10-}$ isomer, are retained in this structure. Both of the cap regions show edge shared octahedra while the belt regions show the alternating pattern of corner and edge shared octahedra. This pattern is obvious from the W-W distances in the two cap and two belt regions. The W-W distances in the two cap regions range from 3.41 to 3.48 Å. In the belt regions, the edge shared octahedra show W-W distances of 3.37 to 3.42 Å, and the W -W distances for the corner shared octahedra range from 3.72 to 3.79 Å. The introduction of the $[Lu(III)(H_2O)_4]^{3+}$ unit into one of the belts disrupts the pattern of edge and corner sharing as the Lu is connected to the two W atoms in the belt by single bridging oxygen atoms. The cap and belt regions are connected via corner shared octahedra. Overall, however, the $Lu(III)(H_2O)_4$ unit introduces a relatively minor perturbation into the parent Wells-Dawson framework.

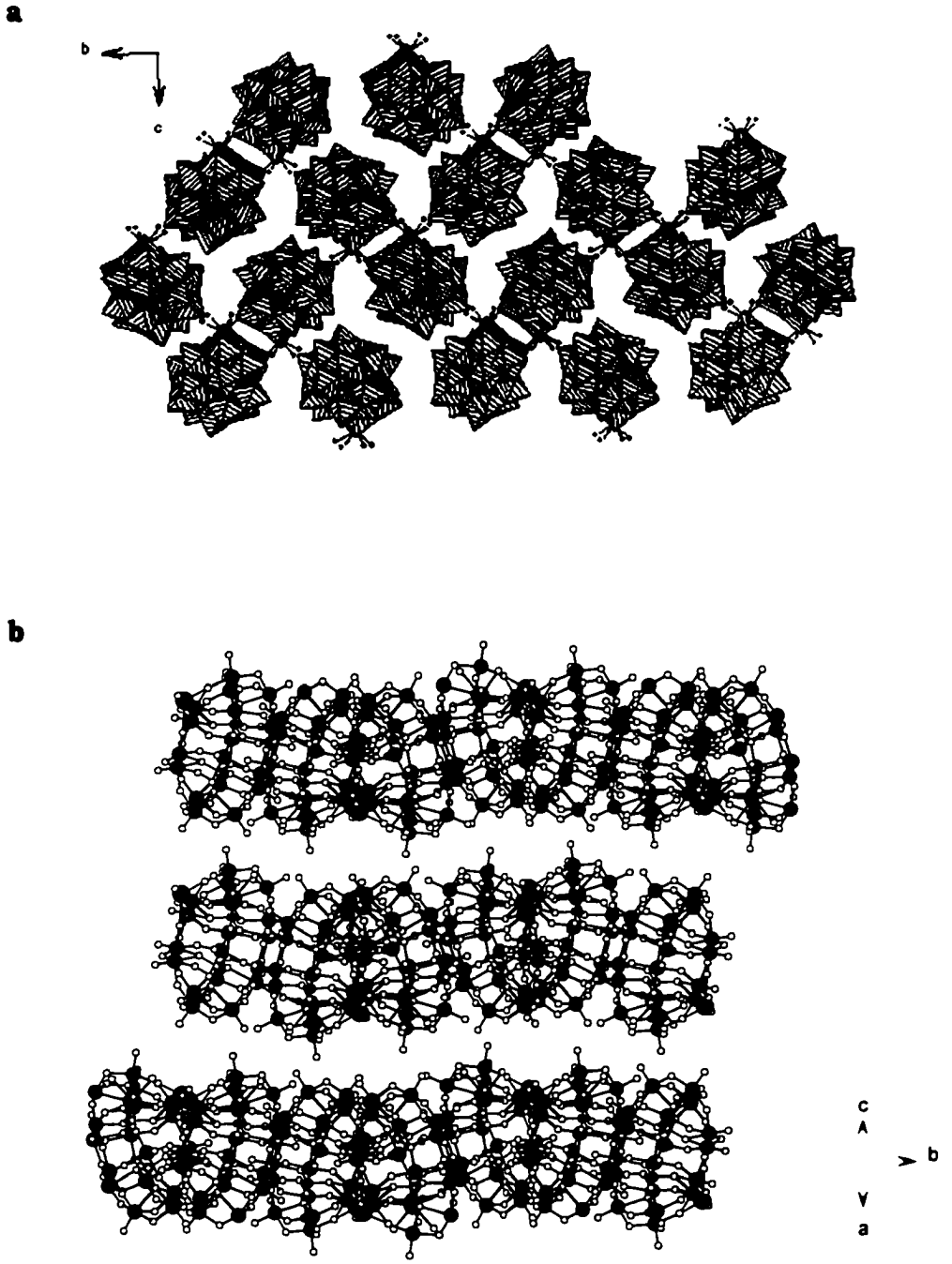

Figure 4.3. Packing diagram of $[Lu(H_2O)_4(\alpha\text{–}1\text{-}P_2W_{17}O_{61})]^{7-}$ anion viewed from different axis respectively.

The crystal structure shows positional disorder in the tungsten framework. The Lu(14) atom is disordered over two sites Lu(14)W(5) and W(6)Lu(15) sites. The model constructed and refined successfully has Lu(14) sharing the position 5/6 of the time with W(5) 1/6 of the time. This type of positional disorder is common in polyoxoanion crystal structures and, in fact, severe positional disorder has been observed before for the lacunary $[\alpha\text{-}2\text{-}P_2W_{17}O_{61}]^{10-}$ species and the $Co(H_2O)$ derivative.[4] Disorder in the counter cations and water molecules are also common in heteropolyoxometalate crystal structures.

Five of the seven potassium ions required for neutrality were found in the crystal structure in close proximity to the anion. The other potassium ions (at least 8 per unit cell, 2 per molecule) are likely disordered along with an unknown amount of water in the channels. The

Table 4.3. Elementary Analysis Data for the crystal of $[Lu(\alpha\text{–}1\text{-}P_2W_{17}O_{61})]^{7-}$ anion.

$K_7[Lu(\alpha\text{–}1\text{-}P_2W_{17}O_{61})] \bullet 18.7H_2O \bullet 1/2CH_3COOK$		
	Observed (%)	Calculated (%)
K	5.80	6.21
P	1.15	1.23
W	59.49	62.11
Lu	3.01	3.47
C	0.16	0.23
H	0.40	0.76
Li	0	0
N	0	0
From TGA result, there are 18.7 water molecules.		

program PLATON/SQUEEZE [5] found a potential solvent volume=1788.8 $Å^3$ / unit cell volume of 9040.6 $Å^3$, or 19.8 % of the total. Elemental Analysis and TGA data (Table 4.3) on a crystalline sample, prepared in a similar fashion as the crystal chosen for crystallography, shows that eight K ions may be present along with acetate ion, which is consistent with this assessment: two to three potassium ions, water and some acetate per molecule are disordered in the infinite channels that lie parallel to the b axis in the unit cell (Fig. 4.3).

4.3. Conclusion

We have solved and refined the crystal and molecular structure of $[Lu(\alpha\text{–}1\text{-}P_2W_{17}O_{61})]^{7-}$ anion. Until now, complete single-crystal X-ray diffraction results have not been available. The Lu(III) ion is 8-coordinate. The Ln-O distances are consistent with literature values. The crystallographic results for $[Lu(\alpha\text{–}1\text{-}P_2W_{17}O_{61})]^{7-}$ reveal 4 water molecules participate in the Lu-O_8 coordination, which in good agreement with the fluorescence results for $[Eu(\alpha\text{–}1\text{-}P_2W_{17}O_{61})]^{7-}$. The molecule has C_1 symmetry which consistent with the ^{183}W NMR results.

4.4. References:

1) Bartis, J.; Dankova, M.; Lessmann, J. J.; Luo, Q. H.; Horrocks, W. D., Jr.; Francesconi, L. C. *Inorganic Chemistry* **1999**, *38*, 1042-1053.

2) Luo, Q. H.; Howell, R. C.; Dankova, M.; Bartis, J.; Williams, C. W.; Horrocks, J., W.DeW.; Young, J., V.G.; Rheingold, A. L.; Francesconi, L. C.; Antonio, M. R. *Inorg. Chem.* **2001**, 40(8), 1894-1901.

3) Bartis, J.; Sukal, S.; Dankova, M.; Kraft, E.; Kronzon, R.; Blumenstein, M.; Francesconi, L. C. *J. Chem. Soc., Dalton Trans.* **1997**, 1937.

4) Weakley, T. J. R. *Polyhedron* **1987**, *6*, 931-937.

5) Spek, A. L. *Acta Cryst.* **1990**, *A46*, C-34.

6) Dawson, B. *Acta Cryst.* **1953**, *6*.

7) Molchanov, V. N.; Kazanskii, L. P.; Torchenkova, E. A.; Simonov, V. I. *Sov. Phys. Crystallogr., Engl. Transl.* **1979**, *24*, 96-97.

8) Ozeki, T.; Yamase, T. *Acta Cryst.* **1994**, *B50*, 128-134.

9) Sugeta, M.; Yamase, T. *Bull. Chem. Soc. Jpn.* **1993**, *66*, 444-449.

10) Yamaguchi, T.; Nomura, M.; Wakita, H.; Ohtaki, H. *J. Chem. Phys.* **1988**, *89*, 5153-5159.

11) Habenschuss, A.; Spedding, F. H. *J. Chem. Phys.* **1979**, *70*, 2797-2806.

Chapter 5

Complexation Study of $[Ln(\alpha\text{-}1\text{-}P_2W_{17}O_{61})]^{7-}$ with $(\alpha\text{-}1\text{-}P_2W_{17}O_{61})^{10-}$ and Other Organic Ligands

Lanthanide ions react with $(\alpha\text{-}1\text{-}P_2W_{17}O_{61})^{10-}$ forming 1:1 and 1:2 complexes. The 1:1 complex was discussed in Chapter 4. The 1:2 complex was observed electrochemically in solution by Contant, in 1993 [1]. Our lab also found from ^{31}P NMR spectroscopy that an unknown species formed while recrystallizing the La complex of $(\alpha\text{-}1\text{-}P_2W_{17}O_{61})^{10-}$ prepared in 1:2 (metal/ligand) stoichiometric ratio [2]. But a pure sample of Ln α-1 1:2 complex has never been isolated. We report here the first time that a Ln α-1 1:2 complex has been synthesized and characterized by ^{31}P, ^{183}W NMR spectroscopy, fluorescence spectroscopy and elemental analysis. The association constants have been measured.

$[Ln(\alpha\text{-}1\text{-}P_2W_{17}O_{61})]^{7-}$ complexes not only react with the $(\alpha\text{-}1\text{-}P_2W_{17}O_{61})^{10-}$ ligand to form 1:2 complexes, but also the 1:1 complexes react with organic ligands to form ternary complexes. The ternary complexes have been observed from ^{31}P NMR spectra for several organic ligands.

5.1. Experiments

5.1.1. Isomerization of $[\alpha\text{-}1\text{-}P_2W_{17}O_{61}]^{10-}$ to $[\alpha\text{-}2\text{-}P_2W_{17}O_{61}]^{10-}$

The $[\alpha\text{-}1\text{-}P_2W_{17}O_{61}]^{10-}$ (0.04g) ligand was dissolved in 2 mL of three different solvents, H_2O, 0.25M of sodium acetate buffer (0.1M NaCl,

pH=4.7) and 0.125M of lithium acetate buffer (0.1M LiCl, pH=5.2). ^{31}P NMR spectra were recorded immediately after mixing and monitored over time.

5.1.2. Synthesis of $[Ln(\alpha\text{-}1\text{-}P_2W_{17}O_{61})_2]^{17-}$ complexes

5.1.2.1. $K_{17}[La(\alpha\text{-}1\text{-}P_2W_{17}O_{61})_2]$

$K_{10}[\alpha\text{-}1\text{-}P_2W_{17}O_{61}]$ (1.5g) (~0.29 mmol) was dissolved in 10 mL of sodium chloride (0.1M) at 35°C-40°C. 0.18mL of aqueous 1 M $LaCl_3$ solution (~0.18 mmol) was added dropwise; the solution was stirred vigorously for 2 minutes followed by addition of potassium chloride (1.05g). The mixture was stirred for 1-2 minutes; the white precipitate was separated by filtration, and dried under air suction.

5.1.2.2. $K_{17}[Nd(\alpha\text{-}1\text{-}P_2W_{17}O_{61})_2]$

$K_{10}[\alpha\text{-}1\text{-}P_2W_{17}O_{61}]$ (1.0g) (~0.19 mmol) was dissolved in 10 mL of water at 35°C-40°C. 0.120 mL of aqueous 1 M $NdCl_3$ solution (~0.12 mmol) was added dropwise; the solution was stirred vigorously for 2 minutes followed by addition of potassium chloride (0.7g). The mixture was stirred for 1-2 minutes; the purple creamy precipitate was separated by filtration and dried under air suction for 2 hours. The precipitate was washed twice in the filter funnel with 1 mL of water added dropwise each time; drying was continued for 2 hours.

5.1.2.3. $K_{17}[Eu(\alpha\text{-}1\text{-}P_2W_{17}O_{61})_2]$

$K_{10}[\alpha\text{-}1\text{-}P_2W_{17}O_{61}]$ (0.76g) (~0.15 mmol) was dissolved in 10 mL of lithium chloride (0.002M) at ca. 40°C, 0.0912 mL of 1M $EuCl_3$ solution (~0.09 mmol) was added dropwise; the solution was stirred vigorously for 2 minutes followed by addition of 0.53g of KCl. After the mixture was stirred for 1-2 minutes, the white precipitate was separated by filtration and dried under air suction for 2 hours.

5.1.3. Characterization of $[Ln(\alpha\text{-}1\text{-}P_2W_{17}O_{61})_2]^{17-}$ by ^{31}P, ^{183}W NMR, Fluorescence Spectroscopy and Elementary Analysis

5.1.3.1. Fluorescence experiments

Luminescence excitation spectra and excited state lifetimes of Eu(III) were measured using the laser luminescence spectroscopic technique [3,4]. A pulsed (10 Hz) Nd : YAG laser-pumped dye laser (Continuum), with a mixture of Rhodamine 590 and 610 dyes, was used to excite the $^7F_0 \rightarrow {}^5D_0$ transition of Eu(III) in the 578-581 nm region; emission ($^5D_2 \rightarrow {}^7F_0$) was monitored at 614 nm.

Excited-state lifetime measurements in H_2O and D_2O solution were used to obtain the number of water molecules coordinated to the ion, using the method of Horrocks and Sudnick [5]. The samples were prepared as described in the experimental section. Samples where the lifetime was recorded in D_2O were recrystallized 2 times from D_2O. The commercially available Peakfit program, which employs a nonlinear regression method, was used in the data analysis [6].

5.1.3.2. Collection of NMR data

NMR spectra were obtained on a Jeol GX-400 spectrometer. ^{31}P spectra at 161.8 MHz were acquired using either a 10 mm broad band probe or the broad band decoupler coil of a 5 mm inverse detection probe. ^{183}W spectra at 16.7 MHz were recorded utilizing a 10 mm low frequency broadband probe. Typical acquisition parameters for ^{31}P spectra included: spectral width: 10,000Hz; acquisition time: 0.8 s; pulse delay: 1s; pulse width: 15μsec (50 degree tip angle). From 200 to 500 scans were required. For ^{183}W spectra, typical conditions included: spectral width: 10,000Hz; acquisition time: 1.6 s; pulse delay: 0.5s; pulse width: 50 μsec (45 degree tip angle). From 1,000 to 30,000 scans were acquired. For all spectra, the temperature was controlled at 20±0.5°C. ^{31}P spectra were referenced to 85% H_3PO_4. ^{183}W spectra were referenced to 2.0 M Na_2WO_4. For ^{31}P and ^{183}W chemical shifts, the convention used is that the more negative chemical shift denote up field resonance.

5.1.4. Observation of Ternary Complex Formation of $[Ln(\alpha\text{-}1\text{-}P_2W_{17}O_{61})]^{7-}$ with organic ligands

5.1.4.1. Titrating $[Eu(\alpha\text{-}1\text{-}P_2W_{17}O_{61})]^{7-}$ with $(CH_2NHCH_2COOH)_2$ (EDDA) (table 6.1)

0.04g (8 μmol) of $(\alpha\text{-}1\text{-}P_2W_{17}O_{61})^{10-}$ dissolved in a mixture of 1.25 mL of lithium acetate buffer (0.5 M, pH=4.7) and 0.5 mL D_2O. 15 μL of 0.5 M $EuCl_3$ (7.5 μmol) was added, the solution was clear after stirring. Using a volumetric pipette, a total of 0.64 mmol of EDDA (sodium salt)

was added in 21 μL (7.35 μmol) increments of 0.35 M EDDA stock solution.

5.1.4.2. Titrating $[Eu(\alpha\text{-}1\text{-}P_2W_{17}O_{61})]^{7-}$ with L-tartaric acid

0.05g (10 μmol) of $(\alpha\text{-}1\text{-}P_2W_{17}O_{61})^{10-}$ was dissolved in 2 mL of lithium acetate buffer (0.5 M, pH=4.5, 20% D_2O). One equivalent of $EuCl_3$ was added, the solution was clear after stirring. Using a volumetric pipette, a total of 0.5 mmol of L-sodium tartrate was added in 30 μL (15 μmol) increments of 0.5 M L-sodium tartrate stock solution.

5.1.4.3. Titrating $[Nd(\alpha\text{-}1\text{-}P_2W_{17}O_{61})]^{7-}$ with L-tartaric acid

0.1g (20 μmol) of $(\alpha\text{-}1\text{-}P_2W_{17}O_{61})^{10-}$ was dissolved in 2 mL of lithium acetate buffer (0.5 M, pH=5.5, 20% D_2O). One equivalent of $NdCl_3$ was added, the solution was clear after stirring. Using a volumetric pipette, a total of 0.45 mmol of L-sodium tartrate was added in 30 μL (15 μmol) increments of 0.5 M L-sodium tartrate stock solution.

5.2. Results and Discussions

5.2.1. Isomerization of $(\alpha\text{-}1\text{-}P_2W_{17}O_{61})^{10-}$ to $(\alpha\text{-}2\text{-}P_2W_{17}O_{61})^{10-}$

The isomerization of $(\alpha\text{-}2\text{-}P_2W_{17}O_{61})^{10-}$ to $(\alpha\text{-}1\text{-}P_2W_{17}O_{61})^{10-}$ has been observed in lithium acetate buffer (pH=4.7) at high temperature (90°C)[2].

$$(\alpha\text{-}1\text{-}P_2W_{17}O_{61})^{10-} \rightleftharpoons (\alpha\text{-}2\text{-}P_2W_{17}O_{61})^{10-}$$

The isomerization of $(\alpha\text{-}1\text{-}P_2W_{17}O_{61})^{10-}$ to $(\alpha\text{-}2\text{-}P_2W_{17}O_{61})^{10-}$ is more favorable than that of $(\alpha\text{-}2\text{-}P_2W_{17}O_{61})^{10-}$ to $(\alpha\text{-}1\text{-}P_2W_{17}O_{61})^{10-}$. We have experienced this phenomenon during the syntheses of Ln complexes of $(\alpha\text{-}1\text{-}P_2W_{17}O_{61})^{10-}$. In synthesizing α-1 complexes, usually we find a small amount of α-2 complex as an impurity while it is easy to prepare pure α-2 complex. After the α-1 ligand binds to lanthanide, the complex is much more stable than α-1 ligand itself. Water, sodium acetate buffer and lithium acetate buffer are the three solvents that are usually used for synthesis. Using lithium acetate buffer (0.25 M, pH=4.7) ca. 50% of α-1 ligand isomerizes to α-2 ligand in about one and half months. In sodium acetate buffer (0.125 M, pH=5.2) 100% of the α-1 ligand isomerized to the α-2 $(P_2W_{17}O_{61})^{10-}$ in 3 days. The isomerization is even faster in pure water; 100% of the α-1 ligand isomerizes to the α-2 ligand in one day. Therefore, the stability of α-1 ligand is in the order of $Li^+ > Na^+ > H^+$. This is due to the interaction of the $[P_2W_{17}O_{61}]^{10-}$ ion with single-charged cations. The binding constants are 3.61, 2.55 and 1.17 for the complexation of Li^+, Na^+ and K^+ to the α-1 ligand respectively [8-10]. It is

postulated that these mono-cations bind to the 'defect' position of the lacunary structure preventing $(\alpha\text{-}1\text{-}P_2W_{17}O_{61})^{10-}$ from isomerizing to $(\alpha\text{-}2\text{-}P_2W_{17}O_{61})^{10-}$. I observed that the more concentrated the ions, the slower the isomerization.

5.2.2. Synthesis of $[Ln(\alpha\text{-}1\text{-}P_2W_{17}O_{61})_2]^{17-}$ complexes

According to above discussion, lithium ion in solution and low temperature slow the process of isomerization of the $[\alpha\text{-}1\text{-}P_2W_{17}O_{61}]^{10-}$ ligand to $[\alpha\text{-}2\text{-}P_2W_{17}O_{61}]^{10-}$. However, high concentration of Lithium ion will interfere with the reaction of $[\alpha\text{-}1\text{-}P_2W_{17}O_{61}]^{10-}$ to lanthanide forming 1:2 complex. Also the formation of Ln α-1 1:2 complex prefers high temperature. Lastly, the ratio of $[\alpha\text{-}1\text{-}P_2W_{17}O_{61}]^{10-}$/Ln (=2) has to be controlled precisely. If the ratio is less than 2, there will be certain amount of Ln α-1 1:1 complex formed. If the ratio is larger than 2, then there will be excess α-1 ligand. Figure 5.1 is the ^{31}P NMR spectrum of one of my early attempts to prepare the La α-1 1:2 complex. Peak ***A*** is La α-2 1:2 complex, peak ***B*** is α-1 ligand; peak ***C*** is La α-1 1:2 complex; peak ***D*** is La α-1 1:1 complex. With careful control of the concentration of lithium ion, the temperature of solution and the ratio of metal/ligand, we can obtain pure peak ***C***; this is shown in Figure 5.4. The synthesis of Nd α-1 1:2 complex is very similar to that of La complex.

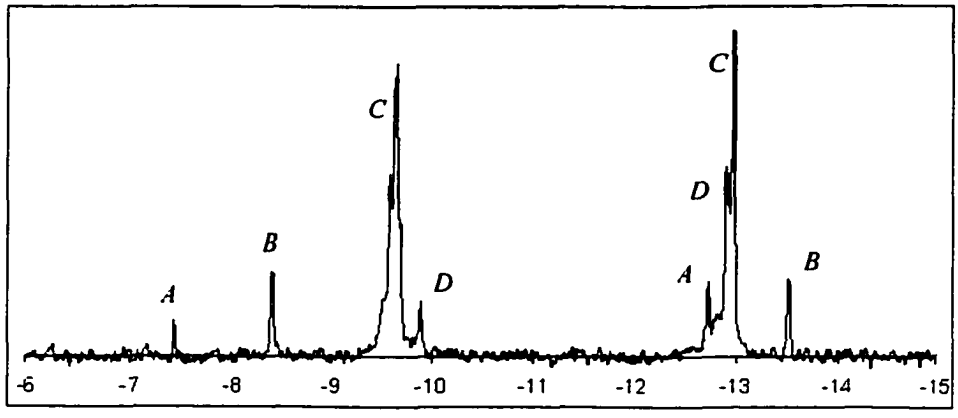

A---La α-2 1:2 *B*---α-1 ligand *C*---La α-1 1:2 *D*---La α-1 1:1

Figure 5.1. ^{31}P NMR spectrum of one of my early attempts to prepare the $[La(\alpha\text{-}1\text{-}P_2W_{17}O_{61})_2]^{17-}$.

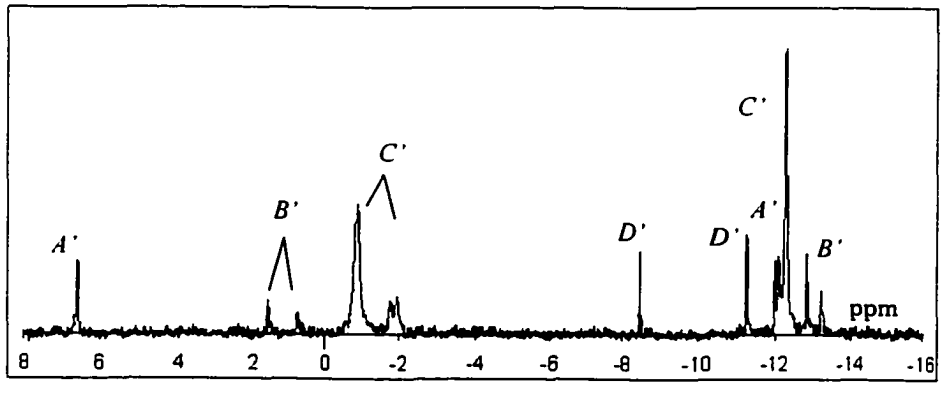

A'---Eu α-1 1:1 *B'*---unknown *C'*---Eu α-1 1:2 *D'*--- α-1 ligand

Figure 5.2. ^{31}P NMR spectrum of one of my early attempts to prepare the $[Eu(\alpha\text{-}1\text{-}P_2W_{17}O_{61})_2]^{17-}$.

It is more difficult to synthesize pure lanthanide α-1 1:2 complexes as one proceeds to the right in the lanthanide series as the size of lanthanide ions decreases. Figure 5.2 is the ^{31}P NMR spectrum of one of my early attempts to prepare the Eu α-1 1:2 complex. Peak ***A'*** is Eu α-1 1:1 complex; peak ***B'*** is unknown; peak ***C'*** is Eu α-1 1:2 complex; peak ***D'*** is α-1 ligand. Compared with the La α-1 1:2 (Fig. 5.1), the good thing is that there is no α-2 complex formed. However a new set of peaks ***B'*** appears, representing an unknown species. In spite of this, it was found that as we increase the concentration of lithium ion in solution, the peaks ***B'*** disappear, but at the same time the amount of Eu α-1 1:1 complex ***A'*** and α-1 ligand ***D'*** increase. Therefore, balancing these two effects is the key to obtain pure complex.

5.2.3. Characterization of $[Ln(\alpha\text{-}1\text{-}P_2W_{17}O_{61})_2]^{17-}$ complex

5.2.3.1. By ^{31}P and ^{183}W NMR spectroscopy

As mentioned before, we previously observed from ^{31}P NMR spectrum that an unknown species formed while recrystallizing La complex of $(\alpha\text{-}1\text{-}P_2W_{17}O_{61})^{10-}$ prepared in 1:2 (metal/ligand) stoichiometric ratio (Fig. 5.3) [2]. The spectrum shows four sets of peaks. **A** represents La α-1 1:1 complex, **C** represents α-1 ligand, **D** represents α-2 ligand. We suspected that peak **B** is due to La α-1 1:2 complex as we only see it in preparation of Ln α-1 1:2 stoichiometry.

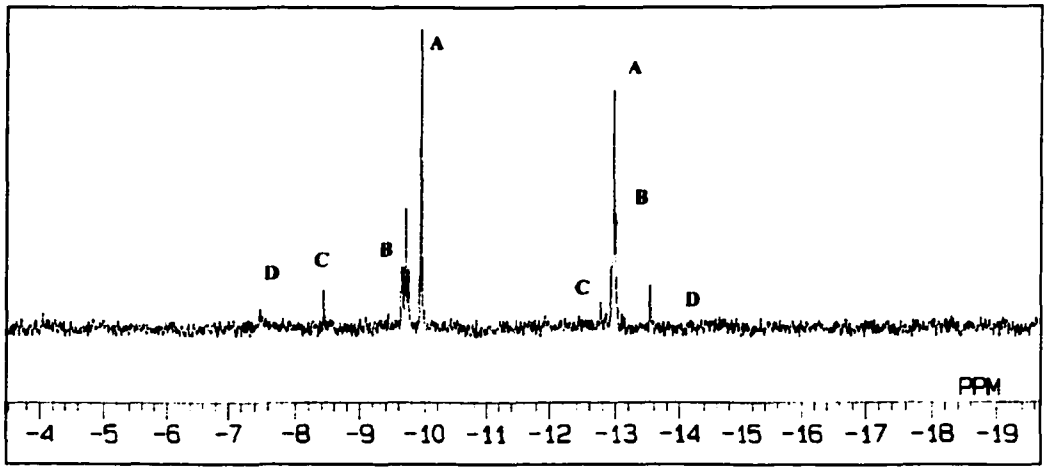

Peak shift (ppm):	A	B	C	D
	-9.94	-9.70	-8.44	-7.53
	-12.98	-12.98	-12.80	-13.54

Figure 5.3. ^{31}P NMR spectrum of the recrystallized La complexes of $[\alpha\text{-}1\text{-}P_2W_{17}O_{61}]^{10-}$ prepared in 1:2 (metal/ligand) stoichiometric ratio.

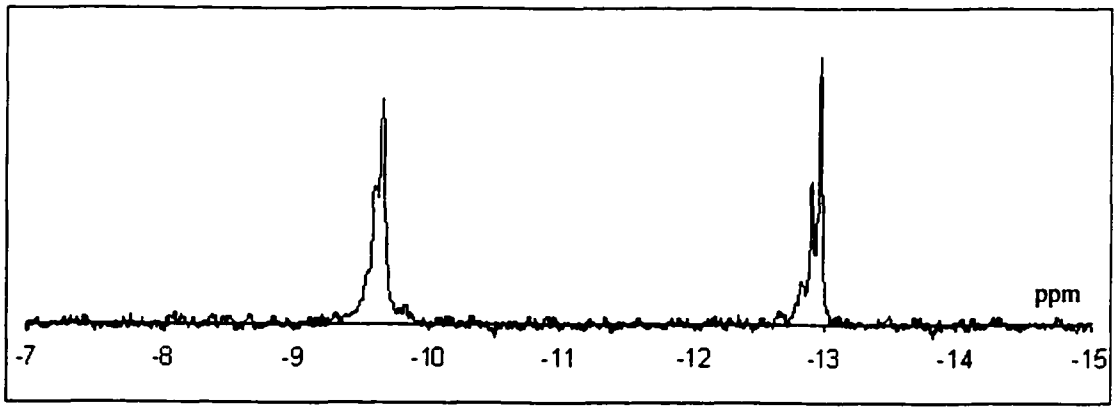

Figure 5.4. ^{31}P NMR spectrum of $[La(\alpha\text{-}1\text{-}P_2W_{17}O_{61})_2]^{17-}$ complex.

From the results of equilibrium between Ln α–2 1:1 and 1: 2 complexes, concentration dependence of Ln α-2 complex, as well as the knowledge of α-1 ligand behavior at different pH values, I changed the reaction conditions to higher temperature (40°C), higher pH (6.0), higher concentration of α-1 ligand (saturated solution). These changes successfully eliminated the peak **A**, **C** and **D** species, to obtain pure peak **B**, which we believe it represents Ln α-1 1:2 complex. Figure 5.4 is ^{31}P spectrum of this newly isolated $[La[\alpha\text{-}1\text{-}P_2W_{17}O_{61})_2]^{17-}$ complex. We can see that the positions of these two peaks are exactly the same as the position of peak **B** in Figure 5.3. Besides the lanthanum, I also synthesized neodymium and europium α-1 1:2 complexes. Figure 5.5 and 5.6 show the ^{31}P NMR spectra of 1:1 and 1:2 complexes for Eu(III) and Nd(III) respectively. The differences between the 1:1 and 1:2 complexes are very clear. Not only the peak shift, but also the pattern of peaks is different; instead of one set of peak, we see three sets of peaks. It is very clear from the spectrum of Eu α-1 1:2 complex, as Eu(III), a shift reagent, dramatically shifts the ^{31}P resonance.

We know that the two peaks in ^{31}P NMR spectrum of the 1:1 complex (Fig. 5.5a) represent the two nonequivalent phosphorus atoms in the anion $[\alpha\text{-}1\text{-}P_2W_{17}O_{61}]^{10-}$. In all of the ^{31}P NMR spectra of the Ln α-1 1:2 complexes, we observe a "triplet" representing this complex-Note that the resonances are clearly separated into a singlet & a doublet in the Eu(III) analog due to the ability of Eu(III) to shift resonances. It is very

likely that the singlet (**N** in Fig. 5.5b) and the doublet (**M** in Fig. 5.5b) represent two conformers, both with Ln : α-1 1:2 stoichiometry. Conformers of the Th(IV) : $(\alpha\text{-}2\text{-}P_2W_{17}O_{61})^{10-}$ 1:2 have been postulated [11]. We have also seen evidence of dynamic behavior in the Lu : $(\alpha\text{-}2\text{-}P_2W_{17}O_{61})^{10-}$ 1:2 compounds [12]. Peaks **N** (Fig. 5.5b) represent the species wherein both of the α-1 units are equivalent to each other by a symmetry operation such as a C_2 axis or an inversion center, resulting in two resonances; each resonance represents two P atoms.

The species represented by the two sets of peaks labeled **M** (Fig. 5.5b) very likely is a conformer wherein the two a-1 units are NOT related by a symmetry element. In this case, we observe four resonances, each resonance represents one P atom. Based on the intensities of the resonances, it appears that the concentration of species **M** is much less than concentration of species **N**.

Figure 5.7 shows the ^{183}W NMR spectra of La α-1 1:1 and 1:2 complexes. Comparing these two spectra, both have 17 peaks, but the peak shifts and pattern are different. For La α-1 1:1 complex, since there is no symmetry existing in the molecule, the 17 tungsten atoms in $[\alpha\text{-}1\text{-}P_2W_{17}O_{61}]^{10-}$ ligand are different, this gives us 17 peaks in ^{183}W NMR spectrum. For La α-1 1:2 complex, we observe 17 peaks very likely representing species **N** wherein both α-1 units are equivalent. Each peak integrates for two tungsten atoms. Species **M** would have 34 different tungsten atoms and should show 34 peaks in ^{183}W NMR spectrum. Since

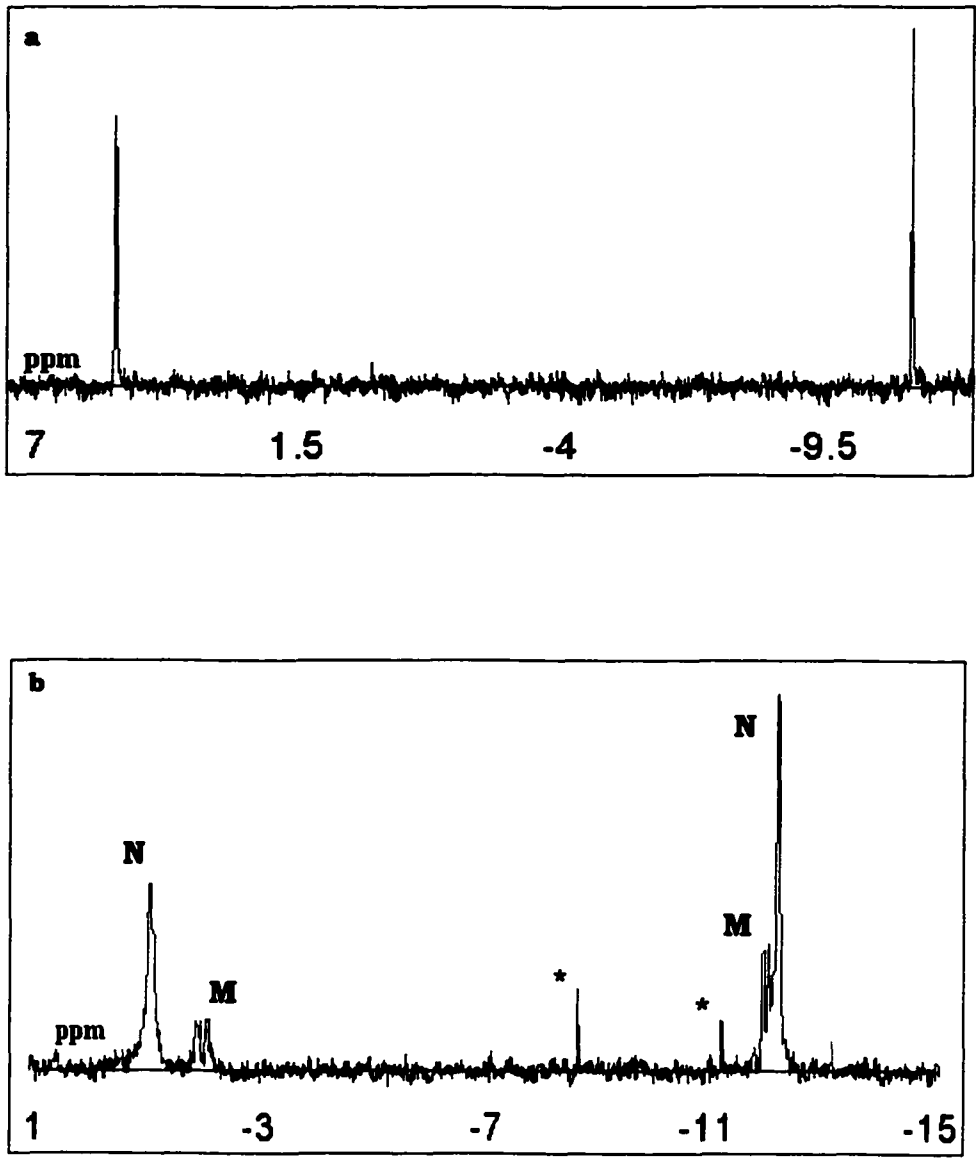

Figure 5.5. a: ^{31}P NMR spectrum of $[Eu(\alpha\text{-}1\text{-}P_2W_{17}O_{61})]^{7-}$. b: ^{31}P NMR spectrum of $[Eu(\alpha\text{-}1\text{-}P_2W_{17}O_{61})_2]^{17-}$. * α-1 ligand.

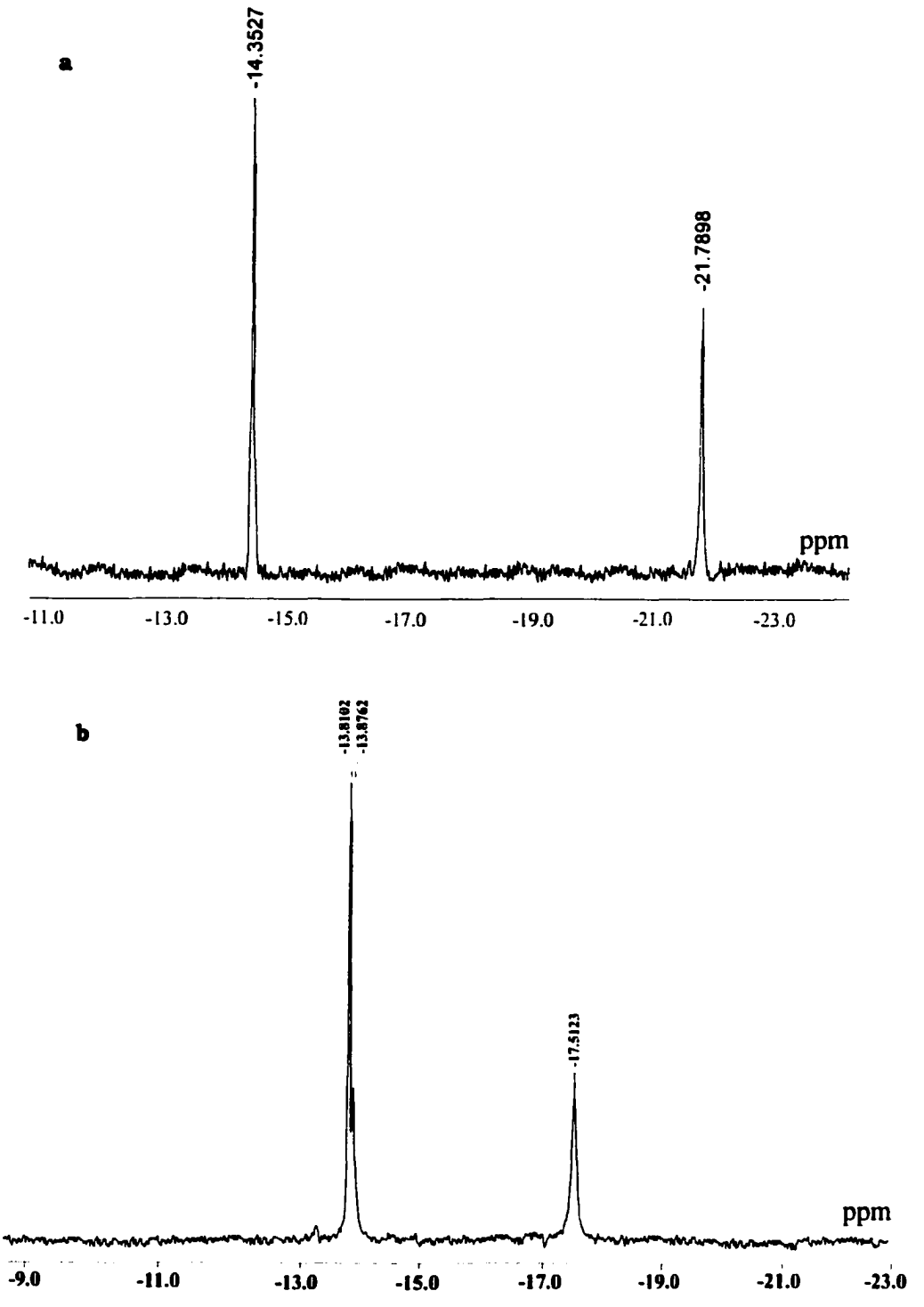

Figure 5.6. a: ^{31}P NMR spectrum of $[Nd(\alpha\text{-}1\text{-}P_2W_{17}O_{61})]^{7-}$. b: ^{31}P NMR spectrum of $[Nd(\alpha\text{-}1\text{-}P_2W_{17}O_{61})_2]^{17-}$.

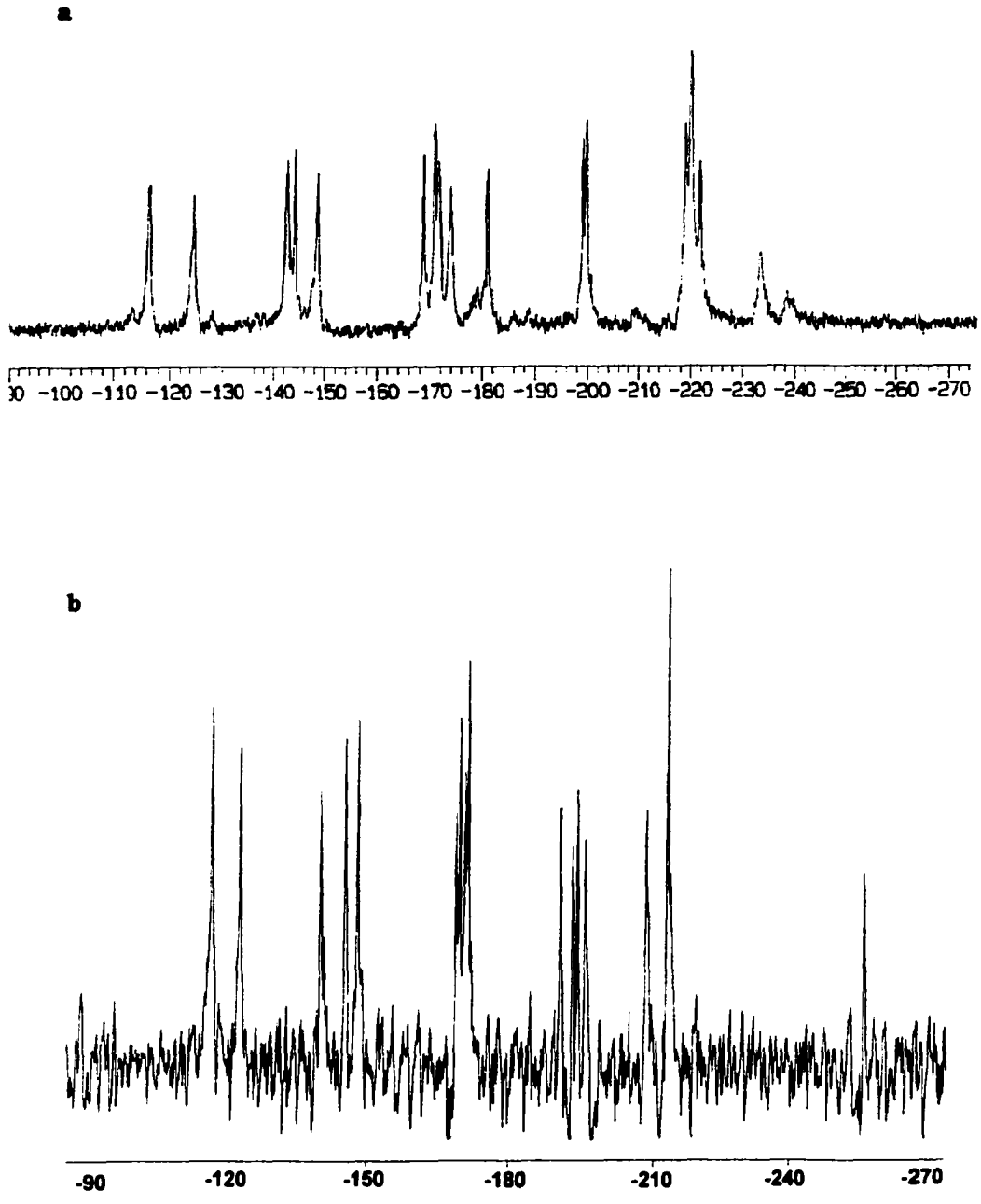

Figure 5.7. a: ^{183}W NMR spectrum of $[La(\alpha\text{-}1\text{-}P_2W_{17}O_{61})]^{7-}$. b: ^{183}W NMR spectrum of $[La(\alpha\text{-}1\text{-}P_2W_{17}O_{61})_2]^{17-}$.

Table 5.1. Elemental Analysis Data for $K_{17}[La(\alpha\text{-}1\text{-}P_2W_{17}O_{61})_2]$ via ICP

Formula: $K_{16}HLa(P_2W_{17}O_{61})_2$		
	Observed (%)	Calculated (%)
K	7.09	6.88
P	1.55	1.36
W	70.40	68.75
La	1.62	1.53

each peak only integrates for one tungsten atom and the concentration of species **M** is much smaller than species **N**, we expect that the peak intensity of species **M** will be much smaller than that of species **N**. The signal to noise ratio for the ^{183}W NMR spectrum is not good, therefore, the 34 weak peaks are most likely buried under the noise; only the 17 peaks for species **N** are clearly observed.

The ^{31}P and ^{183}W NMR results indicate that the complex we isolated is Ln α-1 1:2 complex. The elemental analysis data via ICP for $K_{17}[La(\alpha\text{-}1\text{-}P_2W_{17}O_{61})_2]$ (Table 5.1) also clearly shows the stoichiometric ratio of $[\alpha\text{-}1\text{-}P_2W_{17}O_{61}]^{10-}$ to La is 2.

5.2.3.2. By Eu(III) fluorescence spectroscopy

Eu(III) fluorescence spectroscopy is a very useful technique to characterize lanthanide complexes as demonstrated in Chapter 3. The number of peaks in the excitation spectra give information on the number of Eu(III) species in the solution. The number of water molecules

from lifetime measurements can tell us the coordination information about Eu(III) ion. Figure 5.8a and 5.8b shows the excitation spectra of Eu α-1 1:1 and 1:2 complexes, respectively. In Figure 5.8a, the peak at 579.99 nm represents the Eu α-1 1:1 species; peak at 580.33 nm represents an Eu α-2 1:2 impurity. In Figure 5.8b, the peak at 580 nm represents the Eu α-1 1:2 species, and the peak at 580.41 nm represents an Eu α-2 1:2 impurity. Comparison of these two spectra shows that the peak positions of Eu α-1 1:1 and 1:2 peak are very close. A likely explanation for this similarity can be understood by considering three points. First, the $^7F_0 \rightarrow {}^5D_0$ absorption energy for different Eu(III) environments occurs in a very small range. Second, the chemical coordination environment and electronic environment of the Eu α-1 1:1 species where the Eu is bound to 4 oxygen atoms of the $[\alpha\text{-}1\text{-}P_2W_{17}O_{61}]^{10-}$ and 4 water molecules is not that different from the coordination and electronic environment of the Eu α-1 1:2 species. The α-1 ligand is weakly bound to the Eu compared to the α-2 ligand. This is evident from stability constant measurements, discussed in Chapter 6. This weaker bonding in the Ln $[\alpha\text{-}1\text{-}P_2W_{17}O_{61}]^{10-}$ species will likely render the coordination and electronic environments of the Eu α-1 1:1 species similar to the Eu α-1 1:2 species. A third possibility may be that there is some error in the excitation wavelength measurement; this possibility should be verified by repeating the experiment. Although it is difficult to

differentiate the Eu α-1 1:1 and 1:2 species from their excitation spectra, it is clear that the species are different from lifetime measurements.

From measurements of lifetimes separately in H_2O and D_2O solution, the number of coordinated molecules [5,13], q, bound to Eu can be calculated from:

$$q = 1.11 \times [\tau^{-1}(H_2O) - \tau^{-1}(D_2O) - 0.31] \qquad (\tau : \text{lifetime in msec})$$

The luminescent lifetimes of the $K_7[Eu(\alpha\text{-}1\text{-}P_2W_{17}O_{61})]$ and $K_{17}[Eu(\alpha\text{-}1\text{-}P_2W_{17}O_{61})_2]$ species were measured in H_2O and D_2O.

For $K_7[Eu(\alpha\text{-}1\text{-}P_2W_{17}O_{61})]$:

$$\tau\,(H_2O) = 0.241 \text{ msec}, \quad \tau\,(D_2O) = 2.826 \text{ msec}, \quad q = 3.87$$

For $K_{17}[Eu(\alpha\text{-}1\text{-}P_2W_{17}O_{61})_2]$:

$$\tau\,(H_2O) = 3.110 \text{ msec}, \quad \tau\,(D_2O) = 2.955 \text{ msec}, \quad q = -0.36$$

These results are in excellent agreement with the 1:1 formulation of the $K_7[Eu(\alpha\text{-}1\text{-}P_2W_{17}O_{61})]$ complex where the Eu(III) binds to four oxygen atoms of the polyoxoanion and the other four coordination sites are taken by water molecules (Chapter 4), and the 1:2 formulation of the $K_{17}[Eu(\alpha\text{-}1\text{-}P_2W_{17}O_{61})_2]$ complex where the Eu(III) binds to eight oxygen atoms of the polyoxoanion and no coordination site is taken by water molecule.

To summarize, the Ln α-1 1:2 complexes that I have isolated, have been characterized by fluorescence spectroscopy, ^{31}P, ^{183}W NMR spectroscopy and elemental analysis. All of the results are consistent

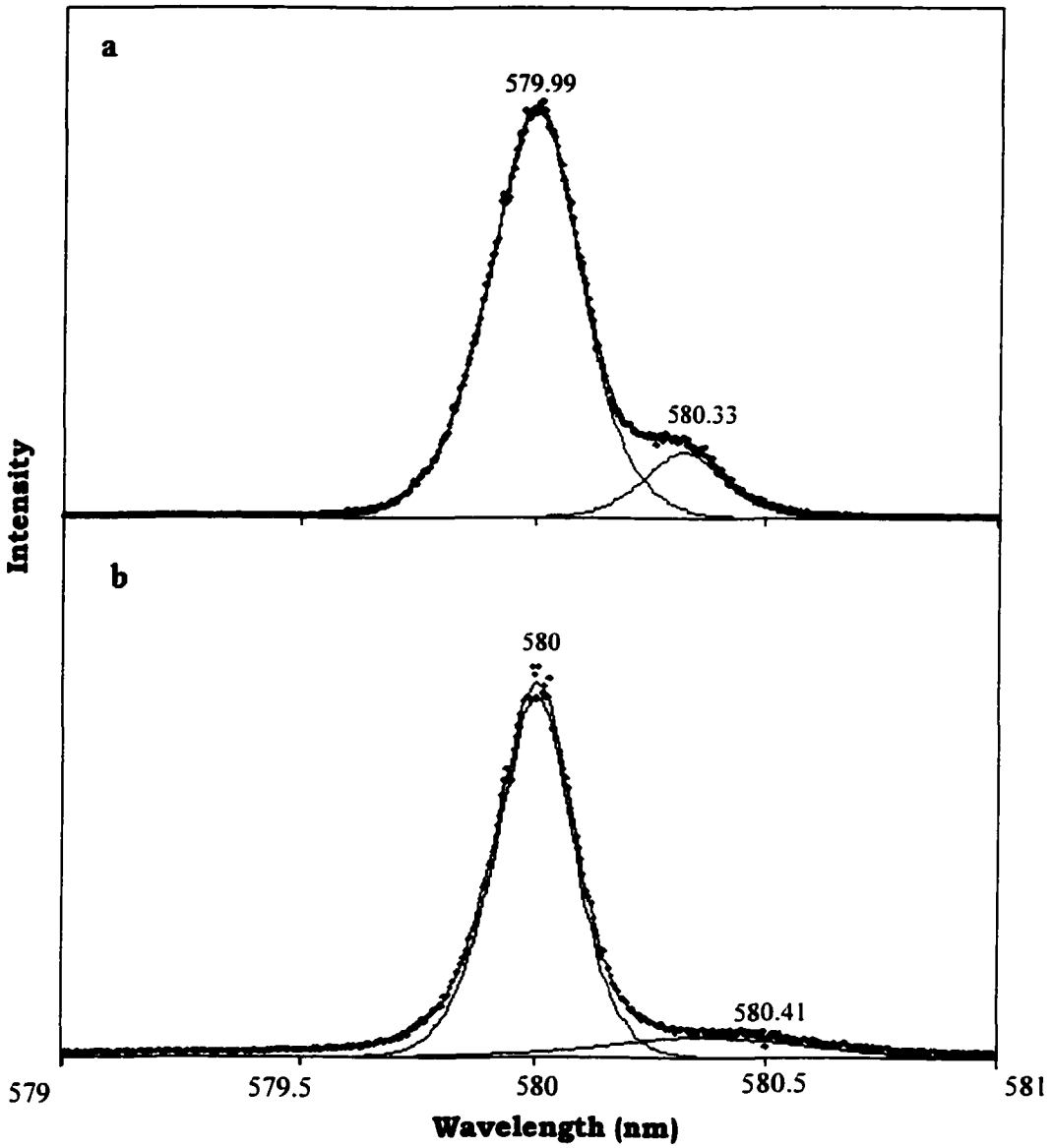

Figure 5.8. Eu(III) $^7F_0 \rightarrow {}^5D_0$ excitation spectra, emission wavelength monitored at 614 nm. a: $[Eu(\alpha\text{-}1\text{-}P_2W_{17}O_{61})]^{7-}$; b: $[Eu(\alpha\text{-}1\text{-}P_2W_{17}O_{61})_2]^{17-}$.

with the formula: $[Ln(\alpha\text{-}1\text{-}P_2W_{17}O_{61})_2]^{-17}$. The lacunary $[\alpha\text{-}1\text{-}P_2W_{17}O_{61}]^{10-}$ species is formally derived from the Wells-Dawson structure by removal of the W=O unit from the 'belt' region, or the equatorial zone [1]. The steric impedance of two α-1 polyoxoanion units renders the Ln α-1 1:2 complexes very unstable in aqueous solution. Compared with Ln α-2 1:2 complexes discussed in Chapter 2, where the two α-2 structures are far away from each other, the two polyoxoanion units in the Ln α-1 1:2 species are likely much closer to each other; the repulsive interactions llikely diminish the stability of the Ln α-1 1:2 complexes.

5.2.4. Observation of Ternary Complex Formation of $[Ln(\alpha\text{-}1\text{-}P_2W_{17}O_{61})]^{7-}$ with Organic Ligands

We know from Chapter 4 that in the Ln α-1 1:1 complex, the Ln(III) binds to four oxygen atoms of the polyoxoanion and the other four coordination sites are occupied by water molecules. These four water molecules can be replaced by another ligand. Lanthanide ions behave as typical "hard" acids and interact preferentially with hard bases such as fluoride and oxygen rather than with softer bases such as nitrogen, sulfur, phosphorous, etc. The bonding strength is dominated by the differences in the electrostatic and steric characteristics of the complex. In the previous section, we have demonstrated that these four water molecules can be replaced by another α-1 ligand to form Ln α-1 1:2 complex. Therefore, by rationally selecting ligands, it is possible to

synthesize ternary complexes that combine inorganic and organic properties.

5.2.4.1. Titrating $K_7[Eu(\alpha\text{-}1\text{-}P_2W_{17}O_{61})]$ with EDDA ($(CH_2NHCH_2COOH)_2$)

A mixture of EDDA and Eu α–1 1:1 complex solution of 1:1 stoichiometry in Lithium acetate buffer can remain at room temperature for one and half months without any decomposition according to ^{31}P

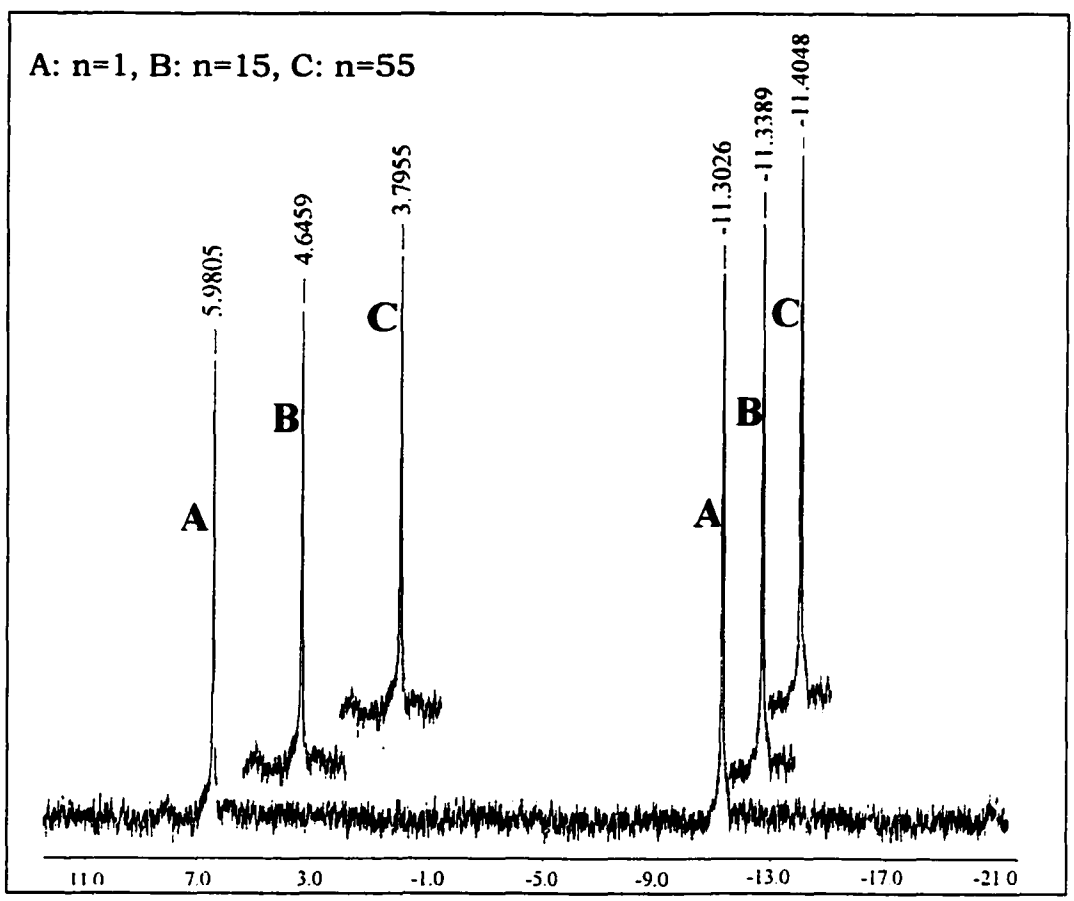

Figure 5.9. The ^{31}P NMR spectra, molar ratio, n= EDDA/Eu(α-1), between 1-55.

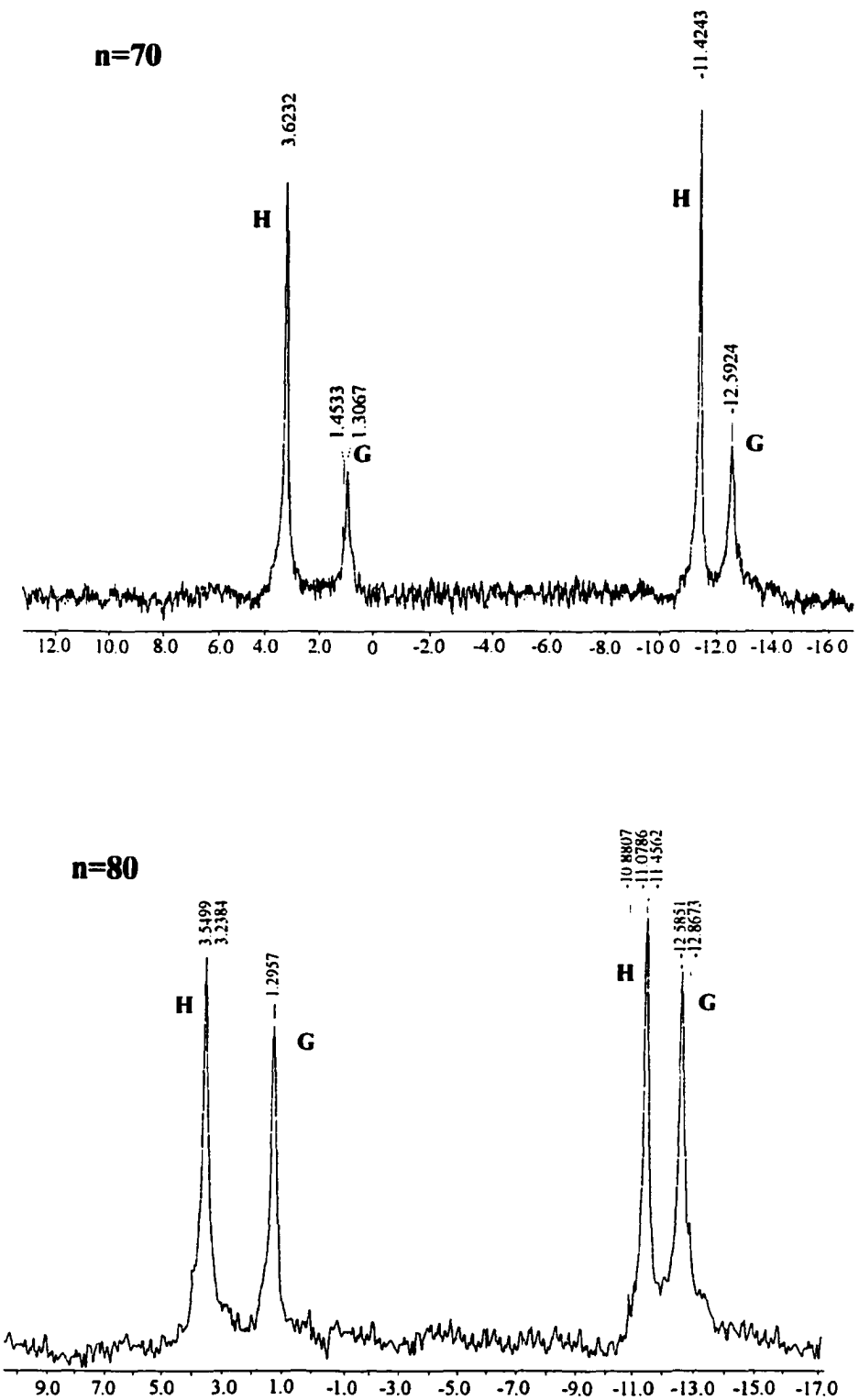

Figure 5.10. The ^{31}P NMR spectra, molar ratio, n= EDDA/Eu(α-1), 70 and 80.

NMR. This is amazing considering the relatively low stability of Ln α–1 complex in aqueous solution. The ^{31}P NMR spectrum shows the average peak of the ternary complex and Eu α–1 1:1 complex; this is typical for all the europium ternary complexes (see below). From the titration experiment (Fig. 5.9), we can see that as the molar ratio of EDDA/Eu α–1 1:1 complex, **n**, increases from 1 to 55, the peaks shift from 6.0 ppm to 3.8 ppm, and from 11.3 ppm to 11.4 ppm. The following equilibrium exists in the solution:

$$Eu(\alpha\text{-}1) + EDDA \rightleftharpoons (EDDA)Eu(\alpha\text{-}1) \qquad (I)$$

There is a fast dynamic exchange between Eu(α–1) and (EDDA)Eu(α–1). In the ^{31}P NMR spectrum, this phenomenon is reflected by an average peak of Eu(α-1) and (EDDA)Eu(α-1).

$$\sigma_{avg} = m_1 \sigma_{Eu(\alpha-1)} + m_2 \sigma_{(EDDA)Eu(\alpha-1)} \qquad (II)$$

m_1, m_2 : molar fraction of Eu(α-1) and (EDDA)Eu(α-1), respectively. $m_1 + m_2 = 1$. σ : NMR chemical shift for the species indicated, ppm.

When the exchange between Eu(α–1) and (EDDA)Eu(α–1) is fast on the NMR timescale, the NMR technique can only detect the average chemical shift of Eu(α–1) and (EDDA)Eu(α–1), σ_{avg}. The equation(II) shows that the average shift, σ_{avg}, is determined by the molar fraction of these two species in the solution, m_1 and m_2, and their chemical shifts, $\sigma_{Eu(\alpha-1)}$ and $\sigma_{(EDDA)Eu(\alpha-1)}$, measured separately. As the molar ratio of EDDA/Eu(α-1), **n**, increases, the molar fraction of (EDDA)Eu(α–1), m_2, is

increased and the molar fraction of Eu(α-1), m_1, is deceased so the average peak moves toward the peak position of (EDDA)Eu(α−1), $\sigma_{(EDDA)Eu(\alpha-1)}$. From the change of NMR shift, we can calculate the binding constant from the equation (III). For detail, see reference [7].

$$L_t/\Delta = (L_t + S_t - [SL])/\Delta_{11} + 1/K\Delta_{11} \qquad \text{(III)}$$

$$\Delta = \sigma_{avg} - \sigma_{Eu(\alpha-1)}\ ,\ \Delta_{11} = \sigma_{(EDDA)Eu(\alpha-1)} - \sigma_{Eu(\alpha-1)}$$

L: the ligand EDDA; S: the complex Eu(α-1); K: binding constant.
t: total concentration; σ: NMR chemical shift for the species indicated, ppm.

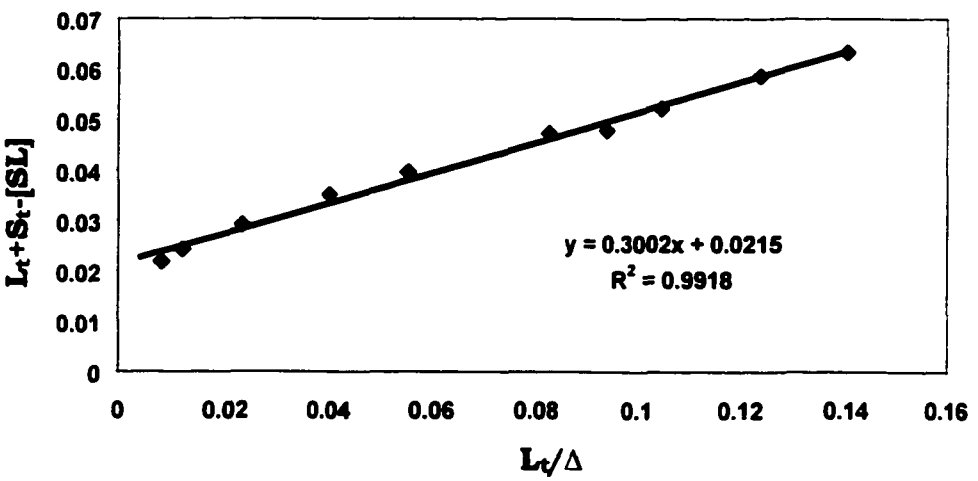

Above is the plot of (L_t + S_t - [SL]) vs. L_t/Δ. According to equation (III), K was calculated, ca. 15 M^{-1}.

As the molar ratio **n** increase to 70 (Fig. 5.10), peak **H** that denotes (EDDA)Eu(α-1) doesn't change anymore, and a new peak **G** appears. As the molar ratio **n** continually increases to 80, peak **H** decreases and peak

G increases. I couldn't isolate each species in this spectrum, but I believe that these spectral changes represent the equilibrium:

$$(EDDA)Eu(\alpha\text{-}1) + EDDA \rightleftharpoons (EDDA)_2Eu(\alpha\text{-}1)$$

5.2.4.2. Titration of Ln α-1 1:1 with chiral ligands

5.2.4.2.1. L-tartaric acid

We have observed the formation of ternary complex of Eu α-1 with EDDA as above. As discussed in Chapter 4, Ln α-1 1:1 molecules have C_1 point group symmetry, which means that Ln α-1 species are chiral. By binding another chiral ligand to Ln α-1 1:1 we should form diastereomeric pairs of polyoxometalate chiral ligand complexes and discriminate between the α-1 enantiomers. Ultimately such stereoselective interactions may allow resolution of polyoxometalate enantiomers. During the course of our study, the interaction of $[(H_2O)_4Ce(III)(\alpha\text{-}1\text{-}P_2W_{17}O_{61})]^{7-}$ with chiral amino acids has been reported [14]. As we find with L-tartaric acid, below, chiral amino acids form diastereomeric pairs of Ce $P_2W_{17}O_{61}$-amino acid complexes.

Figure 5.11, 5.12 are titrations of L-tartrate in Nd and Eu α-1 1:1 complexes, respectively, monitored by ^{31}P NMR. The L-tartrate ligand binds to the two optical isomers of Lnα-1 (Eu, Nd) equally and results in two sets of resonance that represent L-L and L-D ternary complexes.

$$(L+D)\ Ln\alpha\text{-}1 + L\text{-tartrate} \rightleftharpoons (L\text{-tartrate})(L\text{-}Ln\alpha\text{-}1) + (L\text{-tartrate})(D\text{-}Ln\alpha\text{-}1)$$

The fast dynamic exchange between Lnα-1 and ternary complexes gives an average peaks. As the molar ratio of L-tartrate increases, the percentage of ternary complex is increased so the average peak moves toward the peak position of ternary complex (see equation (II), section 5.2.4.1). The binding strength is weak. From the change of NMR shift, the binding constant can be calculated [7] as $K \approx 10\ M^{-1}$.

5.2.4.2.2. D-tartaric acid, $[(OH)CH(CO_2H)]_2$

Figure 5.13a is the ^{31}P NMR spectrum of solution of D-tartaric acid and Eu(α-1) complex mixture in Lithium acetate buffer (pH=4.7, C=0.18M) (acid/Eu(α-1)=1:1). One of the peaks is enlarged in the middle; clearly they are two sets of peaks that are about the same intensity. It very much like the spectrum we just saw for L-tartaric acid. But when the solution remained at room temperature for two days, one set of the peaks disappeared (Fig. 5.13b). The peaks left are at 5.925 ppm and 11.320 ppm. This experiments suggests that one of the two diastereomeric pairs may be more stable than the other.

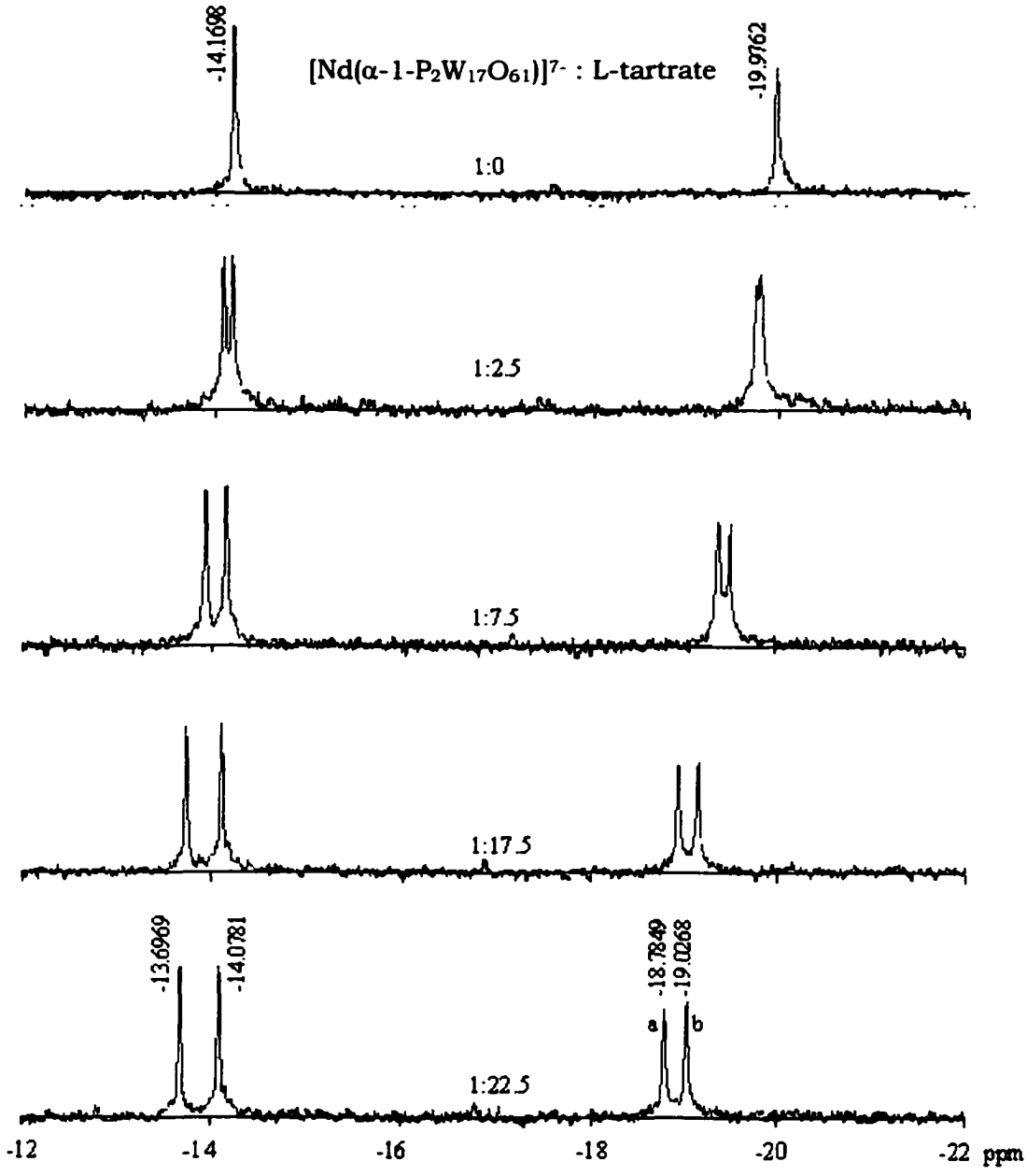

Figure 5.11. Titration of L-tartrate into 10 mM of $[Nd(\alpha\text{-}1\text{-}P_2W_{17}O_{61})]^{7-}$ solution in lithium acetate buffer (pH=5.5, 0.5 M) monitored by ^{31}P NMR.

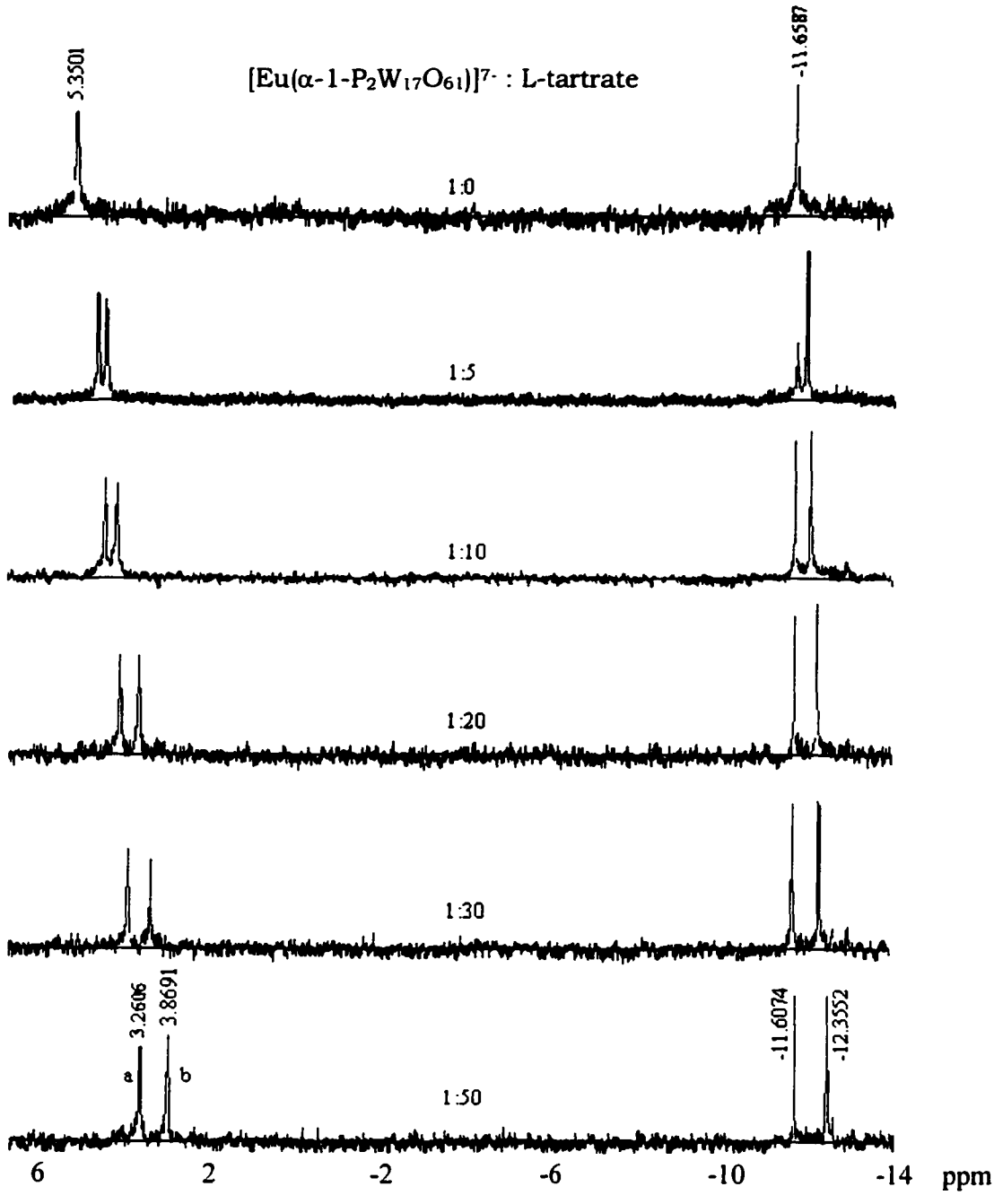

Figure 5.12. Titration of L-tartrate into 5 mM of $[Eu(\alpha\text{-}1\text{-}P_2W_{17}O_{61})]^{7-}$ solution in lithium acetate buffer (pH=4.5, 0.5 M) monitored by ^{31}P NMR.

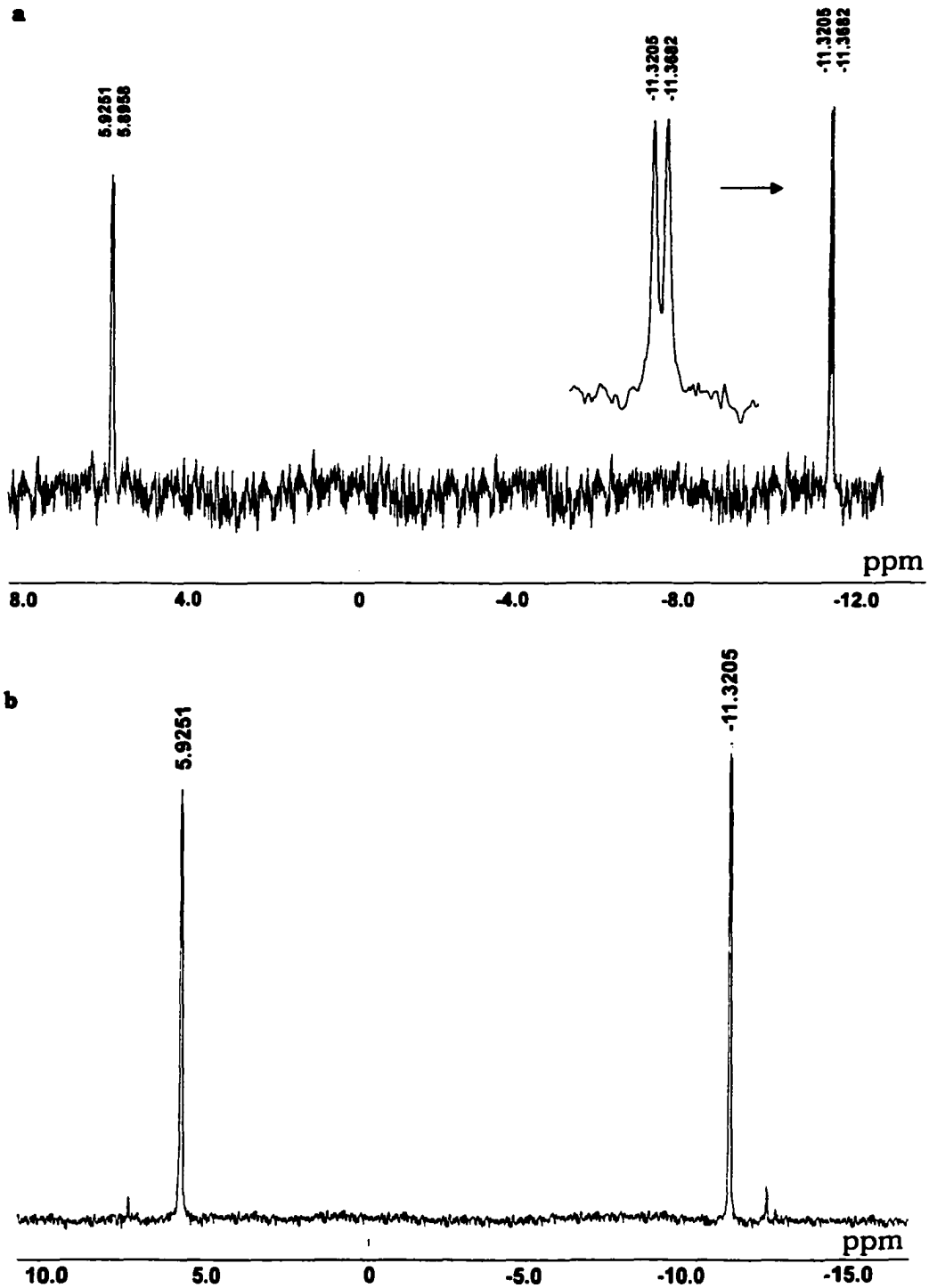

Figure 5.13. ^{31}P NMR spectrum of D-tartaric acid and Eu(α-1) 1:1 complex mixture. Spectrum a: measured after mixing. Spectrum b: sample 'a' measured after two days.

5.3. Conclusion

The kinetics of $(\alpha\text{-}1\text{-}P_2W_{17}O_{61})^{10-}$ isomerizing to $(\alpha\text{-}2\text{-}P_2W_{17}O_{61})^{10-}$ in different media has been studied; this provides guidance for synthesis of new $(\alpha\text{-}1\text{-}P_2W_{17}O_{61})^{10-}$ complexes. A new complex of lanthanide $(\alpha\text{-}1\text{-}P_2W_{17}O_{61})^{10-}$ has been isolated. Elemental analysis, ^{31}P, ^{183}W NMR spectroscopy and fluorescence spectroscopy have been applied to characterize this new complex. ^{31}P and ^{183}W NMR results indicate that it is a complex of α-1. Fluorescence lifetime measurement reveals that no water molecules participate in the Ln coordination. The elemental analysis data show the molar ratio of $(\alpha\text{-}1\text{-}P_2W_{17}O_{61})^{10-}$/Ln is 2. Heretofore, all of the results confirm the formula of this new complex is $[Ln(\alpha\text{-}1\text{-}P_2W_{17}O_{61})_2]^{17-}$.

Ternary complexes of $[Ln(\alpha\text{-}1\text{-}P_2W_{17}O_{61})]^{7-}$ with organic ligands have been observed from titration of organic ligands to $[Ln(\alpha\text{-}1\text{-}P_2W_{17}O_{61})]^{7-}$ monitored by ^{31}P NMR. Monitoring the changes of ^{31}P NMR shift, the conditional binding constants have been calculated from the titration. A chiral organic ligand, L-tartaric acid, was bound to the two optical isomers of $[Ln(\alpha\text{-}1\text{-}P_2W_{17}O_{61})]^{7-}$, as revealed from ^{31}P NMR titration to form diastereomeric pairs of Ln α-1-$P_2W_{17}O_{61}$ - L-tartaric acid complexes.

5.4. References

1) Ciabrini, J. P.; Contant, R. *J. Chem. Res., Synop.* **1993**, *10*, 391.

2) Batis, J., *Doctoral Dissertation*, Chemistry Department of The City University of New York, **1997.**

3) Horrocks, W. DeW., Jr. *Methods Enzymol.* **1993**, *226*, 495.

4) Horrocks, W. DeW., Jr.; Sudnick, D. R. *Acc. Chem. Res.* **1981**, *14*, 384

5) Horrocks, W. DeW., Jr.; Sudnick, D. R. *J. Am. Chem. Soc.* **1979**, *101*, 334.

6) Horrocks, W. DeW., Jr.; Wu, S. R. *Inorg. Chem.* **1995**, *34*, 3724.

7) Kenneth, A. C., *Binding constants-The measurement of molecular complex stability,* John Wiley & Sons, Inc. **1987**.

8) Yusov, V. P.; *Radiokhimiya,* **1980**, vol. 22, no. 5, 727-732.

9) Kulyko, Yu. M.; Lebedev, I. A.; Trofimov, T. I., *et al., Zh. Neorg. Khim.*, **1981**, vol. 26, no. 5, 1254-1260.

10) Contant, R.; Ciabrini, J. P., *J. Chem. Res.* (s), 1982, no. 2, 50-51; *J. Chem. Res.* (M), **1982**, no. 3-7, 641-660.

11) Kirby, J. F.; Baker, L. C. W., *Inorg. Chem.* **1998**, 37, 5537-5543.

12) Bartis, J.; Sukal, S.; Dankova, M.; Kraft, E.; Kronzon, R.; Blumenstein, M.; Francesconi, L. C. *J. Chem. Soc., Dalton Trans.* **1997**, 1937.

13) Supkouski, R. M.; Horrocks, W. DeW., Jr., *Inorg. Chem.* Acta. **2002**, in press.

14) Sadakane, M.; Dickman, M. H.; Pope, M. T., *Inorg. Chem.* **2001**, 40, 2715-2719.

Chapter 6

Determination of Stability Constants of Lanthanide Polyoxometalates

In this chapter, I report the determination of stability constants for the lanthanide complexes of $[\alpha\text{-}1\text{-}P_2W_{17}O_{61}]^{10-}$ and $[\alpha\text{-}2\text{-}P_2W_{17}O_{61}]^{10-}$. Two methods were employed for these measurements, ligand-ligand and Ln-Ln competition monitored by ^{31}P NMR spectroscopy and Ln-ligand titrations monitored by luminescence. We traverse the lanthanide series in this study.

Determination of stability constants for these molecules is of primary importance for a comprehensive understanding of complexation and the relationships that govern their formation and structure. Knowledge of the stability constants and the selectivity of these ligands for different lanthanide and actinide ions is also important for understanding their coordination chemistry and their application in actinide separation. In spite of the significance, the stability constant determination is still far from systematic. The main reasons for this are: first, the system is extremely complicated, especially in aqueous solution. The counter ion type and concentration will take part in the equilibrium of complexation; the pH will affect the species formed in solution. Second, the complexation reactions often exhibit extremely high stability and frequently very fast complexation rates. These factors sometimes

lead to difficulty in measuring their stability constants using conventional methods, e.g. pH-potentiometry.

As discussed above, speciation and structural studies in solution and solid state are pre-requisites for determination of stability constant. We have thoroughly studied the Ln $[\alpha\text{-}1\text{-}P_2W_{17}O_{61}]^{10-}$ and Ln $[\alpha\text{-}2\text{-}P_2W_{17}O_{61}]^{10-}$ systems; therefore, it is possible for us to develop methods to measure the binding constants.

Two methods have been developed. For Ln α-1 1:1 complex, a ligand-ligand competition method monitored by ^{31}P NMR was employed. For Ln α-2 1:1 and 1:2 complexes, metal-ligand titration monitored by Eu(III) fluorescence excitation combined with lanthanide-lanthanide competition experiments were performed. Before the formation constant measurements, the stability of α-1, α-2 ligand and their lanthanide complexes at different pH was studied. The protonation constants for α-2 ligand have been obtained through potentiometric titration.

6.1. Experiments

6.1.1. General

All common laboratory chemicals were reagent grade, purchased from commercial sources and used without further purification. Distilled, deionized water was used throughout. All experiments were performed at room temperature unless specified. The Wells-Dawson anion, $(P_2W_{18}O_{62})^{6-}$ as the potassium salt, was prepared using literature methods [1]. The lacunary isomer, $K_{10}[\alpha\text{-}1\text{-}P_2W_{17}O_{61}]$ was prepared

following the method of Contant [2,3], $K_{10}[\alpha\text{-}2\text{-}P_2W_{17}O_{61}]$ were prepared following the method of Finke [4]. The potassium salt of $[\alpha\text{-}2\text{-}P_2W_{17}O_{61}]^{10-}$ was ion exchanged to the more soluble Li^+ salt or Na^+ salt using ion exchange at pH=4.7 or 5.5, respectively, as described previously [5]. The standardizations of the K^+, Li^+ or Na^+ salt of $[\alpha\text{-}2\text{-}P_2W_{17}O_{61}]^{10-}$, $[\alpha\text{-}2\text{-}P_2W_{17}O_{61}]^{10-}$ were accomplished by spectrophotometric titration with cobalt(II) as described previously for the $[\alpha\text{-}1\text{-}P_2W_{17}O_{61}]^{10-}$ complex [6]. The standard HCl solution is obtained by titration with standard NaOH solution. All lanthanides were standardized by EDTA (standard solution, Aldrich) with arsenazo as indicator (5 drops of pyridine was added to sharpen the end point). The pH measurements were performed using an Orion Research digital pH/millivolt meter 611. Three pH standard buffers (4, 7, 10, Fisher chemicals) were used to calibrate the pH meter before each measurement. NaOH was freshly prepared and stored in sealed container to avoid carbonate formation.

6.1.2. The stability study of $[\alpha\text{-}1\text{-}P_2W_{17}O_{61}]^{10-}$, $[\alpha\text{-}2\text{-}P_2W_{17}O_{61}]^{10-}$ and their complexes with Eu(III) at different pH by ^{31}P NMR

^{31}P NMR was used to monitor at different pH the stability of the $[\alpha\text{-}2\text{-}P_2W_{17}O_{61}]^{10-}$ and $[\alpha\text{-}1\text{-}P_2W_{17}O_{61}]^{10-}$ ligand in 0.1 M lithium chloride or sodium chloride. The spectra were run on a Jeol GX-400 spectrometer. ^{31}P spectra at 161.8MHz were acquired using the broad band decoupler coil of a 5mm reverse detection probe. Typical acquisition parameters for ^{31}P spectra included: spectral width: 10,000Hz; resolution: 1.59266Hz;

acquisition time: 1.68732s; pulse delay: 1s; pulse width: 12.5μsec (45 degree tip angle). Concentration of the samples used for the measurements was in 1-10 mM range.

6.1.3. Potentiometric titration to determine protonation constant of $[\alpha\text{-}2\text{-}P_2W_{17}O_{61}]^{10-}$.

The protonation constants of $[\alpha\text{-}2\text{-}P_2W_{17}O_{61}]^{10-}$ were determined by potentiometric titration [7]. The reaction solution was made by adding 1.5 mL of $[\alpha\text{-}2\text{-}P_2W_{17}O_{61}]^{10-}$ (7.72565 mM in 0.1 M NaCl) solution, 0.4 mL standard acid HCl (0.12173 M in 0.1 M NaCl) and 3.1 mL supporting electrolyte NaCl (0.1 M). The final solution has a pH ~2.4.

Experimental procedure: To the gently stirred acid solution of the ligand prepared as described above, standard base NaOH (0.09647 M) was added in 0.004 mL increments to provide about 100 experimental points for each run. Equilibrium conditions, determined by a constant meter reading falling within an interval of 0.5 mv/min was obtained for each experimental point before proceeding with the next step. The pH profile obtained is then used to calculate the protonation constants of $K_{10}[\alpha\text{-}2\text{-}P_2W_{17}O_{61}]$ by the BEST program [7].

6.1.4. Selection of competitive ligand for competition experiment

0.13g (26 μmol) of $[\alpha\text{-}1\text{-}P_2W_{17}O_{61}]^{10-}$ dissolved in a mixture of 1.25 mL of lithium acetate buffer (0.5 M, pH=3-6.5) and 0.5 mL D_2O. 53 μL of 1 M $EuCl_3$ (26 μmol) was added, the solution was clear after stirring.

Then various amount of competitive ligand was added. ^{31}P NMR was collected after equilibrium was reached.

6.1.5. Determination of the Formation Constant

6.1.5.1. General

The NMR measurements were run on a Jeol GX-400 spectrometer. ^{31}P spectra at 161.8MHz were acquired using the broadband decoupler coil of a 10mm inverse detection probe. Typical acquisition parameters for ^{31}P NMR spectra included: spectral width: 10,000Hz; resolution: 0.39507Hz; acquisition time: 2.53118s; relaxation time: 1s; x-pulse: 12.5μsec (45 degree tip angle).

All NMR experiments were performed at 20 ± 0.5°C on solution with the ionic strength adjusted to 0.10 M with sodium chloride or lithium chloride. An external standard (STD) was used to quantitatively monitor the concentrations of $[\alpha\text{-}2\text{-}P_2W_{17}O_{61}]^{10-}$, $[\alpha\text{-}1\text{-}P_2W_{17}O_{61}]^{10-}$ and the Ln(III) complexes with these two ligands. The external standard was phosphoric acid (0.009-0.013 M in water) in a small tube, which is placed inside a 10 mm NMR tube. Calibration curves of $[\alpha\text{-}2\text{-}P_2W_{17}O_{61}]^{10-}$, $[\alpha\text{-}1\text{-}P_2W_{17}O_{61}]^{10-}$ and lanthanide complexes vs. STD were obtained by monitoring ^{31}P NMR of four concentrations, 0.5 mM, 1.0 mM, 2.0 mM and 3.0 mM under the same condition as of competition experiments. The figure below shows an example of calibration curve for $[\alpha\text{-}2\text{-}P_2W_{17}O_{61}]^{10-}$.

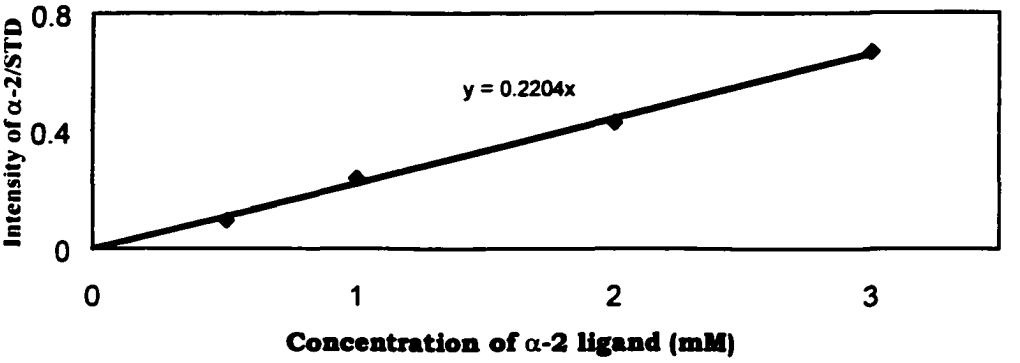

Luminescence titrations were performed by monitoring the luminescence excitation spectra of Eu(III) [8-11]. A pulsed (10 Hz) Nd : YAG laser-pumped dye laser (Continuum), with a mixture of Rhodamine 590 and 610 dyes, was used to excite the $^7F_0 \rightarrow {}^5D_0$ transition of Eu(III) in the 578-581 nm region; emission ($^5D_0 \rightarrow {}^7F_2$) was monitored at 614nm.

6.1.5.2. Ln(III) α-1 1:1 complexes: Ligand-ligand Competition monitored by ^{31}P NMR

0.025g of $K_{10}[\alpha\text{-}1\text{-}P_2W_{17}O_{61}]$ was dissolved in 2 ml of lithium acetate buffer (pH=4.72, 0.5 M, 20% D_2O), 30 μL of $LnCl_3$ (0.17M-0.16M) and 20 μL of EDTA (0.0974M) were added. The solution was clear. After 8 hours at room temperature the solution reached its equilibrium, ^{31}P NMR spectrum was recorded. At least three experiments were run for each lanthanide.

6.1.5.3. Ln(III) α-2 1:1 and 1:2 complexes

6.1.5.3.1. By ligand-ligand competition monitored by ^{31}P NMR

Equilibrium $LnL_2 + L' \rightleftharpoons LnL' + 2L$:

0.05g (9.60 μmol) of $K_{10}[\alpha\text{-}2\text{-}P_2W_{17}O_{61}]$ was dissolved in 0.5 ml of sodium acetate buffer (pH=6, 2.5 M, 95% D_2O), then 2 equivalents of Ln(III) was added followed by 2 ml of EDTA (0.0974M). The solution was clear. After one day at room temperature the solution reached its equilibrium, ^{31}P NMR was recorded. The final pH is 6.10.

Equilibrium $2LnL + L' \rightleftharpoons LnL' + LnL_2$:

0.05g (9.60 μmol) of $K_{10}[\alpha\text{-}2\text{-}P_2W_{17}O_{61}]$ was dissolved in 2 ml of sodium formate buffer (pH=3.0, 0.5 M, 20% D_2O), one equivalent of Ln(III) solution was added and after 15 minutes, 80 μL of EDTA(0.0974 M) was added. The solution was clear. ^{31}P NMR was recorded after the solution stayed at room temperature for one day.

6.1.5.3.2. By laser-excited Eu(III) luminescence excitation

Titration of Eu(III) into a solution of $[\alpha\text{-}2\text{-}P_2W_{17}O_{61}]^{10-}$ or titration of $[\alpha\text{-}2\text{-}P_2W_{17}O_{61}]^{10-}$ into $EuCl_3$ solution was monitored by measurement of excitation photon flux needed by $[Eu(\alpha\text{-}2\text{-}P_2W_{17}O_{61})]^{7-}$ or $[Eu(\alpha\text{-}2\text{-}P_2W_{17}O_{61})_2]^{17-}$ complex. The emission ($^5D_0 \rightarrow {}^7F_2$) was controlled at 614 nm.

Measurement of formation constant for 1:1 complex (K_1):

2mL of standardized $[\alpha\text{-}2\text{-}P_2W_{17}O_{61}]^{10-}$ (1 μM) solution (2 nmol) is placed into a 4mL quartz sample cell, using volumetric pipette. A 20 μM

$EuCl_3$ stock solution was added in 40 μL increments and the excitation spectra were recorded. The commercially available Peakfit program, which employs a nonlinear regression method, was used to analyze the excitation spectra. After all titration data was collected, SigmaPlot 2000, a commercially available program, was used to fit the data, which resulted in conditional formation constant K_{1cond}.

Measurement of formation constant for 1:2 complex (K_2):

2mL of standardized Eu(III) (0.8 μM) solution (1.6 nmol) is placed into a 4mL quartz sample cell, using volumetric pipette. 0.10719 mM [α-2-$P_2W_{17}O_{61}$]$^{10-}$ solution was added in 20 μL increments and the excitation spectra were recorded. The commercially available Peakfit program, which employs a nonlinear regression method, was used to analyze the excitation spectra. After all titration data was collected, SigmaPlot 2000, a commercially available program, was used to fit the data, which resulted in conditional formation constant K_{2cond}.

6.1.5.3.3. Lanthanide-lanthanide competition method monitored by ^{31}P NMR

0.025g of K_{10}[α-2-$P_2W_{17}O_{61}$] (5.15 μmol) was dissolved in 2 mL of sodium acetate buffer (pH=5, 0.5 M, 20% D_2O). 35 μL of $EuCl_3$ solution (0.1533 M) was added. 35 μL of $LnCl_3$ solution (0.15-0.20 M) was added together after 15 minutes. The solution was clear. After the solution stayed at room temperature for one day, ^{31}P NMR was recorded.

6.2. Results and Discussions

6.2.1. The stability study for $[\alpha\text{-}1\text{-}P_2W_{17}O_{61}]^{10-}$, $[\alpha\text{-}2\text{-}P_2W_{17}O_{61}]^{10-}$ and their complexes with Eu(III) at different pH.

We have investigated the pH profile of $[\alpha\text{-}2\text{-}P_2W_{17}O_{61}]^{10-}$ and $[\alpha\text{-}1\text{-}P_2W_{17}O_{61}]^{10-}$ at various pH values with NMR. Figure 6.1 shows the ^{31}P NMR spectra of $[\alpha\text{-}2\text{-}P_2W_{17}O_{61}]^{10-}$ at pH 2 and 7. We observe a peak shift, especially the downfield peak that denotes the phosphorus atom closer to the 'defect' position as the pH is changed. The shift is changed from –6.7 ppm at pH 7 to –7.9 ppm at pH 2. This change in chemical shift is due to protonation of $[\alpha\text{-}2\text{-}P_2W_{17}O_{61}]^{10-}$ as the solution pH decreases [12]. Both spectra show two clean peaks that indicated $[\alpha\text{-}2\text{-}P_2W_{17}O_{61}]^{10-}$ is stable in the pH range of 2-7. The same results we have obtained for lanthanide α-2 1:1 and 1:2 complexes, both complexes are stable from pH 2 to pH 7.

The $[\alpha\text{-}1\text{-}P_2W_{17}O_{61}]^{10-}$ species is not as stable as $[\alpha\text{-}2\text{-}P_2W_{17}O_{61}]^{10-}$. As we discussed in section 5.2.1, $[\alpha\text{-}1\text{-}P_2W_{17}O_{61}]^{10-}$ will isomerize to $[\alpha\text{-}2\text{-}P_2W_{17}O_{61}]^{10-}$ after a period of time depending on the solvents used. Figure 6.2 shows the ^{31}P NMR spectra of $[\alpha\text{-}1\text{-}P_2W_{17}O_{61}]^{10-}$ at pH 2 and 6. As we observed for $[\alpha\text{-}2\text{-}P_2W_{17}O_{61}]^{10-}$, the spectra show a chemical shift change with pH, due to the protonation. Even at 5°C we observe a small amount of decomposition of the α-1 ligand at pH 2.

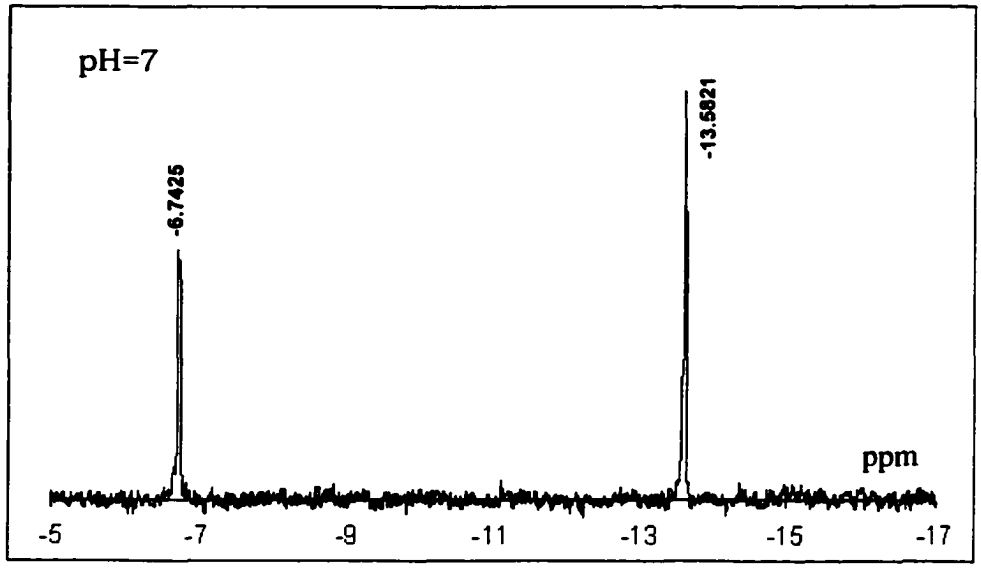

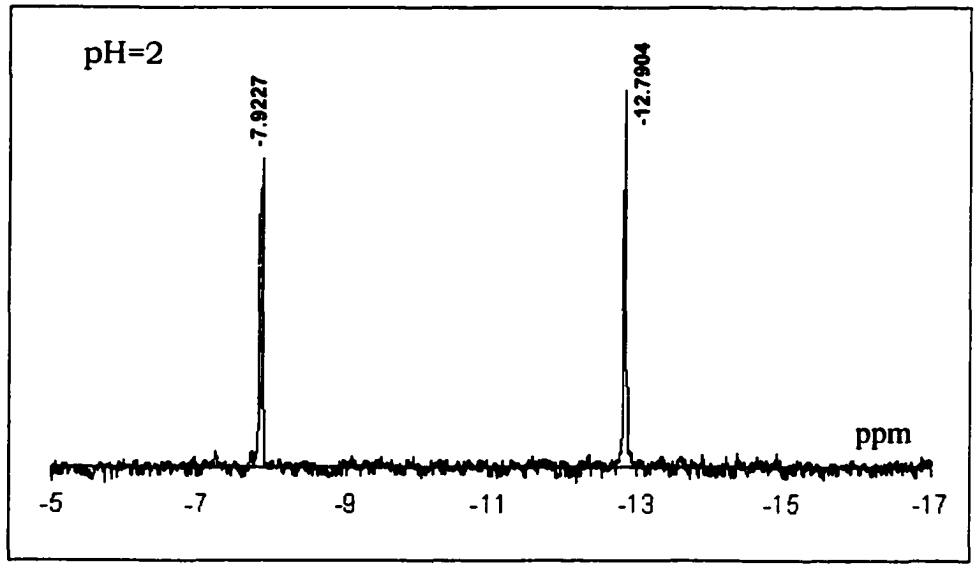

Figure 6.1. ^{31}P NMR spectra of $[\alpha\text{-}2\text{-}P_2W_{17}O_{61}]^{10-}$ at different pH values.

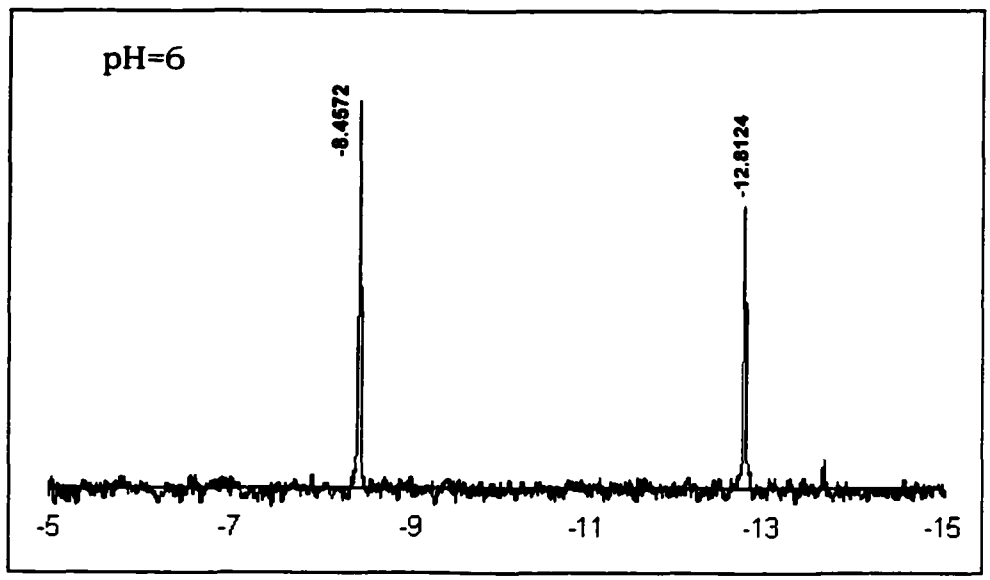

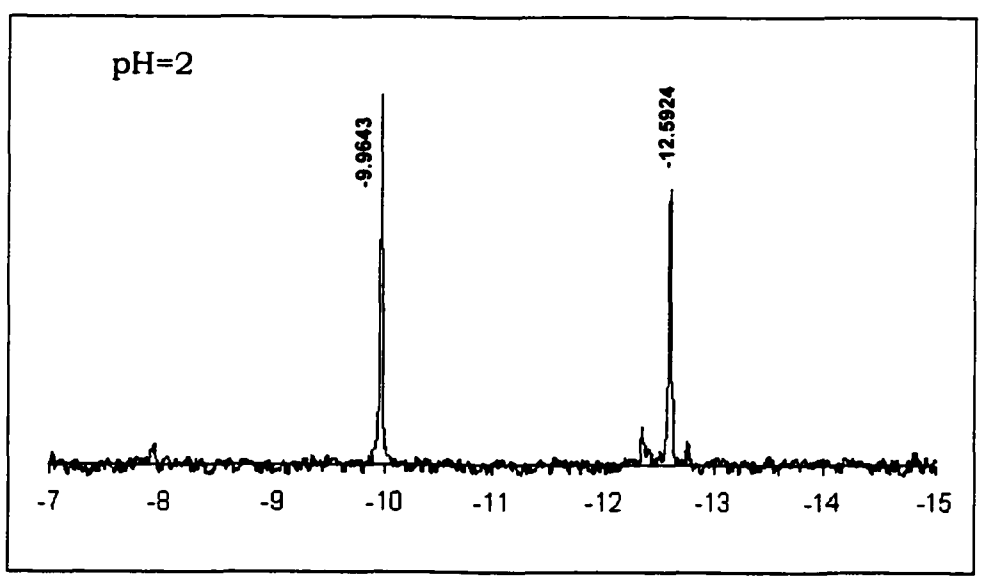

Figure 6.2. ^{31}P NMR spectra of $[\alpha\text{-}1\text{-}P_2W_{17}O_{61}]^{10-}$ at different pH values (T=5°C).

6.2.2. Potentiometric titration to determine protonation constant of $[\alpha\text{-}2\text{-}P_2W_{17}O_{61}]^{10-}$

We used potentiometric titration and the BEST program to determine the protonation constants of $[\alpha\text{-}2\text{-}P_2W_{17}O_{61}]^{10-}$. The BEST program [7] is very flexible; at first we may just guess the number of the protons, then adjust the number of the protons according to the calculation results until no further minimization of the standard deviation can be obtained. Figure 6.3 is the titration curve of $[\alpha\text{-}2\text{-}P_2W_{17}O_{61}]^{10-}$. We used the BEST program to calculate the protonation constants and obtained: $\log K_1 = 3.53$, $\log K_2 = 4.46$, $\log K_3 = 2.42$.

These results are in very good accordance with logK values for $(\alpha\text{-}2\text{-}P_2W_{17}O_{61})^{-10}$ obtained in the references [12-14]. The $(P_2W_{17}O_{61})^{-10}$ anion can bind three protons and the acidity constants depend on the nature and concentration of the counter ions and electrolytes, because the alkaline cations of the supporting electrolyte can also bond to the 'defect' position of $[P_2W_{17}O_{61}]^{-10}$ anion. The binding constants for Li^+, Na^+ and K^+ ion with $[\alpha\text{-}2\text{-}P_2W_{17}O_{61}]^{10-}$ are 3.61, 2.55 and 1.17, respectively [17,18]. Therefore, it is critical to compare the constants under the exact condition. Contant and Ciabrini [13] tried several different conditions to measure protonation constants of $[\alpha\text{-}2\text{-}P_2W_{17}O_{61}]^{10-}$. In the condition of 1.0 M Tris-(hydoxymethyl)methyl(ammonium) chloride (TrisH) and 0.1 M K^+ (which is the closest condition to ours: 0.1 M Na^+), the protonation constants were $\log K_1 = 4.49$, $\log K_2 = 3.75$, $\log K_3 = 2.0$, very close to our

values. The difference is that the $\log K_1$ = 3.53 is smaller than $\log K_2$ = 4.46 from our measurement. This phenomenon has been observed previously [13,19]. With increasing concentration of the supporting electrolyte, especially Li^+ and Na^+, the K_2 increases, and K_1 and β ($=K_1K_2K_3$) decrease. For instance, Contant and Ciabrini reported protonation constants for $[\alpha\text{-}2\text{-}P_2W_{17}O_{61}]^{10-}$ [13] at the conditions of 0.9 M TrisH, 0.1 M Li^+ and 0.1 M K^+, where $\log K_1$ = 2.86, $\log K_2$ = 3.24, $\log K_3$ = 2.0. The decrease in K_1 is due to increased association of $[\alpha\text{-}2\text{-}P_2W_{17}O_{61}]^{10-}$ with single-charged alkaline cations and decreased the Coulomb attraction between proton and $[\alpha\text{-}2\text{-}P_2W_{17}O_{61}]^{10-}$.

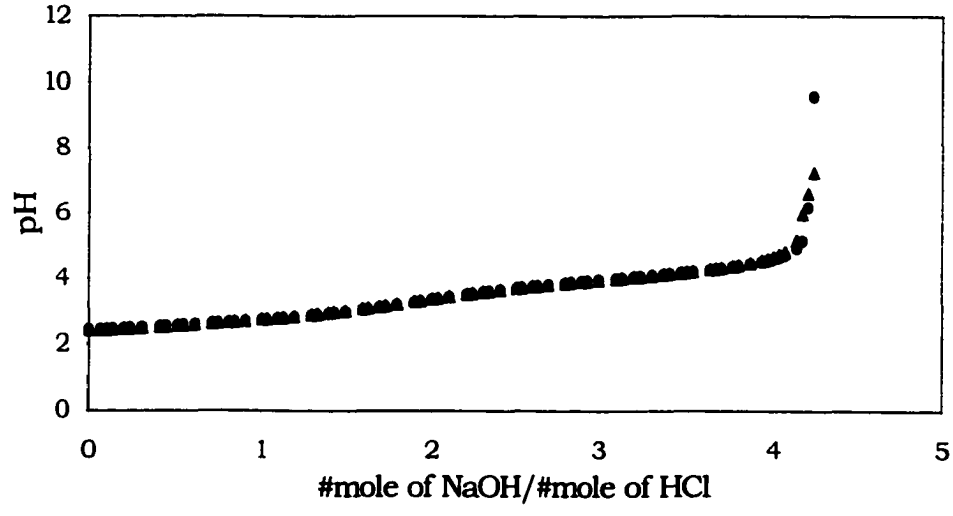

Figure 6.3. Titration curve of $[\alpha\text{-}2\text{-}P_2W_{17}O_{61}]^{10-}$. •: calculated pH value, ▲: experimental pH value.

6.2.3. Selection of competitive ligand for competition experiment

The formation constant K_l (=[ML]/[M][L]) for Cerium binding with $[\alpha\text{-}2\text{-}P_2W_{17}O_{61}]^{10-}$ and $[\alpha\text{-}1\text{-}P_2W_{17}O_{61}]^{10-}$ is about 10^6-10^9 M^{-1} from the work of Contant and Ciabrini [12]. Initially I tried to use a titration method to measure their formation constants with ^{31}P NMR. The sensitivity of NMR technique is relatively low (detection limit is millimolar) compared with fluorescence. The equilibrium concentrations for lanthanide complexation with $[\alpha\text{-}1\text{-}P_2W_{17}O_{61}]^{10-}$ and $[\alpha\text{-}2\text{-}P_2W_{17}O_{61}]^{10-}$ are too small to be detected by the NMR technique. At the same time I also tried to decrease the solution pH to decrease the basicity of $[\alpha\text{-}1\text{-}P_2W_{17}O_{61}]^{10-}$ in order to decrease the conditional formation constant. But since its protonation constants are small, the formation constant does not decrease dramatically by decreasing the solution pH. After a lot of tries and failures, I finally choose to use a competition method monitored by ^{31}P NMR to measure formation constant.

For the competition method, the selection of proper competitive ligand is critical in successfully measuring the formation constant. The competitive ligand has to meet the following standards:

(1) The system should have been well characterized, only the 1:1 complex forms and the thermodynamic formation constant are known.

(2) This ligand should not interfere in the interaction of $[\alpha\text{-}1\text{-}P_2W_{17}O_{61}]^{10-}$, $[\alpha\text{-}2\text{-}P_2W_{17}O_{61}]^{10-}$ with Lanthanide.

(3) The value of formation constant of this ligand with Ln should be compatible with the formation constant of α-1 ligand with Ln, which is believed about log $K \approx 10$.

I followed the book "Critical stability constant" by Martell [15] to choose suitable ligands. Nine ligands (Table 6.1) have been tried according to their values of stability constant with lanthanides. The respectively experimental results are below:

6.2.3.1. HIDA

Two solvents were tried, water and lithium acetate buffer (0.18M, pH=4.9). The ratio of HIDA/Eu(α–1) varied from 1 to 20, the ^{31}P NMR spectra only show one set of peak for Eu(α-1) complex, no change of peak shifts, no peak for α-1 ligand. It was clear that HIDA is not strong enough to replace the α-1 ligand.

6.2.3.2. Dipicolinic acid

Dipicolinic acid reacts with Eu(III) forming 1:1, 1:2 and 1:3 complexes, which makes the competitive system very complicated. Furthermore, $(\alpha\text{-}1\text{-}P_2W_{17}O_{61})^{10-}$ and $(\alpha\text{-}2\text{-}P_2W_{17}O_{61})^{10-}$ ligands and Eu complexes are not stable in the presence of dipicolinic acid. So this ligand is not suitable for competitive ligand.

Table 6.1. Nine organic ligands tested for selection of competitive ligand.

1	HIDA	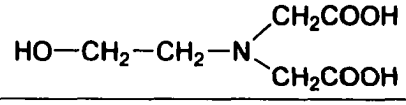
2	Dipicolinic acid	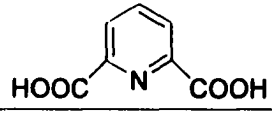
3	Iminobis(methylphosphone acid)	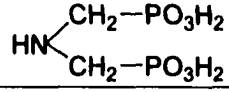
4	1.3-Diamino-2-hydroxypropane-N,N,N',N'-tetraacetic acid	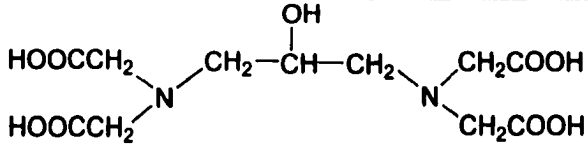
5	N-methyl-D-gluocamine	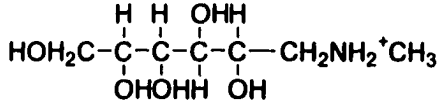
6	D-tartaric acid	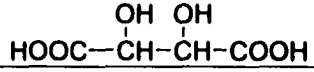
7	EDDA	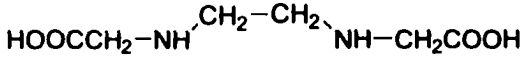
8	Citric acid	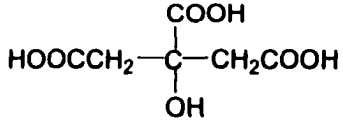
9	EDTA	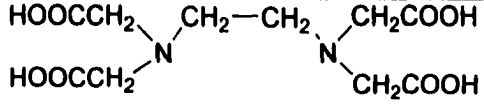

6.2.3.3. Iminobis(methylphosphone acid)

I tried this ligand in H_2O (pH is not controlled) and in lithium acetate buffer (0.18M, pH=4.9). Both solutions of the ligand and Eu α-1 1:1 are stable at room temperature for ca. two months. Both give the ternary complex peak but it takes high ratio (1:20) to observe the peak in water solution. We don't know its formation constant with Eu(III) yet, but it is a good candidate for synthesis of a ternary complex, especially since the ligand can be observed by ^{31}P NMR. Since the mixture is stable, it also will be interesting to try to crystallize this mixture to see if this organic acid will crystallize together with Lnα-1 complex, e.g., as solvent distributing in the void space or as ternary complex.

6.2.3.4. 1.3-Diamino-2-hydroxypropane-N,N,N',N'-tetraacetic acid,

For this ligand, three different values of pH have been tried, pH 6.5, 5.5 and 5.0 in lithium acetate buffer. At pH 6.5 and 5.5, the ^{31}P NMR spectra show that almost all of the α-1 ligand was replaced by this ligand, very small amount of Eu(α–1) complex exists at equilibrium. At pH 5.0, the spectrum shows that the α-1 ligand replaced by this ligand was decreased. Furthermore, this ligand forms 1:1 complex with Eu(III) and its formation constant is well documented. So this ligand is a suitable ligand for competition experiments.

6.2.3.5. N-methyl-D-gluocamine

This ligand is chiral as is Eu(α–1) complex. The purpose of trying this ligand was to see if we can observe the two optical isomers of Eu(α-1) complex by binding this ligand to Eu(α–1). Lu(III) and Eu(III) α-1 complexes were reacted with N-methyl-D-gluocamine in lithium acetate buffer (0.36m, pH=4.7). For Lu(III) α-1 complex, the ^{31}P NMR spectra show the replacement of α–1 ligand by this ligand. And for Eu(III), the ^{31}P NMR spectra show resonance shifting. We did not observe two sets of peaks that indicates the chiral ligand is bound to two optical isomers of Eu(α-1) complex as found with L-tartrate (Fig. 5.11).

6.2.3.6. EDDA and Citric acid

This ligand was discussed in detail at section 5.2.4.1. Citric acid is very similar to EDDA.

6.2.3.7. EDTA

Strong complexation of EDTA with Eu(III) is well known and the binding constant is about 10^{17}-10^{19}. The binding constant is much larger than $(P_2W_{17}O_{61})^{10-}$ with Eu(III), so we did not consider that EDTA would be suitable ligand for the competitive method. However, when pH of the solution was decreased to 3.5 in lithium acetate buffer, the ^{31}P NMR spectrum only showed one set of peaks for Eu α–1 1:1 complex; the EDTA did not replace the $(P_2W_{17}O_{61})^{10-}$. Therefore, by changing the pH, EDTA can be a very good ligand for competition method.

EDTA has five protonation constants [15]: log K_1^H: 10.19, log K_2^H: 6.13, log K_3^H: 2.69, log K_4^H: 2, log K_5^H: 1.5. At pH 2-6, the conditional formation constants for EuEDTA are shown in table 6.2. We can see that they change dramatically from 3.91 to 12.76 as pH changes from 2-6. Therefore, by varying the solution pH, EDTA can be used as a competitive ligand for measurements of formation constant of variety of lanthanide complexes that have different binding strengths.

Table 6.2. The conditional formation constant for *EuEDTA* at different pH (Log K_{EuEDTA} =17.32) [15]

pH	2	3	4	5	6
Log $\alpha_{L'}$	-13.41	-10.51	-8.34	-6.35	-4.56
Log K'_{cond}	3.91	6.81	8.98	10.97	12.76

(Reproduced from reference 15)

6.2.4. Measurement of formation constant

6.2.4.1. Ln(III) α-1 1:1 complexes: Ligand-ligand Competition monitored by ^{31}P NMR

6.2.4.1.1. Computational Method

The equilibrium between Ln(III) and two multidentate ligands, L and L', (negative charges omitted) which form 1:1 complexes with Ln(III) can be written:

$$LnL + L' \overset{K_{eq}}{\rightleftharpoons} LnL' + L \qquad (1)$$

Ln-----lanthanide, L----- $(\alpha\text{-}1\text{-}P_2W_{17}O_{61})^{10-}$, L'-----EDTA

We can write the expression for the equilibrium constant (K_{eq}) as:

$$K_{eq} = \frac{[LnL][L]_t}{[LnL][L']_t} = \frac{K_{cond}}{K_{cond}} = \frac{K\alpha_L'}{K\alpha_L} \qquad (2)$$

K and K' are the thermodynamic formation constants corresponding to equation 3 and 4, respectively:

$$Ln + L \rightleftharpoons LnL \qquad K \qquad (3)$$

$$Ln + L' \rightleftharpoons LnL' \qquad K' \qquad (4)$$

The thermodynamic formation constant does not directly reflect the degree of Ln(III) ion chelation at a given pH. Each ligand has a different response to proton competition for the Ln(III) ion binding which depends on its intrinsic basicity. The affinity of a ligand for Ln(III) at a given pH is described by the conditional formation constant (K_{cond}):

$$K_{cond} = \frac{[LnL]}{[Ln][L]_t} = K\alpha_L \qquad (5)$$

$[L]_t$ is the sum of the equilibrium concentrations of the nonprotonated and all of the protonated forms of ligand L.

$$[L]_t = [L^{n-}] + [HL^{(n-1)-}] + [H_2L^{(n-2)-}] + \bullet\bullet\bullet \qquad (6)$$

$$\alpha_L = \frac{[L]}{[L]_t} = \frac{1}{(1 + K_1^H[H] + K_1^H K_2^H [H]^2 + \bullet\bullet\bullet)} \qquad (7)$$

K_n^H: nth protonation constant of L; analogous expression apply for the competitive ligand, L'.

The present experiments were carried out at pH 4.72. The initial concentrations of Ln present in the samples, $[Ln]_i$, were in the range of 2.0–3.0mM, and the initial ligand concentrations was much greater than

lanthanide concentration. Since both ligands used form strong 1:1 complexes with Ln(III), the concentration of free Ln(III) ion at equilibrium can be considered negligible.

Although $[\alpha\text{-}1\text{-}P_2W_{17}O_{61}]^{10-}$ is charge negative 10, most of the charge is distributed over the entire framework. The basicity of the molecule is not very strong [13]. The most basic atoms are the four oxygens at the defect position. After the Ln(III) binds to these four oxygens, the basicity of the molecule is even decreased. Therefore it is reasonable to assume to a first approximation that the complexes, LnL and LnL', were not protonated under these conditions.

The mass balance equations for eq 1 are:

$$[Ln]_i = [LnL] + [LnL'] \quad (8)$$

$$[L]_i = [LnL] + [L]_t \quad (9)$$

$$[L']_i = [LnL'] + [L']_t \quad (10)$$

i: the initial concentration of the species indicated.

Combing eq 8-10, the equilibrium expression for eq 1 is reduced to a function of $[L]_t$, and the initial concentrations:

$$K_{eq} = \frac{([Ln]_i - [L]_i + [L]_t)[L]_t}{([L]_i - [L]_t)([L']_i - [Ln]_i + [L]_i - [L]_t)} \quad (11)$$

Figure 6.4 is an example of ^{31}P NMR of equilibrium solution of Eu(III), α-1 ligand L and competitive ligand; STD is the external standard (0.01228M of H_3PO_4 in H_2O). The peaks represent the species marked on the spectrum. Each species has two phosphorous atoms giving two

peaks. There is no phosphorous atom in the competitive ligand, so LnL' and L' will not be observed from ^{31}P NMR spectrum. The intensity of [α-1-$P_2W_{17}O_{61}]^{10-}$ peak at –8.4 ppm I_L *vs* intensity of STD peak I_{STD} is proportional to the concentration of [α-1-$P_2W_{17}O_{61}]^{10-}$.

$$S_g = \frac{I_L}{I_{STD}} = \kappa[L]_t \qquad (12)$$

κ is the proportionality constant determined from the calibration curve of S_g vs $[L]_t$ over the 0.5 – 3.0 mM range at the same condition as the equilibrium. So the eq 11 can be expressed as:

$$K_{eq} = \frac{([Ln]_i - [L]_i + S_g/\kappa)(S_g/\kappa)}{([L]_i - S_g/\kappa)([L']_i - [Ln]_i + [L]_i - S_g/\kappa)} \qquad (13)$$

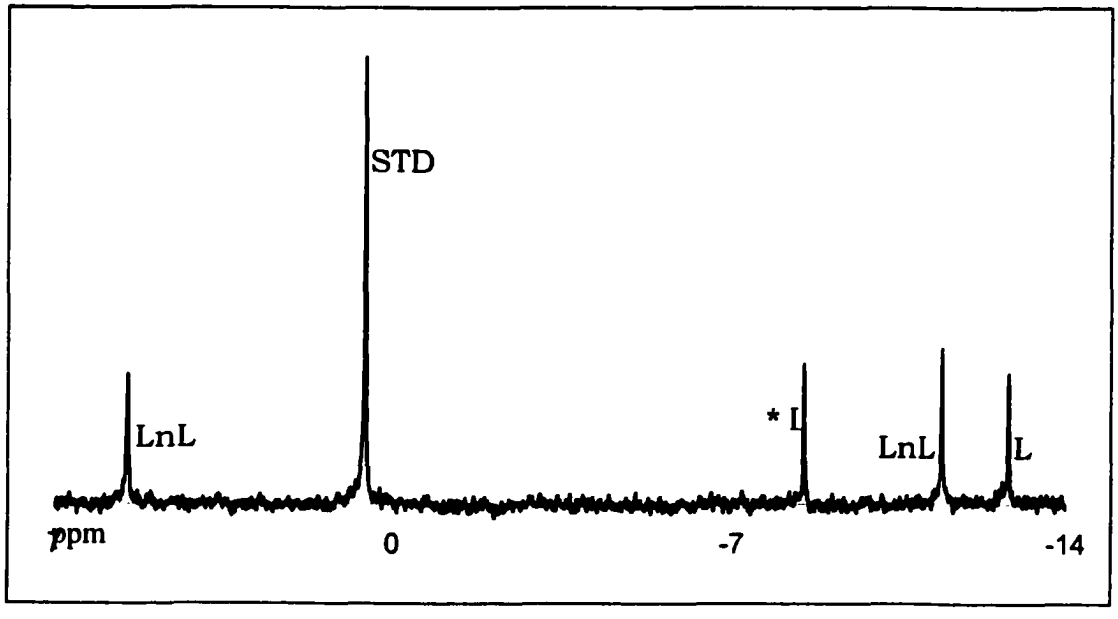

Figure 6.4. Ln = Eu, L=[α-1-$P_2W_{17}O_{61}]^{10-}$, ^{31}P NMR spectrum of the solution in equilibrium. * the peak intensity as I_L.

If the initial concentration of Ln(III) and L are equal, $[Ln]_i=[L]_i$, then eq 13 can be simplified as:

$$K_{eq} = \frac{(S_g/\kappa)^2}{([L]_i - S_g/\kappa)([L']_i - S_g/\kappa)} \qquad (14)$$

After K_{eq} is obtained, from the equation 2, we can calculate K_{cond} since K'_{cond} is known.

6.2.4.1.2. The results

From section 5.2.1, we know that α-1 ligand is not stable in solution for long period of time. Although lithium ion in solution will slow the isomerization process, the solution cannot be left at room temperature for a long time. The shortest equilibrium time should be chosen in order to prevent the α-1 ligand from isomerizing to the α-2 ligand. At least three experiments at different concentrations were run for each Ln ion. Using the NMR spectrum to obtain S_g that is related to $[L]_i$, the initial concentrations of (α-1-$P_2W_{17}O_{61}$)$^{10-}$ $[L]_i$, and EDTA $[L']_i$, we calculated K_{eq} (eq 14). To obtain the conditional formation constant, we

Table 6.3. Conditional formation constants for Ln(III) α-1 1:1 complexes obtained from ligand-ligand competition studies

Ln	La	Nd	Eu	Er	Lu
$LogK_1$[b]	8.93±0.20[a]	9.77±0.10	10.42±0.08	12.31±0.17	13.21±0.26

[a] average deviation for three K determinations. [b] pH=4.72, 0.5M lithium acetate buffer, 20°C, 0.1M LiCl.

use equation 2 and the appropriate value of K'_{cond} for EDTA. The conditional formation constants are obtained because the protonation constants of α-1 ligand under these conditions have not been determined yet. The conditional formation constants are shown in Table 6.3.

We can see that crossing the periodic table from left to right; the conditional formation constants increase as the size of lanthanides decreases. These are in agreement with my synthesis observations for lanthanide α-1 complexes. The lutetium complex is very easy to prepare and crystallize and Lu forms the most stable complex with α-1 ligand.

6.2.4.2. Ln(III) α-2 1:1 and 1:2 complexes

6.2.4.2.1. Ligand-ligand competition monitored by ^{31}P NMR

Lanthanide reacts with $[\alpha\text{-}2\text{-}P_2W_{17}O_{61}]^{10-}$ (L) to form two complexes, 1:1 and 1:2, shown by equation 15 and 16.

$$Ln + L \rightleftharpoons LnL \qquad K_1 \qquad (15)$$

$$LnL + L \rightleftharpoons LnL_2 \qquad K_2 \qquad (16)$$

The general ligand-ligand competition method requires only one product 1:1 formed as we see from eq 1. The simple competition method used for Ln α-1 1:1 complex can't be used here. But if we carefully control the conditions of the reaction between Ln, $[\alpha\text{-}2\text{-}P_2W_{17}O_{61}]^{10-}$ and the competitive ligand, EDTA, we can get one product related to $[\alpha\text{-}2\text{-}P_2W_{17}O_{61}]^{10-}$. The two reactions are:

$$LnL_2 + L' \rightleftharpoons LnL' + 2L \qquad K_{eq}(1) \qquad (17)$$

$$2LnL + L' \rightleftharpoons LnL' + LnL_2 \quad K_{eq}(2) \qquad (18)$$

The equilibrium constant for these two reactions, 17 and 18, are:

$$K_{eq}(1) = \frac{[LnL'][L]_t^2}{[LnL_2][L']_t} = \frac{K'_{cond}}{K_{1cond}K_{2cond}} \qquad (19)$$

$$K_{eq}(2) = \frac{[LnL'][LnL_2]}{[LnL]^2[L']_t} = \frac{K'_{cond}K_{2cond}}{K_{1cond}} \qquad (20)$$

The conditional formation constant of *LnEDTA* (K'_{cond}) is known, K_{1cond} and K_{2cond} (the conditional formation constant for LnL and LnL_2) are unknown; we are trying to solve for these. So if we are able tc obtain $K_{eq}(1)$ and $K_{eq}(2)$, then we can solve the two equations 19 and 20 to get K_{1cond} and K_{2cond}.

For both equilibrium 17 and 18, in order to measure the equilibrium constants under NMR sensitivity limit, we have to carefully control the solution pH (species are stable in the range, pH 2-7, section 6.2.1) and the $[L]_i:[L']_i$ ratio so that there is a comparable distribution of Ln(III) ion between the two ligands in solution. For equilibrium 17, if the pH is too low, then EDTA is not strong enough to compete with [α-2-$P_2W_{17}O_{61}]^{10-}$ and then we will not observe [α-2-$P_2W_{17}O_{61}]^{10-}$ peaks from ^{31}P NMR spectra. On the other hand, for equilibrium 18, if the pH is too high, then EDTA will be too strong a competitor for [α-2-$P_2W_{17}O_{61}]^{10-}$. In this situation, we can observe different species in the ^{31}P NMR spectra: LnL_2, LnL; or LnL_2, L; or only L. We can easily detect the problem if [α-2-

$P_2W_{17}O_{61}]^{10-}$ (L) peaks are observed in the ^{31}P NMR spectra. But even if only LnL_2 and LnL peaks are observed, as required by equation 18, we have to check that each species in equilibrium has at least a significant concentration with the NMR technique. So an easy approach is starting from the lowest pH 2.

The initial concentrations of Ln present in the samples, $[Ln]_i$, were in the range of 4.0-6.0 mM, and the initial ligand concentrations was much greater than lanthanide concentration. Since each ligand forms a strong 1:1 complex with Ln(III), the concentration of free Ln(III) ion at equilibrium is negligible.

Similar to the $[\alpha\text{-}1\text{-}P_2W_{17}O_{61}]^{10-}$, most of the charge of $[\alpha\text{-}2\text{-}P_2W_{17}O_{61}]^{10-}$ is distributed over the entire framework. The basicity of the molecule is not very strong [13]. The most basic atoms are the four oxygen atoms at the defect position. After the Ln(III) binds to those four oxygen atoms, the basicity of the molecule is decreased further. Therefore it is reasonable to assume to a first approximation that the complexes are not protonated at slightly acidic to neutral pH. For low pH, please see the discussion at page 145, section 6.2.4.2.2.

So we can write the mass balance for equilibrium 17:

$$[\mathrm{Ln}]_i = [LnL'] + [LnL_2] \quad (21)$$

$$[L]_i = 2[LnL_2] + [L]_t \quad (22)$$

$$[L']_i = [LnL'] + [L']_t \quad (23)$$

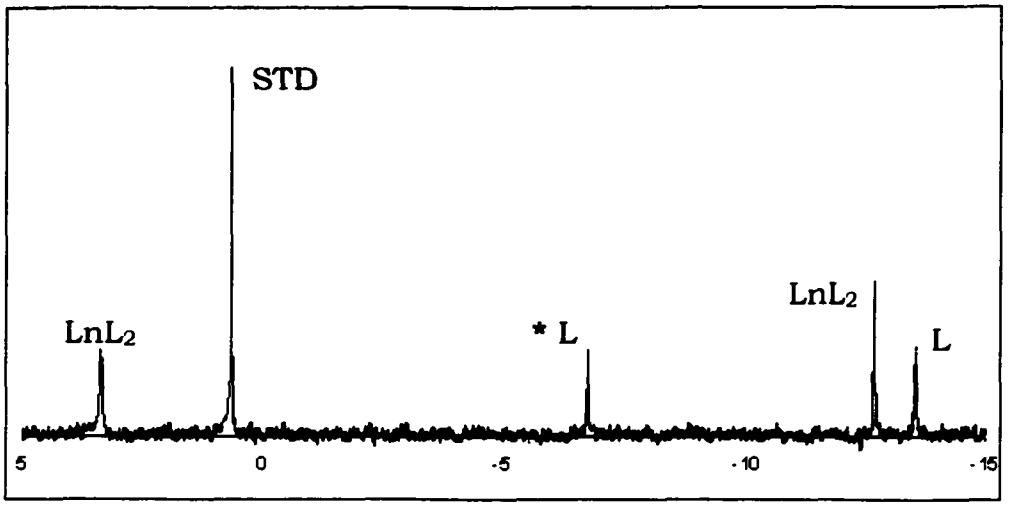

Figure 6.5. An example of ^{31}P NMR spectrum of the solution for equilibrium 17. $LnL_2 + L' \rightleftharpoons LnL' + 2L$, L---$[\alpha\text{-}2\text{-}P_2W_{17}O_{61}]^{10-}$, L'---EDTA, Ln---Eu. * the peak intensity as I_L.

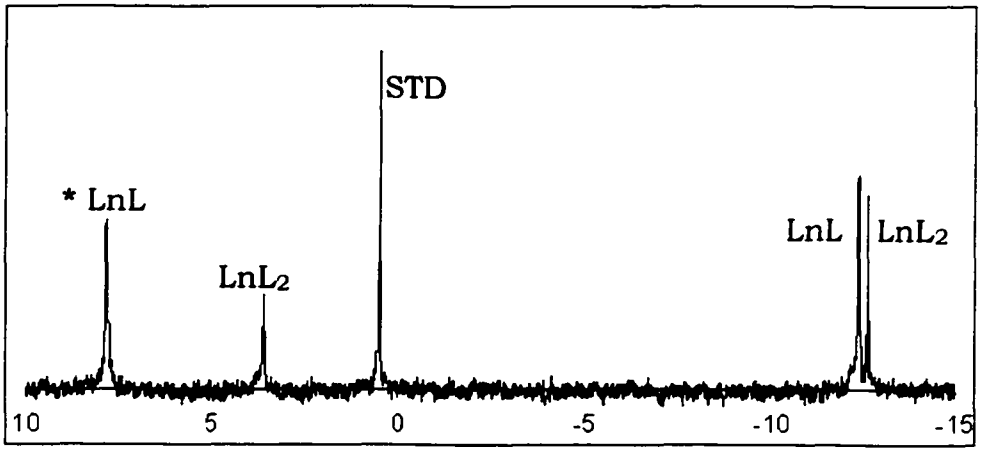

Figure 6.6. An example of ^{31}P NMR spectrum of the solution for equilibrium 18. $2LnL + L' \rightleftharpoons LnL' + LnL_2$, L---$[\alpha\text{-}2\text{-}P_2W_{17}O_{61}]^{10-}$, L'---EDTA, Ln---Eu. * the peak intensity as I_{LnL}.

Combining eq 21-23, the equilibrium expression of eq 19 is reduced to a function of $[L]_t$ and the initial concentrations:

$$K_{eq}(1) = \frac{([Ln]_i - 1/2[L]_i + 1/2[L]_t)[L]_t^2}{1/2([L]_i - [L]_t)([L']_i - [Ln]_i + 1/2[L]_i - 1/2[L]_t)} \quad (24)$$

The mass balance equations for equilibrium 18 are:

$$[\mathrm{Ln}]_i = [LnL'] + [LnL_2] + [LnL] \quad (25)$$

$$[L]_i = 2[LnL_2] + [LnL] \quad (26)$$

$$[L']_i = [LnL'] + [L']_t \quad (27)$$

Combining eq 25-27, the equilibrium expression of eq 20 is reduced to a function of $[LnL]$ and the initial concentrations:

$$K_{eq}(2) = \frac{1/2([Ln]_i - 1/2[L]_i - 1/2[LnL])([L]_i - [LnL])}{[LnL]^2([L']_i - [LnL]_i + 1/2[L]_i + 1/2[LnL])} \quad (28)$$

Figure 6.5, 6.6 are examples of ^{31}P NMR spectra of solution of equilibrium 17 and 18. EDTA is the competing ligand. STD is the external standard as before. The peaks represent the species marked on the spectra. Each species has two phosphorous atoms giving two peaks. There is no phosphorous atom in the competitive ligand, so LnL' and L' will not be observed from ^{31}P NMR spectra. The intensity of $[\alpha\text{-}2\text{-}P_2W_{17}O_{61}]^{10-}$ peak at –6.4 ppm I_L (Fig. 6.5) and intensity of LnL peak at 7.34 ppm (Fig. 6.6) I_{LnL} *vs* intensity of STD peak I_{STD} is proportional to the concentration of $[\alpha\text{-}2\text{-}P_2W_{17}O_{61}]^{10-}$ L and LnL, respectively.

$$S_g = \frac{I_L}{I_{STD}} = \kappa[L]_t \quad (29)$$

$$S_g' = \frac{I_{LnL}}{I_{STD}} = \kappa'[LnL] \qquad (30)$$

κ, κ' is the proportionality constant determined from calibration curves of S_g vs $[L]_t$ and S_g' vs $[LnL]$ over the 0.5 – 3.0 mM range.

If the initial concentration of Ln(III) and L are controlled as, $2[Ln]_i=[L]_i$ for equilibrium 17, and $[Ln]_i=[L]_i$ for equilibrium 18, then eq 24 and 28 can be simplified as:

$$K_{eq}(1) = \frac{[L]_t^3}{([L]_i - [L]_t)([L'] - 0.5[L]_t)} = \frac{(S_g/\kappa)^3}{([L]_i - S_g/\kappa)([L']_i - 0.5S_g/\kappa)} \qquad (31)$$

$$K_{eq}(2) = \frac{([L]_i - [LnL])^2}{2[LnL]^2(2[L']_i - [L]_i + [LnL])} = \frac{([L]_i - S_g'/\kappa')^2}{2(S_g'/\kappa')^2(2[L']_i - [L]_i + S_g'/\kappa')} \qquad (32)$$

Substituting the measured values for S_g, k, $[L]_i$ and $[L']_i$ into these two equations, we can calculate the $K_{eq}(1)$ and $K_{eq}(2)$. From equation 19 and 20, knowing the K_{cond} for EuEDTA, we can calculate the K_{1cond} and K_{2cond}.

The protonation constants for $[\alpha\text{-}2\text{-}P_2W_{17}O_{61}]^{10-}$ (Section 6.2.2) are: Log K_1^H=3.53, Log K_2^H=4.46, LogK_3^H=2.43. So we are able to calculate the

Table 6.4. Thermodynamic formation constants for Ln(III) α-2 1:1 and 1:2 complexes obtained from ligand-ligand competition studies.

Ln	La	Nd	Eu
Log K_1	11.33±0.27[a]	11.71±0.20	11.21±0.19
Log K_2	5.79±0.27	6.21±0.20	6.61±0.19

[a] average deviation for three K determinations.

thermodynamic formation constant for lanthanide α-2 complexes. The results are shown at Table 6.4.

6.2.4.2.2. By laser-excited Eu(III) luminescence excitation

Measurement of formation constant K_1: To measure the formation constant of the 1:1 complex, $[\alpha\text{-}2\text{-}P_2W_{17}O_{61}]^{10-}$ (L) was titrated by a Eu(III) solution while monitoring complex formation at the excitation maximum (579.77 nm) of EuL. Figure 6.7 shows an example of the excitation spectra. During the titration, either having excess Eu(III) or excess $[\alpha\text{-}2\text{-}P_2W_{17}O_{61}]^{10-}$ in the solution, results in formation of only EuL 1:1 complex.

$$Eu + L \rightleftharpoons EuL \qquad K_1 \qquad (33)$$

We can write the conditional formation constant as:

$$K_{1cond} = \frac{[EuL]}{[Eu][L]_t} = K_1 \alpha_L \qquad (34)$$

The mass balance equations for eq 33 are:

$$[Eu]_i = [EuL] + [Eu] \qquad (35)$$

$$[L]_i = [L]_t + [EuL] \qquad (36)$$

For excitation at 579.77 nm wavelength, the intensity I_1,

$$I_1 = k_1[EuL] \qquad (37)$$

k_1 is the proportionality constant between intensity and concentration which is kept as a variable in the non-regression fit.

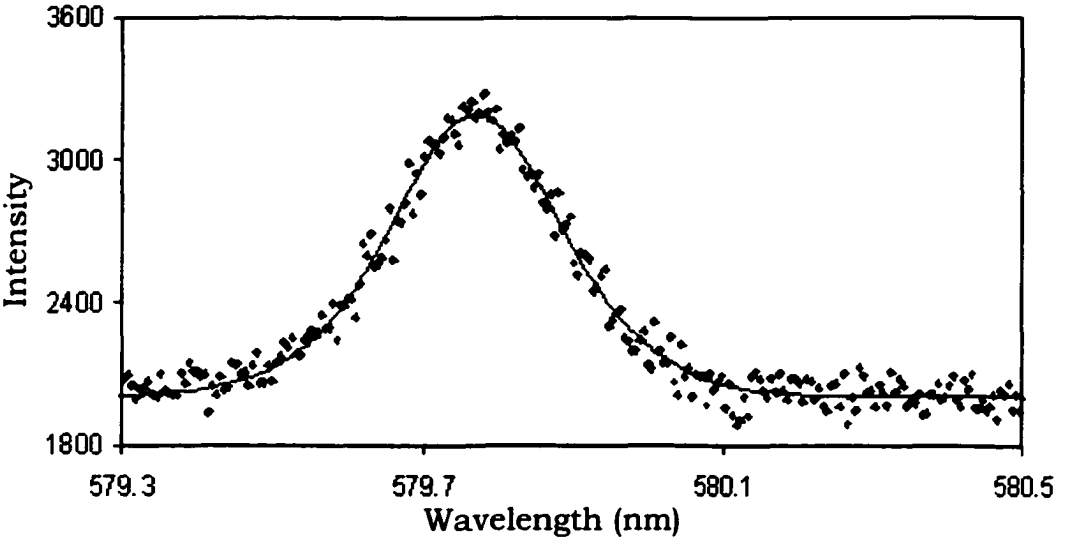

Figure 6.7. $^7F_0 \rightarrow {}^5D_0$ excitation spectrum at [*Eu*]=2.906 mM, emission wavelength monitored at 614 nm.

Combining eq 35-37, the equilibrium expression of eq 34 is reduced to a function of I_1, k_1 and the initial concentrations:

$$K_{1cond} = \frac{[EuL]}{([Eu]_i - [EuL])([L]_i - [EuL])} = \frac{I_1 / k_1}{([Eu]_i - I_1 / k_1)([L]_i - I_1 / k_1)} \qquad (38)$$

The initial concentrations were changing as the Eu(III) was continuously adding into the $[\alpha\text{-}2\text{-}P_2W_{17}O_{61}]^{10-}$ solution. Equation 39 and 40 show the relationship of initial concentrations of $[\alpha\text{-}2\text{-}P_2W_{17}O_{61}]^{10-}$ and Eu(III) with total volume of Eu(III) added, V_{Eu}. $[L]_0$ is the $[\alpha\text{-}2\text{-}P_2W_{17}O_{61}]^{10-}$ concentration before titrating. $[Eu]_0$ is the concentration of stock solution. 2000 (μL) is the volume of the solution before the titration.

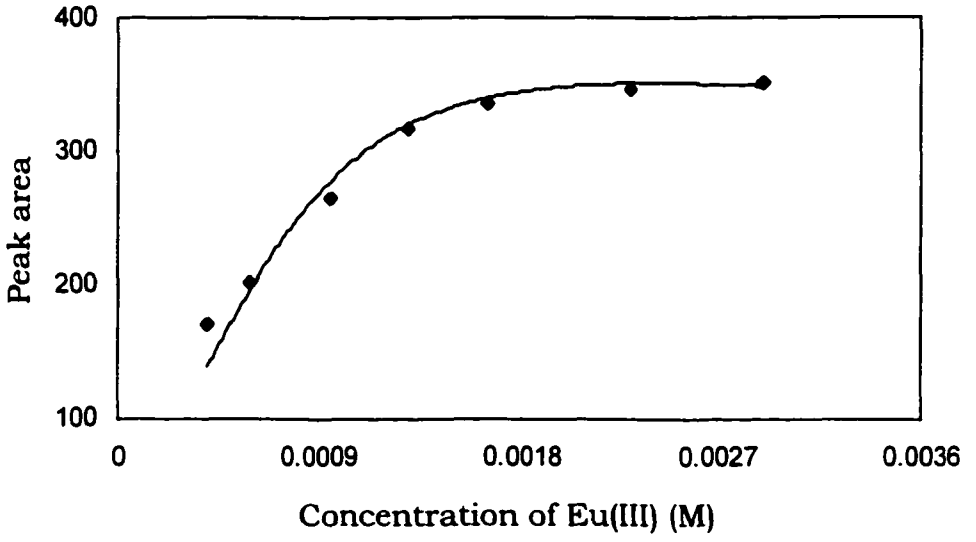

Figure 6.8. Binding curve of $[\alpha\text{-}2\text{-}P_2W_{17}O_{61}]^{10-}$ (1mM) titrated by Eu(III) in NaOOCH buffer (pH=2, 0.5 M). The solid line is the theoretical fit using SigmaPlot 2000.

$$[L]_i = \frac{[L]_0 \times 2000}{2000 + V_{Eu}} \tag{39}$$

$$[Eu]_i = \frac{[Eu]_0 \times V_{Eu}}{2000 + V_{Eu}} \tag{40}$$

For lanthanide α-2 complexes, that have thermodynamic formation constants, log K ≈ 10 for 1:1 complex, conditional stability constants ($K_{cond}=K\alpha$) in the neutral pH region are such that K_{cond} values are much lower than the working sensitivity limit of the luminescent instrumentation. Under such neutral pH conditions a titration of metal ion with ligand would reveal quantitative binding with a sharp break in the titration curve at a 1:1 stoichiometry (which was shown in Fig. 3.8).

Such a titration curve does not yield a formation constant. By reducing the pH to a value that the titration curve will show some curvature, the data can be analyzed using equations 38-40 and non-linear regression methods, which results in K_{1cond} and k_1. The results of these experiments and calculations are shown at Table 6.5.

At such low pH 2, it would be expected that some EuL is protonated to form EuHL:

$$EuL + H^+ \rightleftharpoons EuHL \qquad K_H \qquad (41)$$

In the reference 9, Horrocks at al discussed the effect of K_H on the formation constant at low pH. They tried to fit the data in three different ways. First, the K_H values were held constant at their known values. Second, they were set equal to zero as an approximation. Lastly the K_H values were allowed to vary in the non-linear regression fit. Comparison of the results from the three fitting approaches suggests that final log K values are not very sensitive to the K_H value. The respective log K_H values were in the range of –6 to 3. Therefore, here for simplicity we set K_H equals to zero as an approximation. From the goodness of the curve fitting in Figure 6 we can see the assumption is reasonable.

Measurement of formation constant K_2: To determine K_2 for Euα-2 1:2 complex, Eu(III) was titrated by $[\alpha\text{-}2\text{-}P_2W_{17}O_{61}]^{10-}$ solution while monitoring complex formation at the excitation maximum of EuL_2. Figure 6.9 shows one of the excitation spectra of the titration. Wavelength at

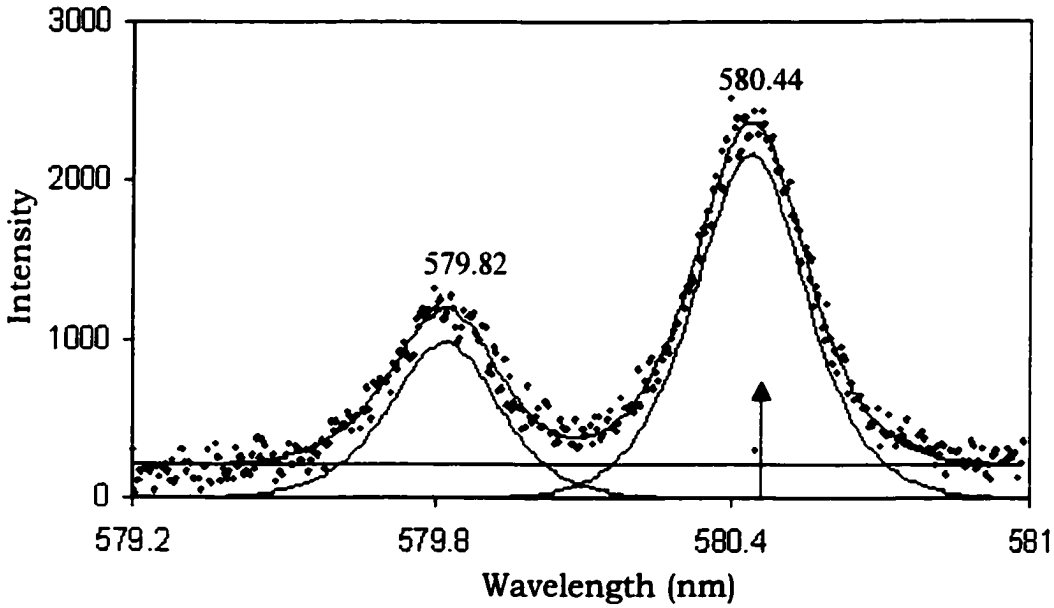

Figure 6.9. $^7F_0 \rightarrow {}^5D_0$ excitation spectrum of mixture solution of Eu(III) and $[\alpha\text{-}2\text{-}P_2W_{17}O_{61}]^{10-}$ at $[L]$=12.541 mM, emission wavelength was monitored at 614 nm.

579.82 nm is the peak for EuL, wavelength at 580.44 nm is the peak for EuL_2. The same computational method as 1:1 complex was employed:

$$EuL + L \rightleftharpoons EuL_2 \quad K_2 \tag{42}$$

$$K_{2cond} = \frac{[EuL_2]}{[EuL][L]_t} = K_2\alpha_L \tag{43}$$

The mass balance equations are:

$$[Eu]_i = [EuL] + [EuL_2] \tag{44}$$

$$[L]_i = [L]_t + 2[EuL_2] + [EuL] \tag{45}$$

For excitation at wavelength 580.44 nm, the intensity I_2,

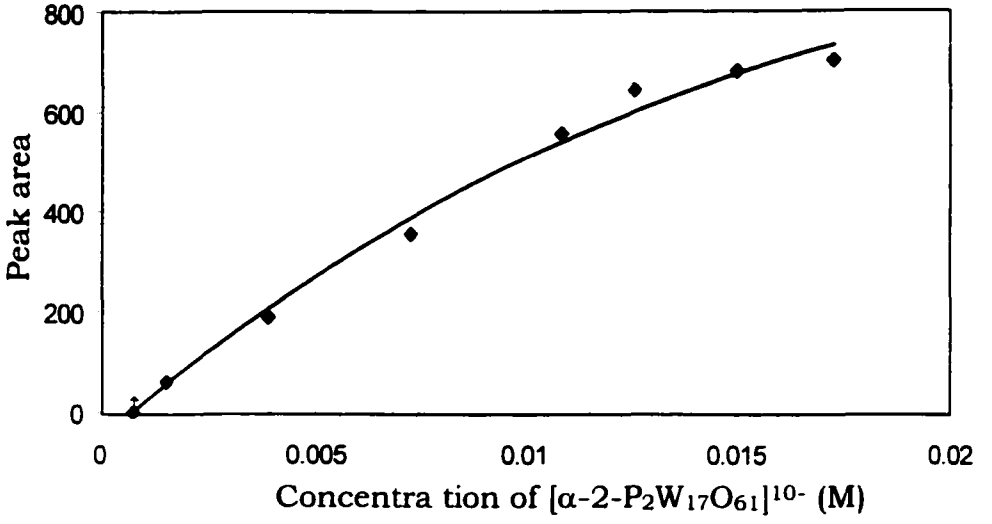

Figure 6.10. Binding curve of Eu(III) (0.8 μM) titrated by [α-2-$P_2W_{17}O_{61}]^{10-}$ in NaOOCH buffer (pH=3, 0.5 M). The first point represents the case where one equivalent of α-2 ligand is added to the Eu(III) solution. This results in formation of the 1:1 complex, EuL, exclusively, no 1:2 complex is formed. The solid line is the theoretical fit using SigmaPlot 2000.

$$I_2 = k_2[EuL_2] \tag{46}$$

k_2 is the proportionality constant which was kept as a variable in the non-linear regression curve fit.

Combining eq 44-46, the equilibrium expression of eq 43 is reduced to a function of I_2, k_2 and the initial concentrations:

$$K_{2cond} = \frac{[EuL_2]}{([Eu]_i - [EuL_2])([L]_i - [Eu]_i - [EuL_2])} = \frac{I_2/k_2}{([Eu]_i - I_2/k_2)([L]_i - [Eu]_i - I_2/k_2)} \tag{47}$$

The initial concentrations were changing as the $[\alpha\text{-}2\text{-}P_2W_{17}O_{61}]^{10-}$ was continuously adding into the titrating solution. Equation 48 and 49 show the relationship of initial concentrations of α-2 ligand and Eu(III) with total volume of $[\alpha\text{-}2\text{-}P_2W_{17}O_{61}]^{10-}$ added, V_L. $[Eu]_0$ is the concentration before titration. $[L]_0$ is the concentration of stock solution. 2000 (μL) represents the total solution volume before titrating.

$$[Eu]_i = \frac{[Eu]_0 \times 2000}{2000 + V_L} \tag{48}$$

$$[L]_i = \frac{[L]_0 \times V_L}{2000 + V_L} \tag{49}$$

Equations 47-49 was used to fit the experiment data (Fig. 6.10) by SigmaPlot 2000, which gave us the values of K_{2cond} and k_2, the result is shown at Table 6.5.

6.2.4.2.3. By lanthanide-lanthanide competition.

Having established a reliable values for the formation constant of $[\alpha\text{-}2\text{-}P_2W_{17}O_{61}]^{10-}$ with Eu(III) (1:1), we can measure the formation constant of $[\alpha\text{-}2\text{-}P_2W_{17}O_{61}]^{10-}$ with other lanthanides by lanthanide-lanthanide competition experiments. The following equation shows the equilibrium expression:

$$Ln + EuL \rightleftharpoons LnL + Eu \qquad K_{rel} \tag{50}$$

$$K_{rel} = \frac{[LnL][Eu]}{[Ln][EuL]} = \frac{K_{LnL}}{K_{EuL}} \tag{51}$$

Figure 6.11 is the ^{31}P NMR of equilibrium mixture of Eu(III), La(III) and $[\alpha\text{-}2\text{-}P_2W_{17}O_{61}]^{10-}$ L. Following almost the same computational method as ligand-ligand competition method to calculate the K_{rel}.

$$K_{rel} = \frac{([L]_i - S_g/k)([Eu]_i - S_g/k)}{([Ln]_i - [L]_i + S_g/k)(S_g/k)} \quad (52)$$

$$S_g = \frac{I_{EuL}}{I_{STD}} = k[EuL] \quad (53)$$

The results are shown in Table 6.5.

Comparing Table 6.4 with Table 6.5, we can see that through two different approaches, one by ligand-ligand competition, another by fluorescence titration combined with lanthanide-lanthanide competition,

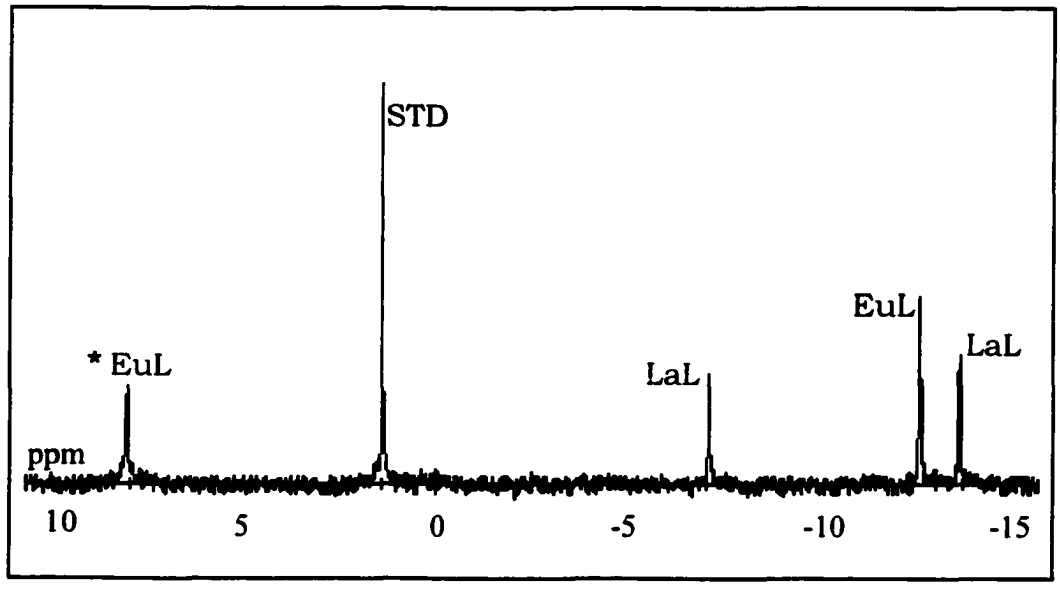

Figure 6.11. An example of ^{31}P NMR spectrum of equilibrium solution of lanthanide competition experiment. * the peak intensity as I_{EuL}.

Table 6.5. Formation constants of Ln α-2 complexes.

Ln	Eu [a]	La [b]	Nd [b]	Lu [b]
Log K_1	11.34±0.17[c]	11.34±0.08	11.53±0.25	12.00±0.25
Log K_2	6.54±0.19			

[a] from luminescence titration. [b] from lanthanide-lanthanide competition. [c] average deviation for three K determinations.

these results are extremely close. This indicates the reliability of the data.

Since the supporting counter ions and their concentrations will affect formation constant value [12,13,19]. it is very important to compare our values under the same condition. The more concentrated the alkaline cation is in the solution, the less the formation constant value will be. Considering this trend and comparing the data, we find our data are comparable with the references [12,20] where $\log\beta$ (=$\log K_1K_2$) for Ce(III) α-2 1:2 was reported as 17.7 in 0.4 M Na^+ solution (K_1 and K_2 were not determined). Calculations for $\log\beta$ using the data from reference 12 correcting for the media resulted in $\log\beta$ =17.72 at 0.4 M Na^+ [12]. The concentration of supporting electrolyte for our studies of the Ln α-2 complexes is 0.5 M. The formation constants for the α-2 complexes that we determined (Table 6.4 and 6,5) are in excellent agreement with those found by Contant and Ciabini [12] and Spitzyn [20] for the Ce(III) complexes.

In reference [14], the formation constants of Ln α-2 complexes have been measured by luminescence. The values for Eu(III) complexes were $\log K_1$=7.5, $\log K_2$=5.7 in 1.0 M Na^+ solution and $\log K_1$=7.36 in 0.1 M Na^+ solution. These values do not agree with my own data. From the above discussion, we know that the nature and concentration of the supporting alkaline cation will affect the measured formation constant value and this is common for polyoxometalates system. But we did see such phenomenon in the results of reference [14]; the binding constant values in 0.1 M Na^+ and 1.0 M Na^+ are very close.

The work by Ciabrini and Contant [12] is the only reference we find that reports the formation constant for Ln α-1 complexes; they determine $\log K_1$=6.6 and $\log K_2$=1.5 for the Ce(III) α-1 complexes in 1.0 M Li^+ solution. Considering the trend of decreasing ionic radius across Ln series, our values of K_{cond} for Ln α-1 1:1 complexes are in excellent agreement with the work of Contant [12]. The weak binding constant for 1:2 complex explains the instability of Ln α-1 1:2 complexes in solution discussed in Chapter 5.

Comparing the formation constant value of Ln α-1 complex (Table 6.3) with Ln α-2 complex (Table 6.4, 6.5), it is interesting to find that across the lanthanide, as the size to lanthanide decrease, the formation constants increase for Ln α-1 complexes, but are constant for Ln α-2 complexes. There may be two reasons for this trend. First, the basicity of $[\alpha\text{-}1\text{-}P_2W_{17}O_{61}]^{10-}$ is larger than $[\alpha\text{-}2\text{-}P_2W_{17}O_{61}]^{10-}$[12]. Figure 2.1 and 4.2

are the crystal structures of Ln α-2 and α-1 complexes. The oxygen atoms marked * is bonded to only one tungsten atom W4 in [α-1-$P_2W_{17}O_{61}]^{10-}$ anion, but to two tungsten atoms W1B, W2B in [α-2-$P_2W_{17}O_{61}]^{10-}$ anion. These renders the [α-1-$P_2W_{17}O_{61}]^{10-}$ anion more basic than [α-2-$P_2W_{17}O_{61}]^{10-}$ anion. The negative charge is mostly located on the four oxygen atoms of the vacancy. As the size of lanthanide decreases from La to Lu, the charge density (charge/diameter) increases. Therefore, it is reasonable for the more basic anion [α-1-$P_2W_{17}O_{61}]^{10-}$, the binding constant increases as the size of lanthanide decreases, that is as the charge/size increases.

Another reason for the stability constant trends observed in Table 6.3, 6.4 and 6.5 may be the flexibility of the defect holes of the [α-2-$P_2W_{17}O_{61}]^{10-}$ and [α-1-$P_2W_{17}O_{61}]^{10-}$ anions.

According to the crystal structures of Ln α-2 1:2 (Ln=Eu, Gd, Lu) (Chapter 2), the defect hole size decreases as the size of Lanthanide ion decreases. The α-2 defect hole that obtained by removal of a WO unit from "cap" region of the plenary [α-$P_2W_{18}O_{62}]^{6-}$ (Figure 1.7), may adjust to the size of the lanthanide, therefore, shows no selectivity between lanthanide ions. The α-1 defect hole that obtained by removal of a WO unit from "belt" region of the plenary [α-$P_2W_{18}O_{62}]^{6-}$ (Figure 1.7), on the other hand, is less flexible and more basic. Therefore, the α-1 ligand is selective to the heavier lanthanide ions with high charge/size ratio.

Unfortunately, we do not have the crystal structure for the Lu α-2 1:1 or Eu α-1 1:1 complexes for an exact comparison.

6.3. Conclusion

The protonation constants for $(\alpha\text{-}2\text{-}P_2W_{17}O_{61})^{10-}$ have been measured by potentiometric titration and are $\log\beta_1$ = 3.53, $\log\beta_2$ = 7.99, $\log\beta_3$ =10.41. EDTA was chosen as competitive ligand after 9 ligands had been tried. Two methods have been developed to measure formation constant for Ln α-1 and Ln α-2 complexes, ligand-ligand competition method monitored by ^{31}P NMR and metal-ligand titration monitored by Eu(III) fluorescence excitation combined with lanthanide-lanthanide competition. The results from both methods are in good accord with each other, implying the reliability of the data, the methods and the suitability of the mathematic model. For Ln α-1 complex, the conditional formation constants are in $10^{8.9}$-$10^{13.2}$ M^{-1} ranges. Crossing the lanthanide series, from La to Lu, as the size of lanthanide ions decrease, the formation constants increase from $10^{8.9}$ M^{-1} to $10^{13.2}$ M^{-1}. However for Ln α-2 complexes, the thermodynamic formation constants are almost constant from La to Lu, about 10^{11} M^{-1} for K_1 and 10^6 M^{-1} for K_2. This may due to the different strength of basicity of $(\alpha\text{-}1\text{-}P_2W_{17}O_{61})^{10-}$ and $(\alpha\text{-}2\text{-}P_2W_{17}O_{61})^{10-}$ anions in solution, and different flexibility of the hole size of 'defect' position in $(\alpha\text{-}1\text{-}P_2W_{17}O_{61})^{10-}$ and $(\alpha\text{-}2\text{-}P_2W_{17}O_{61})^{10-}$ molecule structures.

6.4. References

1) Contant ; Klemperer, Ed., **1990**; Vol. 27, 71.

2) Contant, R.; Ciabrini, J.-P. *J. Chem. Res. Synop.* **1977**, 222; The syntheses are reported in more detail in ref 3.

3) Contant, R. *Inorg. Synth.* **1990**, *27*, 71.

4) Lyon, D. K.; Miller, W. K.; Novet, T.; Domaille, P. J.; Evitt, E.; Johnson, D. C.; Finke, R. G. *J. Amer. Chem. Soc.* **1991**, *113*, 7209.

5) Bartis, J.; Kunina, Y.; Blumenstein, M.; Francescone, L. C. *Inorg. Chem.* **1996**, *35*, 1497.

6) Bartis, J.; Dankova, M.; Lessmann, J. J.; Luo, Q.-H.; Horrocks, W. D., Jr.; Francesconi, L. C. *Inorganic Chemistry* **1999**, *38*, 1042-1053.

7) Martell, A. E.; Motekaitis. R. J. *Determination and Use of Stability Constants*. 2nd ed.; VCH: New York, **1992**.

8) Horrocks, W. DeW., Jr. *Methods Enzymol.* **1993**, *226*, 495.

9) Horrocks, W. DeW., Jr.; Sudnick, D. R. *Acc. Chem. Res.* **1981**, *14*, 384

10) Horrocks, W. DeW., Jr.; Sudnick, D. R. *J. Am. Chem. Soc.* **1979**, *101*, 334.

11) Horrocks, W. DeW., Jr.; Wu, S. R. *Inorg. Chem.* **1995**, *34*, 3724.

12) Ciabrini, J.-P.; Contant, R. *J. Chem. Research (M).* **1993**, 2720-2744.

13) Contant R.; Ciabrini J., *J. Chem. Research, (S),* **1982,** 50-51; *J. Chem. Res. (M),* **1982**, no. 3-7, 641-660.

14) Craig E. Van Pelt; William J. Crooks III; Gregory R. Choppin, *Dissertation,* **1998,** Dept. of Chem., The Florida State University.

15) Martell, A. E.; Motekaitis, R. J., *Determination and use of stability constants,* New York, VCH Publishers, **1992**.

16) Wu, Sh. L.; Horrocks, W. DeW. Jr., *Anal. Chem.* **1996**, 68, 394.

17) Yusov, V. P.; *Radiokhimiya,* **1980**, vol. 22, no. 5, 727-732.

18) Kulyko, Yu. M.; Lebedev, I. A.; Trofimov, T. I., *et al., Zh. Neorg. Khim.,* **1981**, vol. 26, no. 5, 1254-1260.

19) Yusov, A. B.; Shilov, V. P., *Radiochem.* **1999**, Vol. 41, no. 1, 1-23, Translated from *Radiokhimiya.* Vol. 41, no. 1, **1999**, 3-24.

20) Spitzyn, V. I.; Orlova, M. M.; Krot, N. N.; Saprykin, A. S., *Zh. Neorg. Khim.* **1978**, 13, 1227.

Reference

Chapter 1

1) Katsoulis, D. E., *Chem. Rev.* **1998**, 98, 359.

2) Sadakane, M.; Dickman, M. H.; Pope, M. T., *Angew. Chem. Int. Ed.* **2000**, 39(16), 2914.

3) Belai, N.; Sadakane, M.; Pope, M. T., *J. Am. Chem. Soc.* **2001**, 123(9), 2087.

4) Clegg, W.; Elsegood, M. R. J.; Errington, R. J.; Havelock, J., *J. Chem. Soc., Dalton Trans.* **1996**, 681-690.

5) Gouzerh, P.; Proust, A., *Chem. Rev.* **1998**, 98, 77.

6) Kwen, H.; Young, V. G., Jr.; Maatta, E. A., *Angew. Chem. Int. Ed. Engl.* **1999**, 38, 1145.

7) Müller, A.; Kögerler, P.; Kuhlmann, C., *Chem. Commun.* **1999**, 1347.

8) Jeannin, Y. J., *Cluster Sci.* **1992**, 3, 55.

9) Müller, A.; Plass, W.; Krichemeyer, E.; Dillinger, S.; Bögge, H.; Armatage, A.; Proust, A.; Bergholt, C.; Bergmann, U., *Angew. Chem. Int. Ed. Engl.* **1994**, 33, 849.

10) Misono, M.; Nojiri, N., *Appl. Catal.* **1990**, 64,1.

11) Nomiya, K.; Yanogibayashi, H.; Nozaki, C.; Kondoh, K.; Hiramatsu, E.; Shimizu, Y., *J. Mol. Catal. A* **1996**, 114, 181.

12) Shimizu, M.; Orita, H.; Hayakawa, T.; Takehira, T., *Tetrahedron Lett.* **1989**, 30, 471.

13) Kozhevnikov, I. V., *Nato ASI, Polyoxometalate Molecular Science,* **2001**.

14) Zhang, X.Y.; O'Connor, C. J.; Jameson, G. B., *Inorg. Chem.* **1996**, 35(1), 30.

15) Zhang, X.; Chen, Q.; Duncan, D. C., *Inorg. Chem.* **1997**, 36(20), 4381,

16) Hagrman, P. J.; Hagrman, D.; Zubieta, J., *Angew. Chem. Int. Ed.* **1999**, 38(18), 2638.

17) Nazar, L. F.; Koene, B. E.; Britten, J. F., *Chem. Mater.***1996**, 8(2), 327.

18) You, W.; Wang, E., *Inorg. Chem.*, **2001**, in press.

19) Nazar, L. F.; Koene, B. E.; Britten, J. F., *Chem. Mater.***1996**, 8(2), 327.

20) Koene, B. E.; Taylor, N. J.; Nazar, L. F., *Angew. Chem. Int. Ed.* **1999**, 38(19), 2888.

21) Soghomonian, V.; Chen, Q.; Haushalter, R. C.; Zubieta, J., *Angew. Chem. Int. Ed. Engl.* **1995**, 34(2), 223.

22) Niu, J. Y.; You, X. Z.; Duan, C. Y., *Inorg. Chem.* **1996**, 35(14), 4211.

23) Clemente-Juan, J. M.; Coronado, E.; Galán-Mascarós, J. R.; Gómez-Garciá, C. J., *Inorg. Chem.* **1999**, 38, 55.

24) Golhen, S.; Ouahab, L.; Grandjean, D., *Inorg. Chem.* **1998**, 37(7), 1499.

25) Lira-Cantu, M.; Gómez-Romero, P., *In Recent Research Developments in Physical Chemistry*; S. G. Pandalai, Ed.; *Transword Network*, **1997**.

26) Clemente-Leon, M.; Agricole, B.; Mingotaud, C., *Langmuir*, **1997**, 13(8), 2340.

27) Volkmer, D.; Du Chesne, A.; Kurth, D. G., *J. Am. Chem. Soc.* **2000**, 122(9), 1995.

28) Kurth, D. G.; Volkmer, D.; Ruttorf, M., *Chem. Mater.* **2000**, 12(10), 2829.

29) Cheng, L.; Niu, L.; Gong, J., *Chem. Mater.* **1999**, 11(6), 1465.

30) Tang, Z.; Liu, S.; Wang, E., *Langmuir*, **2000**, 16(13), 5806.

31) Rhule, J. T.; Hill, C. L.; Judd, D. A., *Chem. Rev.* **1998**, 98, 327.

32) Sarafianos, S. G.; Kortz, V.; Pope, M. T.; Modak, M. J., *Biochem. J.* **1996**, 319, 619.

33) Yamase, T., *Mol. Eng.* **1993**, 3, 241.

34) Chottard, G.; Michelon, M.; Hervé, M., *Biochim, Biophys. Acta.* **1987**, 916, 402.

35) Peacock, R.D.; R. Weakley, T. J., *J. Chem. Soc. A.* **1971**, 11, 1836.

36) Madic, C.; Bourges, J.; Dozol, J. F., *AIP Conf. Proc*, **1995**, *346*, 628.

37) Kamoshida, M.; Fukasawa, T.; Kawamura, F., *J. Nucl. Sci. Technol.* **1998**, *35*, 185- 189.

38) Saprykin, A. S.; Shilov, V. P.; Spitsyn, V. I.; Krot, N. N., *Doklady Chem., Engl. Trans.* **1976**, *226*, 114-116.

39) Kosyakov, V. N.; Timofeev, G. A.; Erin, E. A.; Andreev, V. I.; Kopytov, V. V.; Simakin, G. A., *Soviet Radiochem., Engl. Transl.* **1977**, *19*, 418.

40) Erine, E. A.; Baranov, A. A.; Yu, V. A.; Chistyakov, V. M.; Timofeev, G. A., *J. Alloys Compd.* **1998**, *27*, 782.

41) Antonio, M. R.; Williams, C.; Solderholm, L.; Francesconi, L. C. *Chemical & Engineering News* **2001**, *Jan 14*, 48.

42) Milyukova, M. S.; Varezhkina, N. S.; Myasoedov, B. F. *J. Radioanal. Nucl. Chem., Letters* **1986**, *105*, 249-256.

43) Milyukova, M. S.; Varezhkina, N. S.; Myasoedov, B. F. *J. Radioanal. Nucl. Chem., Articles* **1988**, *121*, 403-408.

44) Milyukova, M. S.; Varezhkina, N. S.; Myasoedov, B. F. *Soviet Radiochem., Engl. Transl.* **1990**, *32*, 361-367.

45) Malikov, D. A.; Milyukova, M. S.; Myasoedov, B. F. *Soviet Radiochem., Engl. Transl.* **1989**, *31*, 425-430.

46) Malikov, D. A.; Milyukova, M. S.; Kuzovkina, E. V.; Myasoedov, B. F. *Soviet Radiochem., Engl. Transl.* **1993**, *35*, 465-471.

47) Myasoedov, B. F.; Milyukova, M. S.; Malikov, D. A. *Solv. Extr. Ion Exchan.* **1984**, *2*, 61-77.

48) Varezhkina, N. S.; Milyukova, M. S.; Myasoedov, B. F. *J. Radioanal. Nucl. Chem., Letters* **1989**, *135*, 67-76.

49) Molochnikova, N. P.; Frenkel, V. Y.; Myasoedov, B. F. *J. Radioanal. Nucl. Chem., Articles* **1988**, *121*, 409-413.

50) Molochnikova, N. P.; Frenkel, V. Y.; Myasoedov, B. F. *Sov. Radiochem., Engl. Transl.* **1989**, *31*, 322-326.

51) Bartis, J.; Dankova, M.; Blumenstein, M.; Francesconi, L. C. *Journal of Alloys and Compunds* **1997**, *249*, 56-68.

52) Mizuno, N. *Trends Phys. Chem* **1994**, *4*, 349-362.

53) Mizuno, N.; Misono, M. *Chem. Rev.* **1998**, 199-217.

54) Molchanov, V. N.; Kazanskii, L. P.; Torchenkova, E. A.; Simonov, V. I. *Sov. Phys. Crystallogr., Engl. Transl.* **1979**, *24*, 96-97.

55) Bartis, J.; Dankova, M.; Lessmann, J. J.; Luo, Q. H.; Horrocks, W. D., Jr.; Francesconi, L. C. *Inorganic Chemistry* **1999**, *38*, 1042-1053.

56) Luo, Q.H.; Howell, R. C.; Dankova, M.; Bartis, J.; Williams, C. W.; Horrocks, J., W.DeW.; Young, J., V.G.; Rheingold, A. L.; Francesconi, L. C.; Antonio, M. R. *Inorg. Chem.* **2001**, 40(8), 1894-1901.

57) Sadakane, M.; Dickman, M. H.; Pope, M. T. *Angew. Chem. Int. Ed.* **2000**, *39*, 2914-2916.

Chapter 2

1) Bartis, J.; Sukal, S.; Dankova, M.; Kraft, E.; Kronzon, R.; Blumenstein, M.; Francesconi, L. C. *J. Chem. Soc., Dalton Trans.* **1997**, 1937.

2) Luo, Q. H.; Howell, R. C.; Dankova, M.; Bartis, J.; Williams, C. W.; Horrocks, J., W.DeW.; Young, J., V.G.; Rheingold, A. L.; Francesconi, L. C.; Antonio, M. R. *Inorg. Chem.* **2001**, 40(8), 1894-1901.

3) Walker, N.; Stuart, D. *Acta Cryst.* **1983**, *A39*, 158-166.

4) Casan-Pastor, N.; Gomez-Romero, P.; Jameson, G. B.; Baker, L. C. W. *J. Am. Chem. Soc.* **1991**, *113*, 5658-5663.

5) Ortega, F.; Pope, M. T.; Evans, J., H.G. *Inorg. Chem.* **1997**, *36*, 2166-2169.

6) Sazani, G.; Dickman, M. H.; Pope, M. T. *Inorg. Chem.* **2000**, *39*, 939-943.

7) Wasserman, K.; Lunck, H. J.; Palm, R.; Fuchs, J.; Steinfeldt, N.; Pope, M. T. *Inorg. Chem.* **1996**, *35*(11), 3273-3279.

8) Xin, F.; Pope, M. F. *Inorg. Chem.* **1996**, *35*, 5693-5695.

9) Zhang, X. Y.; O'Connor, C. J.; Jameson, G. B.; Pope, M. T. *Inorg. Chem.* **1996**, *35*, 30-34.

10) Molchanov, V. N.; Kazanskii, L. P.; Torchenkova, E. A.; Simonov, V. I. *Sov. Phys. Crystallogr., Engl. Transl.* **1979**, *24*, 96-97.

11) Weakley, T. J. R. *Polyhedron*, **1987**, 6, 931.

12) Dawson, B. *Acta Cryst.* **1953**, 6, 113.

13) Bartis, J.; Dankova, M.; Blumenstein, M.; Francesconi, L. C. *J. Alloys Compds.* **1997**, 249, 56.

14) Luo, Q. H.; Howell, R. C.; Bartis, J.; Dankova, M.; Horrocks, W. DeW. Jr.; Rheingold, A. L.; Francesconi, L. C., *Inorg. Chem.* **2002**, accepted.

15) *Principles and Applications of Inorganic Geochemistry*, Gunter Faure, Macmillan, New York, **1991**.

16) Batis, J., *Doctoral Dissertation*, Chemistry Department of The City University of New York, **1997**.

Chapter 3

1) Walker, N.; Stuart, D. *Acta Cryst.* **1983**, *A39*, 158-166.

2) Casan-Pastor, N.; Gomez-Romero, P.; Jameson, G. B.; Baker, L. C. W. *J. Am. Chem. Soc.* **1991**, 113, 5658-5663.

3) Ortega, F.; Pope, M. T.; Evans, J., H.G. *Inorg. Chem.* **1997**, 36, 2166-2169.

4) Sazani, G.; Dickman, M. H.; Pope, M. T. *Inorg. Chem.* **2000**, 39, 939-943.

5) Wasserman, K.; Lunck, H. J.; Palm, R.; Fuchs, J.; Steinfeldt, N.; Pope, M. T. *Inorg. Chem.* **1996**, *35*.

6) Xin, F.; Pope, M. F. *Inorg. Chem.* **1996**, *35*, 5693-5695.

7) Zhang, X. Y.; O'Connor, C. J.; Jameson, G. B.; Pope, M. T. *Inorg. Chem.* **1996**, 35, 30.

8) Horrocks, W. DeW., Jr. *Methods Enzymol.* **1993**, *226*, 495.

9) Horrocks, W. DeW., Jr.; Sudnick, D. R. *Acc. Chem. Res.* **1981**, 14, 384.

10) Horrocks, W. DeW., Jr.; Sudnick, D. R. *J. Am. Chem. Soc.* **1979**, 101, 334.

11) Horrocks, W. DeW., Jr.; Wu, S. R. *Inorg. Chem.* **1995**, 34, 3724.

12) Bartis, J.; Sukal, S.; Dankova, M.; Kraft, E.; Kronzon, R.; Blumenstein, M.; Francesconi, L. C. *J. Chem. Soc., Dalton Trans.* **1997**, 1937.

13) Bartis, J.; Dankova, M.; Lessmann, J. J.; Luo, Q. H.; Horrocks, W. D., Jr.; Francesconi, L. C. *Inorg. Chem.* **1999**, 38, 1042-1053.

14) Sadakane, M.; Dickman, M. H.; Pope, M. T. *Angew. Chem. Int. Ed.* **2000**, 39, 2914-2916.

15) Yamase, T.; Ozeki, T.; Ueda, K. *Acta Crystallographica Section C* **1993**, 49, 1572-1574.

16) Yamase, T.; Ozeki, T. *Acta Cryst* **1993**, C49, 1577-1580.

17) Weakley, T. J. R. *Polyhedron*, **1987**, 6, 931.

18) Luo, Q. H.; Howell, R. C.; Dankova, M.; Bartis, J.; Williams, C. W.; Horrocks, J., W.DeW.; Young, J., V.G.; Rheingold, A. L.; Francesconi, L. C.; Antonio, M. R. *Inorg. Chem.* **2001**, 40(8), 1894-1901.

19) Ciabrini, J.-P.; Contant, R. *J. Chem. Research (M).* **1993**, 2720-2744.

20) Son, J.-H.; Choi, H.; Kwon, Y.-U. *J. Am. Chem. Soc.* **2000**, 122, 7432.

21) Müller, A.; Serain, C. *Acc. Chem. Res.* **2000**, 33, 2.

22) Jorris, T. L.; Kozik, M.; Casan-Pastor, N.; Domaille, P. J.; Finke, R. G.; Miller, W. K.; Baker, L. C. W. *J. Am. Chem. Soc.* **1987**, 109, 7402.

23) Bartis, J.; Dankova, M.; Blumenstein, M.; Francesconi, L. C. *Journal of Alloys and Compunds* **1997**, 249, 56-68.

24) Crans, D. C. *Comments Inorg. Chem.* **1994**, 16, 35.

25) Ciabrini, J. P.; Contant, R. *J. Chem. Res., Synop.* **1993**, 10, 391.

26) Luo, Q. H.; W. DeW.;Jr.; Francesconi, L.C., manuscript in preparation.

27) S. L. Wu and W. DeW. Horrocks, Jr. *J. Chem. Soc., Dalton trans.*, **1997**, 1497-1502.

28) Supkouski, R. M.; Horrocks, W. DeW., Jr., *Inorg. Chem.* Acta. **2002**, in press.

Chapter 4

1) Bartis, J.; Dankova, M.; Lessmann, J. J.; Luo, Q. H.; Horrocks, W. D., Jr.; Francesconi, L. C. *Inorganic Chemistry* **1999**, *38*, 1042-1053.

2) Luo, Q. H.; Howell, R. C.; Dankova, M.; Bartis, J.; Williams, C. W.; Horrocks, J., W.DeW.; Young, J., V.G.; Rheingold, A. L.; Francesconi, L. C.; Antonio, M. R. *Inorg. Chem.* **2001**, 40(8), 1894-1901.

3) Bartis, J.; Sukal, S.; Dankova, M.; Kraft, E.; Kronzon, R.; Blumenstein, M.; Francesconi, L. C. *J. Chem. Soc., Dalton Trans.* **1997**, 1937.

4) Weakley, T. J. R. *Polyhedron* **1987**, *6*, 931-937.

5) Spek, A. L. *Acta Cryst.* **1990**, *A46*, C-34.

6) Dawson, B. *Acta Cryst.* **1953**, *6*.

7) Molchanov, V. N.; Kazanskii, L. P.; Torchenkova, E. A.; Simonov, V. I. *Sov. Phys. Crystallogr., Engl. Transl.* **1979**, *24*, 96-97.

8) Ozeki, T.; Yamase, T. *Acta Cryst.* **1994**, *B50*, 128-134.

9) Sugeta, M.; Yamase, T. *Bull. Chem. Soc. Jpn.* **1993**, *66*, 444-449.

10) Yamaguchi, T.; Nomura, M.; Wakita, H.; Ohtaki, H. *J. Chem. Phys.* **1988**, *89*, 5153-5159.

11) Habenschuss, A.; Spedding, F. H. *J. Chem. Phys.* **1979**, *70*, 2797-2806.

Chapter 5

1) Ciabrini, J. P.; Contant, R. *J. Chem. Res., Synop.* **1993**, *10*, 391.

2) Batis, J., *Doctoral Dissertation*, Chemistry Department of The City University of New York, **1997.**

3) Horrocks, W. DeW., Jr. *Methods Enzymol.* **1993**, *226*, 495.

4) Horrocks, W. DeW., Jr.; Sudnick, D. R. *Acc. Chem. Res.* **1981**, *14*, 384

5) Horrocks, W. DeW., Jr.; Sudnick, D. R. *J. Am. Chem. Soc.* **1979**, *101*, 334.

6) Horrocks, W. DeW., Jr.; Wu, S. R. *Inorg. Chem.* **1995**, *34*, 3724.

7) Kenneth, A. C., *Binding constants-The measurement of molecular complex stability,* John Wiley & Sons, Inc. **1987**.

8) Yusov, V. P.; *Radiokhimiya*, **1980**, vol. 22, no. 5, 727-732.

9) Kulyko, Yu. M.; Lebedev, I. A.; Trofimov, T. I., *et al., Zh. Neorg. Khim.*, **1981**, vol. 26, no. 5, 1254-1260.

10) Contant, R.; Ciabrini, J. P., *J. Chem. Res.* (s), 1982, no. 2, 50-51; *J. Chem. Res.* (M), **1982**, no. 3-7, 641-660.

11) Kirby, J. F.; Baker, L. C. W., *Inorg. Chem.* **1998**, 37, 5537-5543.

12) Bartis, J.; Sukal, S.; Dankova, M.; Kraft, E.; Kronzon, R.; Blumenstein, M.; Francesconi, L. C. *J. Chem. Soc., Dalton Trans.* **1997**, 1937.

13) Supkouski, R. M.; Horrocks, W. DeW., Jr., *Inorg. Chem.* Acta. **2002**, in press.

14) Sadakane, M.; Dickman, M. H.; Pope, M. T., *Inorg. Chem.* **2001**, 40, 2715-2719.

Chapter 6

1) Contant ; Klemperer, Ed., **1990**; Vol. 27, 71.

2) Contant, R.; Ciabrini, J.-P. *J. Chem. Res. Synop.* **1977**, 222; The syntheses are reported in more detail in ref 3.

3) Contant, R. *Inorg. Synth.* **1990**, *27*, 71.

4) Lyon, D. K.; Miller, W. K.; Novet, T.; Domaille, P. J.; Evitt, E.; Johnson, D. C.; Finke, R. G. *J. Amer. Chem. Soc.* **1991**, *113*, 7209.

5) Bartis, J.; Kunina, Y.; Blumenstein, M.; Francescone, L. C. *Inorg. Chem.* **1996**, *35*, 1497.

6) Bartis, J.; Dankova, M.; Lessmann, J. J.; Luo, Q.-H.; Horrocks, W. D., Jr.; Francesconi, L. C. *Inorganic Chemistry* **1999**, *38*, 1042-1053.

7) Martell, A. E.; Motekaitis. R. J. *Determination and Use of Stability Constants*. 2nd ed.; VCH: New York, **1992**.

8) Horrocks, W. DeW., Jr. *Methods Enzymol.* **1993**, *226*, 495.

9) Horrocks, W. DeW., Jr.; Sudnick, D. R. *Acc. Chem. Res.* **1981**, *14*, 384

10) Horrocks, W. DeW., Jr.; Sudnick, D. R. *J. Am. Chem. Soc.* **1979**, *101*, 334.

11) Horrocks, W. DeW., Jr.; Wu, S. R. *Inorg. Chem.* **1995**, *34*, 3724.

12) Ciabrini, J.-P.; Contant, R. *J. Chem. Research (M).* **1993**, 2720-2744.

13) Contant R.; Ciabrini J., *J. Chem. Research, (S),* **1982,** 50-51; *J. Chem. Res. (M),* **1982**, no. 3-7, 641-660.

14) Craig E. Van Pelt; William J. Crooks III; Gregory R. Choppin, *Dissertation,* **1998,** Dept. of Chem., The Florida State University.

15) Martell, A. E.; Motekaitis, R. J., *Determination and use of stability constants,* New York, VCH Publishers, **1992**.

16) Wu, Sh. L.; Horrocks, W. DeW. Jr., *Anal. Chem.* **1996**, 68, 394.

17) Yusov, V. P.; *Radiokhimiya,* **1980**, vol. 22, no. 5, 727-732.

18) Kulyko, Yu. M.; Lebedev, I. A.; Trofimov, T. I., *et al., Zh. Neorg. Khim.,* **1981**, vol. 26, no. 5, 1254-1260.

19) Yusov, A. B.; Shilov, V. P., *Radiochem.* **1999**, Vol. 41, no. 1, 1-23, Translated from *Radiokhimiya.* Vol. 41, no. 1, **1999**, 3-24.

20) Spitzyn, V. I.; Orlova, M. M.; Krot, N. N.; Saprykin, A. S., *Zh. Neorg. Khim.* **1978**, 13, 1227.